8-1-2011

A Climatology of High-Wind Events Associated with Post-Tropical Cyclones in the United States

Joshua M. Gilliland
Western Kentucky University, joshua.gilliland847@topper.wku.edu

A CLIMATOLOGY OF HIGH-WIND EVENTS ASSOCIATED WITH POST-TROPICAL CYCLONES IN THE UNITED STATES

A Thesis
Presented to
The Faculty of the Department of Geography and Geology
Western Kentucky University
Bowling Green, Kentucky

In Partial Fulfillment
Of the Requirements for the Degree
Master of Science

By
Joshua M. Gilliland

August 2011

A CLIMATOLOGY OF HIGH-WIND EVENTS ASSOCIATED WITH POST-TROPICAL CYCLONES IN THE UNITED STATES

Date Recommended 05.13.11

Josh Durkee, Director of Thesis

Kevin Cary

Greg Goodrich

Rezaul Mahmood

Richard A. Bowker June 24, 2011

Dean, Graduate Studies and Research Date

I dedicate this thesis to my parents, Hank and Rita, and my brothers, Nick and Adam. I am forever appreciative of having a supportive and close-knit family. Your continuous encouragement and love helped me in the completion of this degree. To my parents, I have always looked up to you for advice and guidance. Without your continual advice and guidance, I would have never been able to complete this degree. So, this thesis is especially dedicated for you. Thank you!

I also dedicate this thesis to my late friend and former high school basketball coach, Cody Betts. You inspired and taught me that the only way to be successful in life is through hard work and determination. The lessons and values that you taught me not only made me triumphant on the basketball court but in life as well. You will never be forgotten and I am forever in gratitude to you.

ACKNOWLEGEMENTS

First, I would like to acknowledge my parents, Hank and Rita. Thank you for giving me the opportunity to pursue my educational dreams at Western Kentucky University. Without your continual support and sacrifices, I would have never of gotten to this point in my life. The values and lessons that you distilled from a young age have encouraged me to reach for the stars and never settle for anything less. Thank you!

I would also like to thank my brothers, Nick and Adam, for their continual support through this part of my life. I could not ask of any better brothers to share my problems and concerns with. Furthermore, I would like to acknowledge my entire extended family, for their immeasurable support and guidance throughout the years.

In addition, I would like to thank my advisor, Dr. Joshua D. Durkee, for sharing his expertise and mentoring me through my research, and guiding me through this part of my educational process. In addition, I would like to acknowledge my committee members, Kevin Cary and Drs. Gregory B. Goodrich, and Rezaul Mahmood, for their advice and guidance through the thesis process.

TABLE OF CONTENTS

LIST OF FIGURES

LIST OF TABLES

A CLIMATOLOGY OF HIGH-WIND EVENTS ASSOCIATED WITH POST-TROPICAL CYCLONES IN THE UNITED STATES

Joshua M. Gilliland August 2011 113 Pages

Directed by: Dr. Joshua D. Durkee

Department of Geography and Geology Western Kentucky University

During 1951-2009, 47% of all tropical systems (TSs) within the Atlantic Basin transitioned to post-tropical (PTC) extratropical classification. These systems have shown the capability of producing hurricane-force winds and gusts for portions of the eastern United States. This study provides a climatological foundation for high-wind observations that were contributed from PTCs. In this study, 76 PTC systems were identified and tracked using six hourly observations from the National Hurricane Center's HURDAT dataset. Mean wind radii buffers were calculated and used to determine the high-wind observations attributed by PTCs. High-wind climatology was developed by using hourly surface wind data from the National Climatic Data Center (NCDC) and deploying the current NWS high-wind criteria. For this study, the geography and climatology of PTCs and resultant high winds were analyzed using geographic information systems (GIS). Findings show that < 1% (270) of all high-winds events that occur within the U.S. were contributed from PTCs. The highest frequencies were found in three regions: Midwest, Mid-Atlantic, and New England. Due to the low number of high-wind events produced from PTCs, an adjusted wind scale was created by using standard deviations of sustained and gust observations. The goal of this study is determine the contribution of high winds from PTCs, with the aim of improving our understanding of the hazardous outcomes of such events.

CHAPTER 1

INTRODUCTION AND LITERATURE REVIEW

1.1 Introduction

The pattern of Atlantic tropical systems (TSs) is primarily driven by atmospheric circulations, sea surface temperatures (SSTs), and physiographic characteristics. The thermohaline circulation provides the energy and heat to warm the Atlantic Ocean and Gulf of Mexico. Converging surface winds along the intertropical convergence zone (ITCZ) creates lift to form thunderstorms and cloud structures. The majority (60%) of easterlies waves or disturbances that develop into TSs originate along the ITCZ near Africa (Landsea 1993; Chen et al. 2008). This combination of tropical easterlies, warm SSTs, and surface wind convergence along the ITCZ help create the TSs that often leave behind devastating impacts across the eastern United States. Surface winds within TSs typically peak prior to landfall and eventually decay in magnitude as the cyclone moves inland (Kaplan and DeMaria 1995). In contrast, changes in SSTs and baroclinic conditions above 40° N can influence the strength and spatial coverage of surface wind fields within the TS. Today forecast meteorologists remain challenged by prognostic determinations of the evolving structure of surface wind fields especially, as TSs encounter various upper-atmospheric and surface conditions (e.g., troughs, jet streams, and SSTs) (Jones et al. 2003).

1.2 Literature Review

TSs (including tropical depressions, tropical storms, and hurricanes) are intense oceanic weather systems that are capable of producing destructive storm surge, damaging winds, flooding rains, and tornadoes. TSs that affect the southeastern U.S. are mostly observed to develop and migrate across the Atlantic and Gulf of Mexico basins during the summer and fall seasons of June-November. At times a certain fraction (i.e., 50%) of these TSs that make initial landfall and/or move into latitudes above 25° N have been observed to transition into an extratropical, or post-tropical (PTC) cyclones (Hart and Evans 2001). PTCs are generally typified by asymmetries in cloud, precipitation, and wind fields, a loss of deep core convection, an outward expansion of gale force winds ($\geq$ 18 m s^{-1}) from the center of circulation, and/or decrease and disappearance of upper-level clouds from satellite imagery (J. Franklin, person communication). However, a formal universal definition of a PTC remains subjective, while a variety of meteorological applications have been used to classify these systems (Merrill 1993; Evans and Hart 2003; Jones et al. 2003). The primary focus of most research is on understanding how various synoptic environments influence the surface wind field structures of PTCs.

a. Identifying PTCs

Various large-scale atmospheric circulation and dynamics are used to justify the transitional phase from a TS to a classified PTC. The National Hurricane Center (NHC) defines a PTC based on two criteria stemming from extratropical cyclones (ETCs) and remnant surface low-pressure circulations. A PTC is a mid-latitude system that has lost

its tropical characteristics (i.e., a warm core non-frontal system that exhibits an organized deep convective with closed surface wind circulation around a well-defined center) with a poleward trajectory that derives its energy source from horizontal temperature differences in the atmosphere (NHC, 2010). In an earlier study, Matano and Sekioka (1971) classified two PTC transition types for the western Pacific based solely on surface pressure. In the first type, a complex transition occurs when a pre-existing mid-latitude front or trough interacts with a TS to create a new PTC along the frontal boundary. The second type, a compound transition develops when an ETC encounters a TS and the warm core system appears to transitions to PTC.

More recently, Klein et al. (2000) defined the PTC transition process based on two phases for the North Pacific basin. First, the transformation stage begins when the outer circulation of the TS interacts with a pre-existing mid-latitude baroclinic environment. The cyclone starts to exhibit an asymmetric cloud structure and decrease in deep convection along the western flank of the system. The transformation stage is completed when the TS becomes embedded within the frontal zone and cold air is present at the surface center (Klein et al. 2000). Second, reintensification maximum occurs after the transformation is completed and the surface sea-level pressure (SLP) gradient is at its strongest before the storm starts to dissipate in strength and magnitude.

Hart (2003) developed a cyclone phase space (CPS) model, which is derived from thermal wind and storm motion thicknesses to determine the complete transition from TS to PTC. The onset of PTC transition begins when the sustained thickness asymmetry (β) reaches a value of > 10 m between the pressure levels of 900-600 hPa. The transition is complete when vertical storm structure corresponds to a cold-core vortex resulting in a

positive thermal wind ($-V_T^L < 0$) (Evans and Hart 2003). Sinclair (2004) also used the CPS method to identify the onset and completion of southwest Pacific PTCs and determined that strong cyclonic vorticity advection (CVA) was critical for surface development of PTCs.

In another study, Kitabatake (2008) examined how strength and magnitude of different frontal boundaries can influence and change the large-scale dynamic structure of PTCs in the western North Pacific basin. In that study, the evolution of PTCs are described with three classification types: cold air (CA), seclusion-occlusion (SO), and open-wave (OW) frontal cyclones (Fig. 1.1). In the first type, CA cyclones develop when the TS approaches a strong pre-existing cold front, which is eventually absorbed into the frontal boundary during PTC transition. A SO cyclone occurs when the TS has a poleward movement over colder SSTs while maintaining a warm-core structure (Kitabatake 2008). When the transition to PTC is completed, the frontal evolution becomes occluded in nature. The OW cyclone exhibits characteristics of both CA and SO systems. This cyclone type is not well organized and dissipates shortly after becoming PTC.

b. Characteristics of PTCs

1. Worldwide PTCs

PTCs have been observed worldwide over all oceanic and continental basins, including southeast Indian (Foley and Hanstrum 1994), southwest Pacific (Sinclair 2002, 2004), western North Pacific (Sinclair 1993; Harr and Elsberry 2000; Harr et al. 2000; Klein et al. 2000; Ritchie and Elsberry 2002; Kitabatake 2002, 2008), and extensively in

the North Atlantic (Hart and Evans 2001; Hart 2003; Arnott el al. 2004; Evans and Prater-Mayes 2004; Hart et al. 2006; Evans and Hart 2008; Hulme and Martin 2009). The transition from a TS to PTC classification characteristics vary among the different oceanic basins and continents. Jones et al. (2003) compiled a comprehensive PTC climatology background of the all oceanic basins (i.e., southeast Indian, western North Pacific, southeastern Pacific, and North Atlantic) from 1970-1999. Jones et al. (2003) indicated that the greatest frequency of PTCs occurs in western North Pacific basin, while the North Atlantic contains the highest percentage TS/PTC transitions. Over the Indian Ocean, relatively few TSs (<10 %) undergo PTC genesis (Jones et al. 2003). Foley and Hanstrum (1984) showed that PTCs most likely occurred when a strong approaching surface cold front is within 1700 km of the Indian Ocean basin.

Sinclair (2002) provided an analysis of TS/PTC transition for the southwest Pacific from 1970-1996 based on the tropical cyclone best and intensity archive developed by the New Zealand Meteorological Service (NZMS). In that study, Sinclair (2002) found that 32% of all TSs made the transition to PTC classification between 23°-25° S and migrated southeasterly. Moreover, the highest frequency of PTCs developed between December-March, with a maximum occurrence in February. Klein et al. (2000) examined the migration, duration, and transition of western North Pacific PTC systems from 1994-1998. PTC transition was defined when visible, infrared, and water vapor imagery started to show asymmetric cloud structure and a decrease in convective on the down flank quadrant of the TS (Klein et al. 2000). As of result, 30% (27/112) of all TSs made PTC transformation and tracked to the northeast or northwest. Klein et al. (2000) also found the mean duration of transition took 46 hours to complete. In contrast,

Kitabatake (2008) showed that a higher percentage (42%) of TSs completed the transition within the North Pacific basin. The primary difference between the two studies is likely due to the fact that Klein et al. (2000) excluded TSs that form and transition during the cool season. Hart and Evans (2001) studied PTC transitions of North Atlantic cyclones from 1950-1996 based on the categorical strengths found within the HURDAT dataset developed by the NHC. The findings from Hart and Evans (2001) showed that roughly 46% of all TSs transformed into PTCs along a northeast trajectory. Further discussion of North Atlantic PTCs is discussed in the below sub-section b2.

2. North Atlantic PTCs

Hart and Evans (2001) provided the first and earliest climatology investigating PTC transition of TSs for the North Atlantic. Over 46% (216/463) of all TSs underwent the transition phase to PTC and tracked in a northeasterly direction. In addition, Hart and Evans (2001) revealed that 50% of the 206 TSs that made landfall north of 25° N transitioned to PTC. Typically, these cyclones tend to develop at higher latitudes from May-August. A noticeable southward trend in PTC development is evident during the months of September and October (Fig. 1.2). The southward movement of baroclinic growth and instability, along with the slow warming of the Atlantic Ocean are key factors that implement the late transition point during the season (Hart and Evans 2001).

PTCs usually form between the latitudes of 24°-55° N, with the highest frequency occurring between 35°-45° N (Hart and Evans 2001). A statistical shift during the months of July- September showed TSs are most likely to transition to PTC at the latitudes of 40°-45° N (Hart and Evans 2001). As of result, Hart and Evans (2001)

determined the transition season can be broken down into three subclasses based on activity: a low latitude quiet early season, high latitude active mid-season, and mid-latitude active late season.

It is clear from monthly frequencies that a higher percentage of TSs transition to PTCs during the peak of the hurricane season. Roughly 50% of all Atlantic TSs from September-October tend to transform and make landfall above 25° N (Hart and Evans 2001). Even with cooler water temperatures at high latitudes, 51% of TSs strengthen when compared after transitioning to PTCs. This high percentage is primarily caused by the magnitude or strength of the TS circulation (Hart and Evans 2001). Furthermore, Hart and Evans (2001) suggested that PTC reintensification can be traced back to the origin of the TS before entering into the baroclinic or synoptic environment. TSs that originate deep in the tropics (below 15° N) tend to form more intense PTCs (Fig. 1.3). Hart and Evans (2001) explain that potential vorticity (PV) anomalies help promote a decrease in static stability and advect warm, moist air into higher latitudes causing the promotion of baroclinic growth to occur during the transition to PTC. In addition, Hart and Evans (2001) found that the central SLP can dictate the transition duration and strength of the PTC. TSs that maintain a minimum pressure greater than 970 hPa usually required a shorter transition time (< 20 hours), and typically intensify in strength and magnitude when interacting within the baroclinic environment. PTCs that do reintensify upon entering middle-to-high latitudes tend to start their transitions between 37°-47° N and south of 65°-50° W (Hart and Evans 2001).

However, TSs that form or enter into the Gulf of Mexico show a lesser likelihood of undergoing PTC transition (Hart and Evans 2001). Hart and Evans found only 31%

(14/45) of TSs underwent and completed PTC classification. Interestingly, none of the 14 PTCs intensified in strength, which commonly occurs with Atlantic-based PTCs. Hart and Evans (2001) explained that a landfalling Gulf of Mexico TS typically weakens or dissipates well before interacting with baroclinic environments to allow post-transition intensification to occur.

c. Characteristics of PTC Surface Wind Fields

Kruk et al. (2010) found that most states located east of the Rocky Mountains have experienced surface winds associated from a PTC (Fig. 1.4). The region most likely to receive winds greater than 17.5 m s^{-1} is primarily along the East Coast with PTC winds every 2-5 years on average (Kruk et al. 2010). Areas located within the interior of the contiguous U.S. (i.e., Great Plains, and upper Great Lakes) or located within the western basin of the Gulf of Mexico (Texas, Louisiana, and Mississippi) demonstrated a lesser likelihood of receiving PTC winds of 17.5 m s^{-1}. Kruk et al. (2010) also showed overland average radii for PTCs are typically larger when compared to all other categories of the Saffir-Simpson Hurricane Wind Scale (SSHWS). This outward expansion in the wind fields is supported by Hart et al. (2006). Hart et al. (2006) revealed that the average radius of gale force surface winds increase from 226 km to 571 km after the storm transitioned from TS to PTC classification.

Specifically, the strongest winds typically develop along the right (left) flank of the storm track in North (South) Hemisphere due to adiabatic cooling to the west (east) side of the system and shift of the maximum inward angle to the landward side of the cyclone (Powell 1982). Merrill (1993) indicated that topographic roughness, baroclinic

environments, and friction help reduce the velocity and allow asymmetry of wind fields to occur within these systems. The wind field expansion of "PTC Bonnie" (1998) demonstrates how a baroclinic environment can influence the size and shape of a PTC surface wind fields (Evans and Hart 2008). Evans and Hart (2008) concluded that conveyor belts transferred warm air to the outer edge of the cyclone's circulation in which caused the wind fields (i.e., right flank) to increase outward away from PTC Bonnie's center.

Kaplan and DeMaria (2001) found that landfalling TSs above (below) 37° N tend to have surface wind fields that decay more (less) rapidly when the velocity was greater (less) than 17 m s^{-1} (Fig. 1.5). Kaplan and DeMaria (2001) attribute this faster decay rate due to higher terrain located along the coastline as well as the mid-latitude environment that the cyclone encounters during landfall. Baroclinic energy at higher latitudes allows for a slower decay rate to occur as the wind speed falls below 17 m s^{-1} (Kaplan and DeMaria 2001). Other studies have also shown that upper-level troughs and the change in SST gradients can cause PTC surface winds to evolve with velocity, size, and shape in high-latitude regions (Merrill 1993; Ritchie and Elsberry 2002; Jones et al. 2003; Arnott el al. 2004; Hart et al. 2006).

d. Impacts of PTC Winds

PTCs have the possibility of producing hurricane force winds ($\geq$ 33 m s^{-1}) over inland and higher latitude cities and communities (Jones et al. 2003). Rappaport (2000) found that wind-relative events were the second (12%) leading cause of death from Atlantic TSs during 1970-1999 in the U.S. Rappaport (2000) also demonstrated that

inland counties and regions are not safe zones from receiving TS surface winds. Since 1970, 35 deaths have been attributed from winds that reach inland counties, and 10% of those fatalities were caused from falling trees (Rappaport 2000).

The impacts from PTC winds can be even more costly and deadly than a tropical or mid-latitude cyclone (Jones et al. 2003). Hurricane Ike (2008) is an excellent example of a PTC storm that produced hurricane strength winds across portions of the Ohio River Valley and Mid-South regions. For example, maximum wind gusts for "PTC Ike" included 37 m s^{-1}, 33 m s^{-1}, and 28 m s^{-1} in Cincinnati, OH, Louisville, KY, and Indianapolis, IN, respectively. Meanwhile, numerous other locations across the region reported wind speeds exceeding 26 m s^{-1} (Stoppkotte et al. 2009). These high winds associated with the remnants of Ike produced nearly $1.5 billion dollars in total damage. Aside from damaging winds, this PTC event left behind 12 fatalities and forced over three million people to lose their electricity, ranging from a few hours to more than one week in certain cities of southwest and central Ohio (NWS 2008; Stoppkotte et al. 2009).

The "Perfect Storm" of 1991 illustrated that PTCs are capable of producing strong winds along coastal and inland regions without making direct landfall. High winds were reported all along the eastern seaboard (Florida to Maine) with gusts ranging from 15-33 m s^{-1} (NCDC, 1991). Damage estimated from the storm resulted in over $300 million dollars across the region (Corderia and Bosart 2010). A similar outcome of high winds occurred as PTC Noel in 2007 tracked along the eastern Atlantic coastline and caused more than 250,000 U.S. and Canadian citizens to lose their electricity (Brown 2008).

Other high-wind events associated with PTCs have been observed throughout the world. Hill (1970) described a tropical disturbance that rapidly reintensified as it

approached New Zealand. Wind gust reports of 75 m s^{-1} were observed in the capital city of Wellington, which unfortunately caused an interisland ferry to sink, resulting in the loss of 51 lives. Overall, these summaries indicate the magnitude of caution and awareness that must be taken regarding PTC winds.

e. PTCs vs. ETCs

One important large-scale atmospheric influence on the strength and magnitude of PTC winds across North America are the influence of ETCs (Bosart and Bartlo 1991; Harr et al. 2000; Klein et al. 2000; Jones et al. 2003; Ritchie and Elsberry 2003; Evans and Prater-Mayes 2004; Hart el al. 2006; Kitabatake 2008; Hulme and Martin 2009). ETCs are defined as synoptic-scale low pressure weather systems that occur poleward of the tropics. Research has shown that ETCs over North America are more tightly confined to higher latitudes (> 45° N) during the early summer months and make an eventual southward move to lower latitudes during the cool season months (Reitan 1974; Whittaker and Horn 1984; Eichler and Higgins 2006; Wernil and Schwierz 2006; Ulbrich et al. 2009).

However, recent studies have found the frequency count of ETC genesis remains steady during July-September (Wang et al. 2006; Raible et al. 2008). With this minimum change, both analyses showed that the mean life span has changed considerably for all intensities of ETCs. Mesquita et al. (2008) found that the average life span of an ETC lasts between 5-7 days. This increase in duration is dependent on the SST gradients, baroclinic environments, relative vorticity, SLP, and available potential energy (APE).

These various conditions contribute for a longer time for a cyclone to develop near or along the eastern Atlantic coastline (Mesquita et al. 2008; Dacre and Gray 2009).

The atmospheric variables mentioned above have also been shown to influence the structure and dynamics of PTCs. Specifically, Hart et al. (2006) provided an analysis of PTC characteristics based on 34 Atlantic PTCs of 1998-2003. From the study, Hart et al. (2006) found that the typical ETC evolution and intensity change is dependent on the magnitude of the interaction of the mid-latitude trough and the TS. TSs that underwent rapid (slow) intensification encountered highly meridional (zonal) mid-latitude longwave flow, SSTs well below (closer to) 27° C, and the system was smaller and weaker (larger and stronger) than average before beginning the transformation to PTC. Even with a change in magnitude of the trough, the final intensity of the TS as its transition to a PTC was not as dependent on the strength of the mid-latitude trough (Ritchie and Elsberry 2002).

A non-hierarchical cluster analysis conducted by Arnott et al. (2004) found that a TS synoptic life cycle (from its genesis to PTC transition) can be identified and grouped by the changes in thermal and relative motion thicknesses based on latitude and longitude coordinates. Arnott et al. (2004) also determined TSs that transition to PTCs tend to resemble similar structural characteristics of an ETC. PV anomalies associated with the TS core becomes broader and are no longer vertically aligned, and start to slope northwest with height as the system approaches the mid-latitude trough. The core of the cyclone initially remains intact but begins to show an asymmetrical structure. As the TS continues to interact with the trough, the PV anomalies merge together causing the system to resemble a mature ETC (Arnott et al. 2004).

f. High-Wind Events (HWEs)

Recent studies have examined atmospheric dynamics and hazard distributions of nonconvective and convective to help explain wind characteristics for the U.S. Understanding how large-scale conditions vary throughout U.S. may help explain and define the wind characteristics of landfalling PTCs.

1. Nonconvective

Knox et al. (2011) illustrated that four mechanisms (topography, isallobaric wind, tropopause folds, and sting jets) have been used to explain the development of nonconvective high-wind events (NCWEs). As of result, Knox et al. (2011) concluded that nonconvective wind dynamics are the result of many atmospheric processes, rather than one dominant contributor (i.e., pressure gradient). Similarly, Durkee et al. (2011) applied ageostrophic wind theory to determine that isallobaric winds, friction, horizontal, and vertical advection were all important contributors in the NCWEs over the Great Lakes region during 12-13 November 2003. Research conducted by Niziol and Paone (2000) suggested that topographic channeling along Lake Erie was the major cause of southwesterly NCWEs over western New York from 1977-1997. However, Lacke et al. (2007) conducted a 44-year cold season climatology (November-April) of NCWEs for the entire Great Lakes region and found that the southwest preference found by Niziol and Paone (2000) was not caused by topography but instead by ETC dynamics. Martin and Konard (2006) also concluded that ETC migration was responsible for high-wind events to occur over a network of 20 Automated Surface Observing System (ASOS) sites in the southeastern U.S. from 1995-2003.

In support of Martin and Konard (2006) and Lacke et al. (2007) findings, Kurtz and Martinell (2010) documented that the primarily factor of driving cold season NCWEs (September-March) over the central Great Plains were caused by mid-latitude dynamics. Asuma (2010) performed a cool season wind and dynamic climatology for the northeastern U.S. from 1993-2008 and showed that the highest frequency of gradient wind days (i.e., NCWEs) occurred during October-December. The largest magnitudes of gradient winds were found in three major regions: Great Lakes, Atlantic coastline, and lee of Appalachian Mountains (Asuma 2010).

2. Convective

Convective high-wind events (CWEs) are primarily the result of downdrafts. The outflow of downdraft air from thunderstorms is an important phenomenon in understanding convective dynamics. Wakimoto (2001) described that diabatic cooling and microphysics of falling precipitation, along with negative buoyancy of the air parcel are key contributors of producing strong downdrafts at the surface of Earth. In addition, condensate loading and downward drag from descending precipitation can also contribute to the initiation of downdrafts (Wakimoto 2001). Numerical models showed that the maintenance of a downdraft by descending precipitation is a function of the drop size, rain intensity, lapse rate, and downdraft velocities (Kamburova and Ludlam 1966; Srivastava 1985).

Wakimoto (2001) also found that the leading edge (gust front) of the downdraft's outflow is another important factor of producing CWEs. Wakimoto (2001) discussed that two types of convective downdrafts (rear-flank and forward flank) are usually associated

with supercell development. Lemon and Doswell (1979) found that forward-flank downdrafts occur downwind of the supercell and is typically associated with a wet-bulb potential temperature that results from the mixing of updraft and mid-level environmental air. Klemp (1987) showed that the leading edge of the outflow play a critical factor in generating horizontal vorticity which is needed to produce tornadic thunderstorm events. In contrast, the strongest downdrafts associated within a supercell are located within the rear-flank of the developing convective system (Wakimoto 2001).

The distribution of high winds produced from convective storms can be spatially explained over the U.S. Kelly et al. (1985) provided a climatology of nontornadic severe thunderstorm events from 1955-1983. As of result, Kelly et al. (1985) concluded that two major axe of CWEs exists over the U.S. The first axis begins in the upper Midwest and stretches over the Great Lakes region with the secondary axis occurring over the Great Plains region. Other research has shown the greatest CWE occurrences arise between late spring and early summer months (Kelly 1985; Wakimoto 2001; Klimowski et al. 2003; Doswell 2005; Horgan et al. 2007; Smith et al. 2010). Horgan et al. (2007) performed a 5-year climatology of elevated severe convective storms and found that the central and eastern U.S. typically experience CWEs during the summer and early fall months, while in the south-central U.S. CWEs developed during the cold season (October-February). Doswell (2005) revealed an apparent preference for CWEs in the Great Plains with a secondary axis into the Ohio Valley region. In addition, a northward shift in CWEs from the lower plains into the higher plains and Ohio Valley region by late summer (Doswell 2005). An analysis of CWEs over the northern high plains from 1996-1999 showed that the highest frequency of CWEs occur later in the season (June-August)

(Klimowski et al. 2003). Additional work by Asuma (2010) showed that convective development in the northeastern U.S. during the cool season (October-April) is quite rare. Furthermore, Asuma (2010) found that only 14% of all high-wind events that occur from 1993-2008 were classified as convective.

3. High-Wind Hazards

Other work has focused on understanding the hazardous contributions of convective and nonconvective high winds (Knox 2004; Ashley and Black 2008; Black and Ashley 2010; Durkee et al. 2011; Schoen and Ashley 2011). Black and Ashley (2010) found that nontornadic convective winds accounted for 32.1% of all wind-related fatalities during 1977-2007. The highest frequencies of nontornadic convective deaths occurred in the late spring and summer months (Black and Ashley 2010). Schoen and Ashley (2011) also found that the location of thunderstorms, among various storm types can impact the number of fatalities. As of result, Schoen and Ashley (2011) established that weakly organized convective thunderstorms (i.e., pulse convection and quasi-cellular thunderstorms) contributed to 45% of all fatalities during 1998-2007. In addition, two distinct fatality thunderstorm regions were recognized: Great Lakes and Mid-South/East Coast regions (Schoen and Ashley 2011). A large number of fatal convective wind deaths over the Great Lakes were contributed by unorganized and nonlinear storms, and bow echoes. For the Mid-South and East Coast, deaths were mainly caused by organized linear convective storms.

However, the number and timing of deaths were different when compared to nonconvective winds. Ashley and Black (2008) determined a lower frequency of deaths

(21.4%) with those fatalities occurring during the cooler months of November-March. Knox (2004) also found that 5% of all U.S. wind deaths were contributed by NCWEs from 1996-2002. Typically, the highest number of NCWE-related fatalities occurs along the Great Lakes to Mid-Atlantic regions and southern states (Ashley and Black 2008; Black and Ashley 2011). Both studies explained that largely dense forest areas, proximity of water, and high population densities caused higher fatally rates to occur in these regions.

1.3 Research questions

PTCs have been shown to produce severe weather events across various regions around the world (Jones et al. 2003). Accurate forecasting of PTC intensity and tracking with operational models is still an obstacle for meteorologists. The motivation of this research is derived from the limited availability and accessibility of PTC research for the U.S.

This thesis provides a climatological assessment of all PTCs and the resultant inland high winds across the eastern U.S. during 1951-2009. The examination of PTC-HWEs is performed using hourly surface wind data from National Climatic Data Center (NCDC). This particular dataset was further processed to select only those observations that meet the current National Weather Service (NWS) high-wind criteria (Table 1.1). In a previous study, Kruk et al. (2010) showed that the highest frequency of PTCs winds occur along the Mid-Atlantic and New England coastlines due to the influence of relatively stronger baroclinic conditions across those areas. However, Kruk et al. (2010) determine these internal years based on estimated wind radii and not using actual surface

wind records from meteorological observation sites. Based on Kruk et al. (2010), it was plausible that high-wind frequency maxima associated with PTCs occur in the northeastern U.S. Given such conditions, any differences found in the physical structure of PTC and its wind field characteristics may enhance our understanding to better forecast and predict the behaviors of PTCs as they approach inland and highly populated areas. Overall, this research will identify how susceptible the eastern U.S. is to PTC-HWEs based on the NWS high-wind criteria. In order to investigate these issues, this study addresses the following questions:

- What percent of TSs transition to PTCs in the U.S.?
- What regions in the U.S. are most susceptible to PTCs?
- How capable are PTCs at producing high winds that meet typical NWS criteria?
- What regions in the U.S. are more susceptible to PTC high-wind events?
- What is the spatial distribution of observed high winds within the PTC storm track?
- Does the origin and/or strength of a TS or STS affect PTC high-wind characteristics?
- Does seasonality influence or change the characteristics of PTCs and subsequent high-wind observations?

1.4 Summary

North Atlantic TSs has been widely studied by scientists during the last century. However, PTC research is still a relative new area of study. PTCs have shown to have

the capability of producing sensible weather-related events similar in magnitude and strength of any major TS study in the Atlantic Ocean basin. Researchers have focused on understanding PTC transition by investigating the various large-scale baroclinic and dynamic environments. Despite these research efforts, no formal studies have focused explicitly on understanding the spatial distribution of HWEs associated with landfalling PTCs.

The purpose of this thesis is to strengthen our understanding of PTCs by constructing a descriptive climatological database of these events from 1951-2009, with special attention given to PTC high-wind characteristics. The results and conclusions found in this thesis will provide a better understanding of PTC surface winds and further prepare forecasters and U.S. citizens of the possible hazards that are unfortunately often associated with Atlantic-based PTC storms.

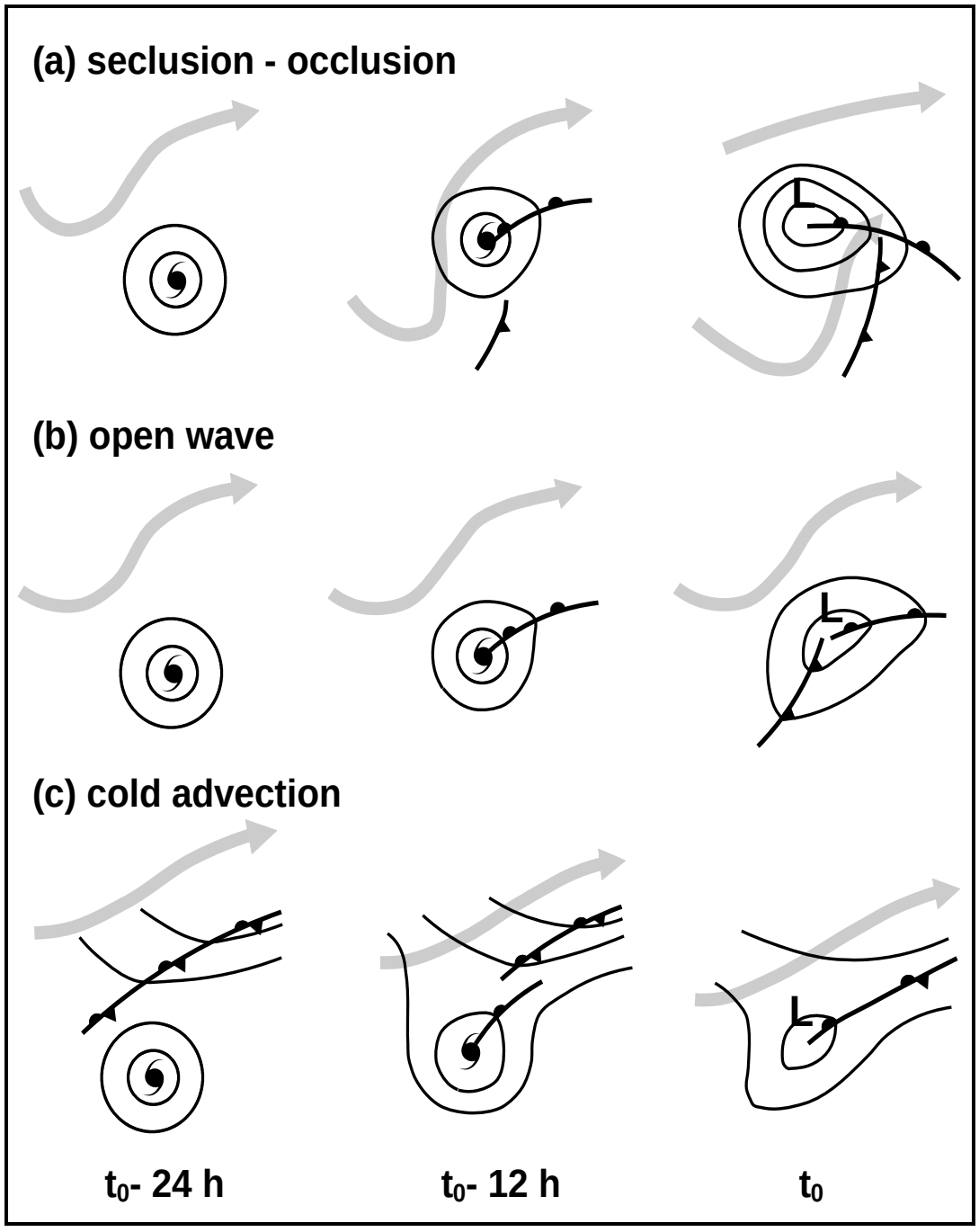

Fig. 1.1. The three different class schemes (SO, OW, and CA) used to classify the transition from TS to PTC under large-scale synoptic conditions. Developed from Kitabatake (2008).

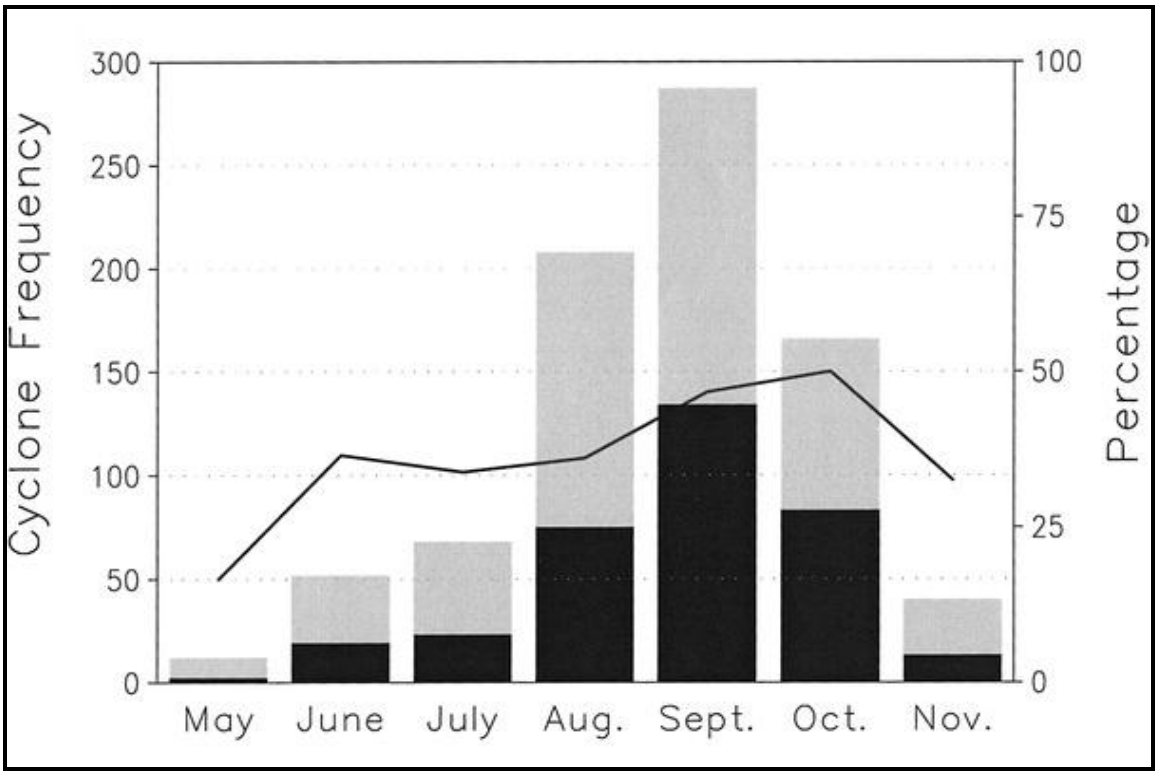

Fig. 1.2. Monthly frequency and distribution of all TSs (light shading) and PTCs (dark shading) that occurred from 1899-1996. The black line represents the percent of TSs classified as PTC during its lifecycle. From Hart and Evans (2001).

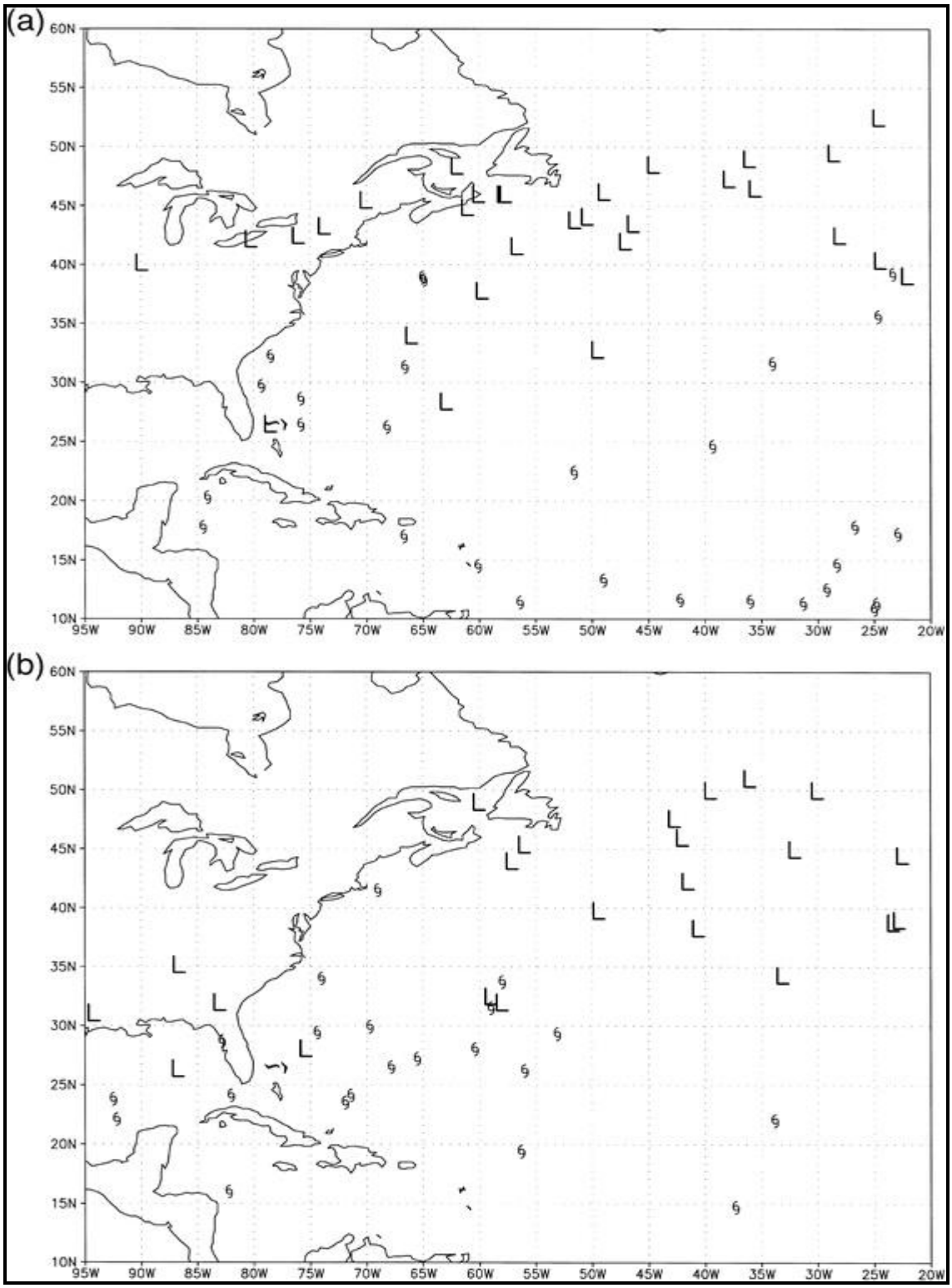

Fig. 1.3. Formation (§) and transition (L) locations of evolving PTCs based on NHC HURDAT dataset from 1978-1993. (a) PTC intensification and (b) decay of transitioning TSs. From Hart and Evans (2001).

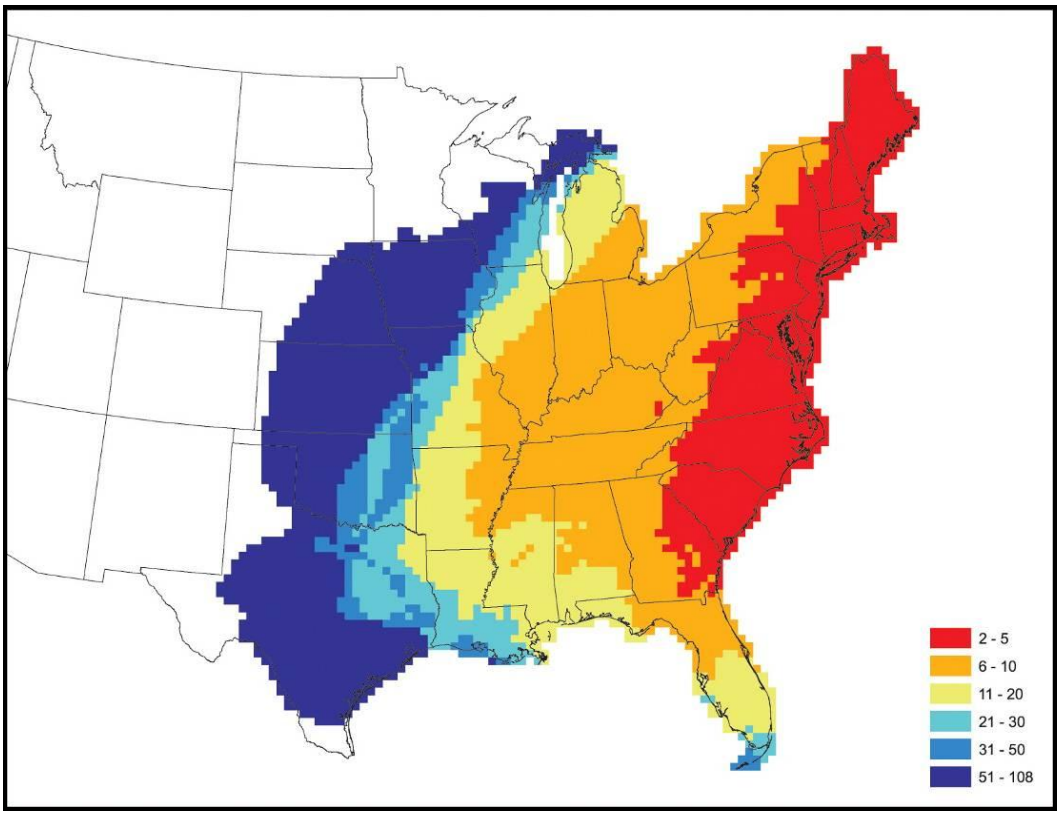

Fig. 1.4. Return intervals in years of PTC cyclones with 17.5 m s^{-1} wind that affected the U.S. From Kruk et al. (2010).

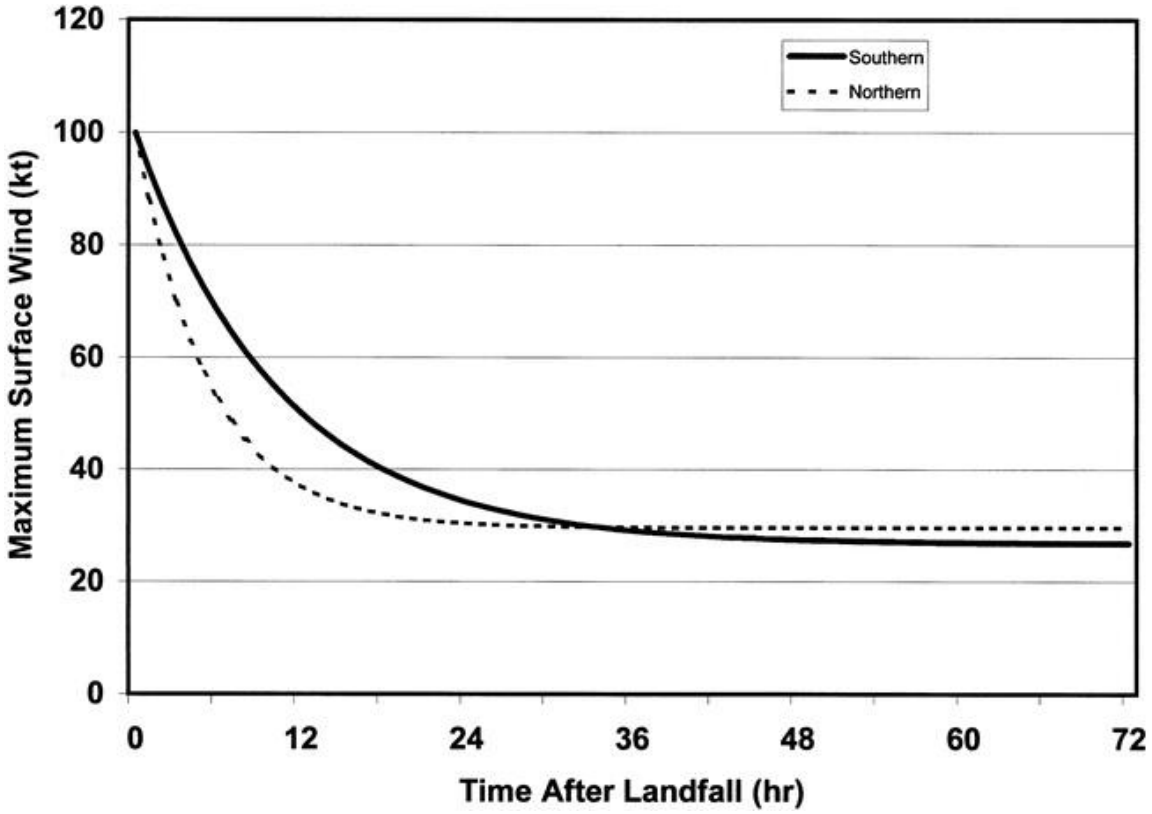

Fig. 1.5. Maximum surface winds as a function of time as the TS landfall based on latitudes [i.e., landfalls above (below) 37° N for northern (southern) storms]. From Kaplan and DeMaria (2001).

Table 1.1. Typical National Weather Service (NWS) high-wind criteria based on sustained and gust observations.

National Weather Service (NWS) High-Wind Criteria		
Criterion	**Speed**	**Duration**
Sustained	≥ 18 m s^{-1} (40 mph)	≥ 1 hour
Gust	≥ 26 m s^{-1} (58 mph)	For any duration

CHAPTER 2

A CLIMATOLOGY OF HIGH-WIND EVENTS ASSOCIATED WITH POST-TROPICAL CYCLONES IN THE UNITED STATES

2.1 Introduction

The Atlantic Ocean and Gulf of Mexico basins are prone to the timing, intensity, and variability of subtropical (STS) and tropical (TS) systems. In recent years, STSs and TSs have become monitored more not only by forecasters, but also local, state, federal governments, media and newspapers coverage and concerned citizens. Much of the resources and time is spent on tracking and predicting the initial landfall position of STSs or TSs as they approach the United States. After the cyclone makes direct landfall and moves into higher latitudes, the level of interest and focus starts to diminish, as well as the official warnings and reports to advise people about potential hazards (Jones et al. 2003). However, a decaying cyclone has been shown to retain the capability of producing hurricane strength winds, intense rainfall and flooding events, and large wave action to coastal and inland regions after landfall (Jones et al. 2003; Stoppkotte et al. 2009).

Recent hazard statistics show that high winds from TSs are capable of producing casualties and substantial storm damage to the U.S. Since 1940, the National Climatic Data Center's (NCDC) Storm Events online database recorded 3,311 casualties from TSs. Rappaport (2000) constructed a TS fatality climatology for the contiguous U.S. and found that 600 casualties were contributed by TSs from 1970-1999. A similar study performed by Czajkowski et al. (2011) analyzed 62 landfalling TSs between 1970 and 2007 and they found that 47% of all TS inland fatalities were contributed by their surface winds. Pielke

et al. (2008) showed that tropical cyclones have produced more than $1 trillion dollars in damages along U.S. coastal counties from 1900-2005. Interestingly, Pielke et al. (2008) also found that weak TSs (subtropical and tropical storms) contributed to 2% (21.8 billion dollars) of the total damages reported from the coastal study region. Therefore, understanding the characteristics of high winds associated with TSs and the affects they have on the U.S. is important.

2.2 Background

a. Post-Tropical Cyclones (PTCs)

Currently, a universally accepted definition of a PTC transition does not presently exist (Merrill 1993; Hart and Evans 2001; Jones et al. 2003). Governmental weather organizations, academic institutions, and private research groups have applied different techniques and methodologies to understand the evolution of PTCs. Previous studies have focused on the interaction between large-scale dynamic atmospheric conditions of mid-latitude weather systems with TSs conducive to PTC transition and development (Matano and Sekioka 1971; Harr and Elsberry 2000; Evans and Prater-Mayes 2004; McTaggart-Cowan et al. 2004; Agustí-Panareda 2008; Kitabatake 2008; Hulme and Martin 2009). However, the majority of those studies are limited on analyzing cyclones that remained over the ocean or have focused to particular storm events. An early study by Palmén (1958) found that potential energy from the atmosphere increased during the initial transition of Hurricane Hazel in 1954 to a PTC. Matano and Sekioka (1971) developed a classification scheme purely based only on surface pressure analyses for the western Pacific: complex and compound transitions. In the first type, a complex

transition occurs when a pre-existing mid-latitude front or trough interacts with a TS to create a new PTC along a frontal boundary. For the second type, a compound transition develops when an extratropical cyclone (ETC) encounters a TS and the warm-core system appears to transition to a PTC. A similar two step process was also used by Klein et al. (2000) to identified 30 PTC transitions over the western North Pacific from 1994-1998.

PTCs have been widely documented and studied in all oceanic and continental basins across the world, including southeast Indian (Foley and Hanstrum 1994), southwest Pacific (Sinclair 2002, 2004), western North Pacific (Sinclair 1993; Harr and Elsberry 2000; Harr et al. 2000; Klein et al. 2000; Ritchie and Elsberry 2002; Kitabatake 2002, 2008), and extensively in the North Atlantic (Hart and Evans 2003; Arnott el al. 2004; Evans and Prater-Mayes 2004; Hart et al. 2006; Evans and Hart 2008; Hulme and Martin 2009). A summary of our current understanding of PTC transition and their characteristics is well documented in Jones et al. (2003), and highlighted below.

Numerous studies have suggested that rapid intensification or decay of PTCs is dependent on the location and magnitude of ETC large-scale dynamics (Foley and Hanstrum 1994; Sinclair 2002, 2004; Hart and Evans 2003; Arnott et al. 2004). The spatial location and distribution of ETC genesis and tracking over North America are generally more confined to higher latitudes (> 45° N) during the early summer months, with greater frequency at lower latitudes (30° N-40° N) during the cooler season months (Reitan 1974; Whittaker and Horn 1984; Eichler and Higgins 2006; Wernil and Schwierz 2006; Ulbrich et al. 2009). The combination of maximum sea surface temperature (SST)

warming across the Atlantic Ocean basin and ETC tracks enhanced PTCs development at higher latitudes (≥ 40° N) during the peak hurricane season (Evans and Hart 2003).

The interaction between ETCs and TSs can cause various conditions to occur within both system types. Kitabatake (2008) examined how the strength and magnitude of different baroclinic conditions (i.e., lower-tropospheric equivalent potential temperatures) and characteristics of TSs can influence the large-scale dynamic structure of a PTC in the western North Pacific basin. In that study, the evolution of PTCs are described with three classification types: cold air (CA), seclusion-occlusion (SO) and open-wave (OW) frontal cyclones. Kitabatake (2008) found during the two-year period that 35% of all PTCs underwent SO development, 12% were absorbed by CA frontal passages, and the remaining 53% (12) TSs were classified as OW cyclones (i.e., the combination of SO and CA characteristics). However, previous research by Ritchie and Elsberry (2002) found that even with the change in magnitude of the mid-latitude trough, the final intensity of the TS as its transitions to PTC was not as dependent on the strength of the mid-latitude trough.

Large-scale atmospheric influences, including baroclinicity, play a fundamental role in determining the strength and magnitude of PTC surface winds (Bosart and Bartlo 1991; Klein et al. 2000; Evans and Hart 2003; Hart 2003; Jones et al. 2003). Bosart and Bartlo (1991) analyzed large-scale conditions associated with the initial evolution of TS Diane (September 1984) in a baroclinic environment. In this case, the TS developed from a baroclinic cyclone which was initially driven by an upper-level trough.

Hart (2003) constructed a three-dimensional cyclone phase space (CPS) model using storm-relative-relative thick asymmetry and thermal wind gradients to understand

the large-scale structural evolution of TSs. Using an equivalent CPS method, Evans and Hart (2003) identified the initiation and completion of 61 PTC transitions from 1979-1993. As of result, Evans and Hart (2003) found that the onset of PTC transition began when the sustained thickness asymmetry (β) is > 10 m between the pressure levels of 900-600 hPa. The transition is defined as "complete" when the vertical storm structure corresponds to a cold-core vortex resulting in a positive thermal wind ($-V_T^L < 0$) (Evans and Hart 2003).

b. High-Wind Characteristics

Kaplan and DeMaria (1995) documented the decay rate of the TS winds is dependent on the intensity and forward motion speed of the cyclone. As of result, Kaplan and DeMaria (2001) found that cyclones that make landfall above (below) 37° N tend to have surface winds that decay more (less) rapidly when the velocity was greater (less) than 17 m s^{-1}. The tendency for TSs to maintain stronger winds for longer durations is based on several critical factors: physiographic and topographic landscape (in the case, of the New England coastline), influence of the baroclinic environment, and the possible dynamic changes that occur when the cyclone is transitioning to PTC classification (Kaplan and DeMaria 2001).

Recent studies have examined large-scale dynamics to help explain both nonconvective and convective high-wind characteristics for the U.S. Knox et al. (2011) illustrated that four mechanisms (topography, isallobaric wind, tropopause folds, and sting jets) have been used to explain the development of nonconvective high-wind events (NCWEs). Similarly, Durkee et al. (2011) applied ageostrophic wind theory to determine

that isallobaric winds, friction, horizontal, and vertical advection were all important contributors in the NCWEs over the Great Lakes region during 12-13 November 2003.

Convective high-wind events (CWEs) are primarily the result of downdrafts. The outflow of downdraft air from thunderstorms is an important phenomenon in understanding convective dynamics. Wakimoto (2001) described that diabatic cooling and microphysics of the descending precipitation, along with negative buoyancy of the air parcel are key components of producing a strong downdraft to occur at the surface of Earth. In addition, condensate loading and downward drag from descending precipitation can also contribute to the initiation of downdrafts (Wakimoto 2001). Numerical models showed that the maintenance of a downdraft by falling precipitation is a function of the drop size, rain intensity, lapse rate, and downdraft velocities (Kamburova and Ludlam 1966; Srivastava 1985).

c. High-Wind Hazards

Other TS and PTC research has shown that these intense systems are capable of producing a variety of hazards outcomes damaging winds, (e.g., flooding rains, tornadoes, and storm surge that impact human society on an annual basis (Jones et al. 2003). Rappaport (2000) found that TS surface winds were the second (12%) leading cause of death from Atlantic TSs during 1970-1999 in the U.S. This result demonstrates that inland counties and regions can be affected by TS winds. Since 1970, 35 deaths have been attributed from winds that reach inland counties, and 10% of those fatalities were caused from falling trees (Rappaport 2000). In addition, Ashley and Black (2008) determined that nearly 80% of all wind-related fatalities during the 1980-2005 for the

conterminous U.S. were caused by ETC- related winds. Ashley and Black (2008) also found that deaths from winds associated with TSs caused the lowest number of deaths (181) compared to tornadic, thunderstorm, and nonconvective wind-relative deaths. In another study, Schmidlin (2009) determined that 31% of casualties caused from all TSs from 1995-2007 [excluding Hurricane Katrina (2005)] were caused by fallen trees that were located within 320 km of the U.S. coastline.

The impacts from PTC winds can be even more costly and deadly than a TS or ETC (Jones et al. 2003). Hurricane Ike (2008) is an example of a TS that transitioned to a PTC and strengthen to produce hurricane-force strength winds ($\geq$ 33 m s^{-1}) across portions of the Ohio River Valley and Mid-South regions. "PTC Ike" left behind 12 fatalities, forced over three million people to lose their electricity, and an estimated damage of $1.5 billion dollars to the area (NWS 2008; Stoppkotte et al. 2009). In another example, the "Perfect Storm" of 1991 demonstrated that PTCs are capable of producing strong winds to coastal and inland regions without making landfall (NCDC 1991; Corderia and Bosart 2010). The interaction of three ETCs, remnants of Hurricane Grace, and large-scale atmospheric conditions (e.g., downstream baroclinic development, and a negative Pacific-North American (PNA) index) produced a PTC that caused high winds to occur along the U.S. eastern coastline, with gusts ranging from 15 to 33 m s^{-1}. These intense storms persisted for over a week and caused an estimated damage of over $300 million dollars to the region (NCDC 1991; Corderia and Bosart 2010). Regardless, a fundamental and climatological understanding of PTCs and resultant high winds across the eastern U.S. has yet to be established.

The purpose of this study is to provide a climatological description of the spatial and physical characteristics of high winds associated with PTC Atlantic systems during 1951-2009. The period of record was chosen based on the accuracies of TS observation data (surface winds). Prior to routine reconnaissance flights into TSs in 1944, TS intensities and surface winds were strictly based on ship or coastal station observations (Landsea 1993). In addition, Landsea (1993) also suggested that TSs could have been omitted or were not detected prior to the use of satellite and post-aircraft eras. Results from this study provide a more comprehensive understanding of PTCs and the evolution of surface high winds as they transition from warm-core to cold-core ETCs.

2.3 Data and Methodology

In this study, various methods and techniques were used to understand the surface wind characteristics of PTCs. HURDAT, a hurricane dataset provided by NHC (Jarvinen et al. 1984) was utilized to first identify all TSs. Secondly, hourly wind observations from the NCDC were used to select only reports that followed NWS high-wind criteria. Geographical Information Systems (GIS) software was used to spatially analyze these datasets. In the end, only those systems that became classified as PTCs and exhibited high-wind observations were examined. A summary of the data and methods used over the U.S. in this study is described below and shown in Fig. 2.1.

a. PTC Identification

In this study, all TSs that were characterized as subtropical or tropical (i.e., systems that were tropical depression intensity or greater) by the NHC were considered.

A STS is defined as a non-frontal low pressure system that displays both tropical and extratropical characteristics, with an upper-low level cold circulation. STSs contain a maximum sustained wind radius of at least 160 km from the center (NHC, 2010). A tropical depression is classified as a warm-core non-frontal synoptic cyclone that originates over tropical or subtropical water and displays a closed surface wind circulation about a defined center with a maximum speed of 17 m s^{-1} (NHC, 2010).

HURDAT dataset was used to determine the tracks and intensities of North Atlantic STSs and TSs for the study period of 1951-2009. Each STS or TS track contained in the database is comprised of six hourly observations (0000, 0600, 1200, and 1800 UTC), longitude, latitude, maximum sustained wind, categorical strength based on Saffir-Simpson Hurricane Scale (SSHS), central surface pressure, and date as classified by the NHC (Table 2.2). The record for each storm starts at its origin and is continually monitored and tracked until the system does not poise threat to land or passes north of 40° N (Hart and Evans 2001). The declaration of transition to PTC is arrived through subjective examination by the NHC from the following factors: asymmetries in cloud structure, a loss of deep convection (< -50° C), an outward expansion of gale force winds, and/or disappearance of upper level clouds analyze from satellite imagery (J. Franklin, personal communication).

From the HURDAT dataset, PTCs included in this study were analyzed using GIS software. First, each six hourly observation for every North Atlantic TS (i.e., remnant lows, subtropical depression, subtropical storms, tropical depressions, tropical storms, and hurricanes) during the study period were plotted. A line segment tool was used to consolidate and merge each data point into a continuous track for each storm based on

unique identification number. Spatial location queries were performed to select only those TSs and STSs transitioned to a PTC according to HURDAT and where the cyclone's center made direct U.S. landfall and after.

PTCs that indirectly impact the continental U.S. without landfall can still affect sensible weather conditions inland. Ho et al. (1987) found that TSs within 275 km of landfall can have outer precipitation bands that reach inland of the U.S. coastline. To account for this possibility, a buffer surrounding the storm track of each event was constructed to determine the PTC systems that potentially had an inland impact from its surface wind circulation. The method of creating and using wind radii to estimate the surface wind distributions of PTCs was described by Kruk et al. (2010). In the study, Kruk et al. (2010) developed wind radii buffers and used them to determine the frequency distribution and return intervals for inland PTC, tropical storm, and hurricane-force winds impacting the U.S.

The extended best track dataset by Demuth et al. (2006) was used to average the distance for each maximum extent of winds threshold of 17.5, 25.7, and 32.9 $m\ s^{-1}$ for each quadrant surrounding the system and categorical strength (i.e., based on Saffir-Simpson Scale) that were within 275 km of landfall (see Kruk et al. 2010 for more detail). Next, the two upstream and two downstream quadrants (relative to the major axis and relative motion of the system) were merged into two, upstream and downstream flanks, respectively. The results of this conversion are found in table 2.3. The final step was to apply the buffers to all TSs and STSs within the HURDAT dataset (e.g., see Fig. 2.2). Fig. 2.3 shows the resulting 76 PTCs observed in this study for potential high-wind observations.

b. High-Wind Observations

All high-wind observations (Table 2.1) were collected from hourly surface wind data from the Climate Data Online (CDO) provided by NCDC (data available at: http://cdo.ncdc.noaa.gov/CDO/cdo). The high-wind dataset used in the current study consists of quality-controlled weather observations of 331 first-order stations for the eastern U.S (Fig. 2.4). DeGaetano (1997) analyzed the quality of hourly wind and directional data for 41 northeastern U.S. first-order stations and found that < 0.1% of the records failed the quality control test (i.e., removal of excessive wind variability and inaccurate wind observations). However, Lacke et al. (2007) highlighted that one drawback from using the NCDC CDO archive was non-accumulated and/or missing data. Therefore, in order to be considered for this study, each station must have contained wind observations for at least 70% of the study period (1951-2009).

Another concern was that a majority of stations had their instruments moved to another site or changed their measurement heights. Most of the instruments moved during the 1960's were removed from building rooftops and relocated to ground surface locations. Further, weather stations that had their anemometers repositioned from the height of 6.1 m to 10 m did this to meet the wind height standard set by the World Meteorological Organization (WMO). Lacke et al. (2007) also found that anemometer heights were not standardized between 1950's and 1960's during their high-wind climatology of the Great Lakes during 1951-1995.

After all high-wind observations were collected, the dataset was classified into two types: convective and nonconvective high-wind events. Following Lacke et al. (2007), the "present weather" data field within the NCDC CDO archive was used to

differentiate convective and nonconvective wind observations within PTC storm tracks. In this case, CWE was defined as any thunderstorm, lightning, hail, or tornado report that was observed during an hourly aviation report. Any other weather type (i.e.,, blowing snow, dust and sand storms, fog, mist, etc) that did not meet the above criteria was recognized as a NCWE (Lacke et al. 2007). Each report was further inspected for erroneous or questionable observations (e.g., a station observed a wind speed = 0 but records a wind direction ≠ 0) as indicated by the NCDC metadata guidelines and was otherwise removed.

c. PTC High-Wind Events (PTC-HWEs)

The final step was to determine high-wind observations attributed to PTCs. A spatial query equation was used to determine both NWS high-wind criteria (see Table 2.1) for all wind reports from each station during the period of record. After identifying these observations, a second query was used to filter high-wind observations into two groups based on NCWE and CWE classifications. Next, the HURDAT and high-wind datasets were examined together to select only those observations that were located within PTC wind radii buffers. To do this, a third spatial query filtered time(s) and date(s) that each cyclone was classified as PTC by the NHC. Lastly, any outlying hourly observations that did not fulfill the wind radii buffers or could not be verified were removed from the dataset. Fig. 2.5 shows the final results of this process, for the case of "PTC Ike (2008)".

2.4 Results

a. PTC Climatology

Out of 635 TSs, 47% (301) transitioned to a PTC as defined by NHC during the 59-year study period (Fig. 2.6). PTC transition has been relatively consistent through the entire study period even though a recent increase in TS activity over the last two decades (Fig. 2.7a). An independent sample t-test showed that the only significant differences in PTC and TS frequencies existed during the last two decades (i.e., 1990s and 2000s) when compared to the rest of the record (Table 2.4). The peak monthly frequencies of PTCs occurred in September (116) and October (76) (Fig. 2.7b), which is a likely consequence of peak TS activity during that time. However, more than 50% of all TSs in September and October transition to a PTC, which may also be connected to mid-latitude wave cyclone interaction during the seasonal transition period. These findings are supported by the Hart and Evans (2001) study, which found an increase in PTC transition probability during these peak months of the North Atlantic hurricane season. However, a greater proportion of PTCs was established in this study when compared to Hart and Evans (2001), likely due to a longer study period in that study and smaller number of TSs observed in this study. Regardless, both studies show that the frequency distribution of PTCs that affect the U.S. is typical of the seasonal frequency pattern of TSs in the Atlantic basin.

Overall, 80% of all PTC transitions occur above 35˚ N. Roughly one-third of all PTCs developed between 41˚-45˚ N. Fig. 2.8 shows that PTCs tend to develop at higher (lower) latitudes during the early (later) months of TS activity over the Atlantic basin. It also showed that PTC transition variability is most prominent during September, the

typical peak of TS activity. The key factors that have been shown to influence PTC transitions are primarily attributed to baroclinic growth and instability, vertical shear, increased Coriolis effect at higher latitudes, along with the slow warming SSTs of the Atlantic Ocean (Hart and Evans 2001; Jones et al. 2003).

During the study period, 205 TSs have made direct landfall over the U.S. The highest number of observations occurred in Florida (96), North Carolina (66), Georgia (53) and Texas (50). A steady decline in TSs is seen over the Midwest, Great Plains, and New England regions (Fig. 2.9a). Systems that arrived in these three regions are typically classified as PTCs. Interestingly, only 47 of the 205 TSs that made a direct landfall along the U.S. coastline transitioned to PTC. The highest number of PTC transitions occurs along the eastern U.S. seaboard (Fig 2.9b). A similar number of PTC frequencies were found along the southeastern U.S. which shows that PTCs usually migrate along equivalent paths across the Appalachian Mountains range from Georgia to Virginia. However, the greatest likelihood of receiving PTCs occurs in the Midwest, Mid-Atlantic and New England states and less likely to develop over the Gulf Coast and southeastern U.S.

The PTC transition frequencies are further supported by the migration and initiation of these systems. Fig. 2.10a shows that PTCs tend to develop primarily across the eastern U.S. with three maxima locations along the U.S. and Canadian coastlines and over Georgia and South Carolina. In addition, PTCs tend to migrate in a northeasterly direction along the U.S. coastline toward the Canadian providence of Nova Scotia (Fig. 2.10b). These findings are supported by Jones et al. (2003) which also found that TSs and PTCs track in a similar direction, especially above 30° N.

Overall, these findings show that PTC frequency patterns closely resemble tropical frequency patterns of Atlantic basin systems, particularly in September-November. Previous research determined that various atmospheric and oceanic conditions (e.g., SST gradients, baroclinic environments, and Coriolis parameter) can influence where PTC transitions can occur in the North Atlantic (Hart and Evans 2001; Jones et al. 2003). Results from this study indicate that coastal regions tend to experience more PTCs and are more favorable at higher latitudes, especially above 35° N.

b. Analysis of PTC-HWEs over the Eastern U.S.

1. Spatial and Temporal Analysis of High-Wind Observations

During 1951-2009, a cumulative total of 18,986 high-wind days were observed by the 331 first-order stations following the NWS high-wind criteria in Table 2.1. The greatest frequency of high-wind days occurred prior to the North Atlantic hurricane season, during the transition season of March (2,577) and April (2,517). The study found that 40% (7,703) of those high-wind day records were observed from June-November. These results indicate that seasonality differences in ETC development and track migration likely affect high-wind frequency.

As a result, this study shows that 76% (14,430) of all high-wind days were sustained winds. These sustained wind events (SWEs) typically occurred during the cool and transition seasons (January-April), with peak frequencies during March and April. Thereafter, a steady decline in SWEs occur until through August. The greatest distribution of SWEs days were located in a region that stretches from the Great Plains through Great Lakes region, and into the eastern U.S. seaboard (Fig. 2.11a and 2.11c).

While, the greatest cumulative gust wind events (GWEs) days were located across similar regions as the SWEs, GWEs exhibited a greater frequency along the Gulf Coast and were rarely observed over the New England and Tennessee Valley regions (Figs. 2.11b and 2.11d). As expected, the maximum frequency of all GWEs (51%) occurred during the peak convective, warm-season months of April-August.

Also in this study, NCWEs accounted for 82% of all high-wind days. Figs. 2.12a and 2.12c show that the regions with the greatest NCWE frequencies were the central Great Plains (Kansas and Oklahoma and Mid-Atlantic (from New Jersey to Massachusetts). The greatest (smallest) proportion of NCWEs was typically during the winter (summer) seasons. In comparison, the maximum number of all (70%) CWE days were observed during May-August. Figs. 2.12b and 2.12d show that the highest number of observed CWEs stretches from Great Plains states into the Upper Great Lakes, and along the Appalachian Mountains, while CWEs are irregularly seen in two distinct regions: New England and Mid-South.

2. Climatology of PTC-HWEs

During the 59-year study period, 76 of the 301 PTCs classified by the NHC were analyzed and examined for high-wind reports following the typical NWS high-wind criteria in Table 2.1. In this study, only 17 (22%) PTCs contained at least one high-wind observation (Table 2.5). Upon further inspection, PTC-HWEs only contributed 0.8% (270) high-wind reports and 0.6% (121) high-wind days to the entire dataset. Only a slight frequency increase (2%) was found when the complied high-wind dataset is limited to the typical North Atlantic hurricane season (June-November). Fig. 2.13 shows that the

highest frequency of high-wind reports produced by PTCs occurred during the peak of the hurricane season (September and October). In fact, 75% (203) of those reports were classified as high-wind events during these two months, which is expected given that the majority of by PTCs develop during that time. However, PTC-HWEs during the peak months of September and October only made up 5% of all high-wind observations across the eastern U.S. Overall, this study shows that while it is relatively uncommon for TSs to transition into PTC, the prosperity for PTCs to produce high winds is an even rarer occurrence.

In terms of the spatial distribution of PTC-HWEs, one can see that the highest frequencies occurred primarily over the Mid-Atlantic, New England, and Midwestern states (Fig. 2.14). Similarly, Kruk et al. (2010) used return intervals to show that the Carolinas northeastward through the New England states have the greatest likelihood of PTC surface winds ≥ 17.5 m s^{-1}. Previous work performed by Kaplan and DeMaria (2001) determined that baroclinic energy available at higher latitudes allowed PTCs to maintain higher wind speeds for longer durations when compared to TSs that made landfall below 37° N. The results from this study further support the previous work conducted by Kruk et al. (2010). The spatial distribution of PTC-HWEs is supported by the minimum number of high-wind events despite having higher frequencies of PTC landfalls along southeastern U.S. Fig. 2.15a shows that the primary axis of SWEs occurred along the eastern U.S., primarily from Virginia to Maine. TSs that make landfall and transition to PTCs along the Gulf of Mexico basin typically do not produce high winds. Hart and Evans (2001) found that TS landfalls along Gulf of Mexico coastlines dissipate more rapidly, preventing them to enter into a baroclinic environment

that can support PTC growth. The only exception to this finding was for PTC-GWEs, where a majority (52%) of all reports were associated with Hurricane Ike (2008) as it tracked over the Mid-South and Midwestern states (Fig. 2.15b).

Further examination of PTC-HWEs showed that 76% (206) were classified as SWEs and were attributed to 16 of the 76 PTCs examined during the study. Specifically, PTC-SWEs only accounted for 0.8% all high-wind observations. The highest SWE maxima occur during the early and late season months [June (27), September (39), and October (115)] of the season (see Fig. 2.13). Even with a decrease in the number of reports during the summer, these observations still only make up < 3% of each monthly cumulative frequency except October (~ 8%).

The study also showed that 78% of all SWEs in the PTC dataset were predominately observed from the southern cardinal flank, particularly out of the east-southeast and south-southwest directions (90°-270°) (Fig. 2.16a). A majority (55%) of the high-wind records that met the criteria were observed within 2 m s^{-1} of the minimal threshold values (Fig. 2.16b). In contrast, Lacke et al. (2007) demonstrated that the strongest winds associated with an ETC occurred along the western cardinal flank, in particularly a west-southwest preference. In addition, PTC-SWEs have two peak frequencies at 18 m s^{-1} and 20.5 m s^{-1}

In comparison, only eight PTCs were capable of producing 64 GWEs. It is possible that the relatively lower number of GWEs could be contributed to, in part, the lack of wind gust data available prior to the 1970's from the NCDC CDO (Lacke et al. 2007). However, given that the 64 PTC-HWEs occurred in only three months (September-November) of the hurricane season, perhaps another reason for the relatively

low PTC high-wind reports is due to the location of peak TS frequency and interacting with extratropical wave cyclones during the transition season. The frequency of these GWEs comprised of < 1% of all GWEs for the entire study region.

PTC-GWEs wind directions were mostly prevalently observed from northeasterly and southwesterly directions (Fig. 2.17a). In addition, a steady decrease in wind velocity is evident for GWEs, with 43% of all reports within 2 m s^{-1} of the gust threshold (Fig. 2.17b). Powell (1982) found that the strongest winds associated with TS are usually located on the right flank (specifically, front right quadrant) of the system. Similar results were found with landfalling PTC-HWE for this study. Over 87% (235) of all PTC-HWEs were located on the upstream flank of PTCs.

It is interesting to note that 98% (266) of all PTC-HWEs were classified as NCWEs. The highest NCWEs frequencies also occur during the months of September (84) and October (116). Furthermore, these findings reveal that PTCs irregularly produce CWEs that meet the high-wind criteria and follows the trend found in the previous section. Despite the fact, that one-quarter of all CWEs occurred along the coastal U.S. and over the months of the hurricane season.

The strength at its peak and initial landfall location, as well as the origin of TSs can indicate the likelihood of high-wind events associated with PTCs. TSs classified by the NHC as a "major hurricane" (category strength ≥ 3 according to the Saffir-Simpson Scale) during their peak magnitude were more likely to produce high-wind reports as they became PTCs (Fig 2.18). This is further evident upon the initial strength at landfall. Weak and disorganized landfalling systems such as STSs, PTCs, tropical depressions, and tropical storms irregularly produce PTC-HWEs (Fig. 2.19). Hart and Evans (2001)

showed that the origin of a TS can determine the strength and magnitude of a PTC before entering into a baroclinic or synoptic environment. In the current study, TSs that originated between 10°-15° N produced the highest frequency of high-wind reports (Fig. 2.20). Storms that form within this latitude band usually develop and intensify into major TSs within the Atlantic Ocean. In contrast, only 21% of all PTC-HWEs formed from storms that originally developed within the Gulf of Mexico and Caribbean basins (Fig. 2.21). These statistics indicate that most PTC-HWEs, while relative rare, arise from strong well-organized TSs deep within the Atlantic Ocean basin.

In summary, PTC-HWEs that met the NWS criteria are characterized as NCWEs. Results from the previous sub-section 1b showed that the greatest frequency of NCWEs occurred along eastern U.S. coast and Great Lakes region. However, it was also found that the lowest distribution of CWEs occurred over the northeastern U.S as well. Based on the migration and initiation of PTCs, it can be concluded that PTCs only produced NCWEs upon landfall over the eastern U.S. Finally, the study also revealed that the strength and origin of TSs can indicate the likelihood of high-wind events associated with PTCs. TSs that originated deep within the Atlantic Ocean basin are the most likely to produce high-wind events.

d. Reduction in NWS High-Wind Criteria for PTC-HWEs

This study showed that the capability for PTCs to produce high-wind observation is relatively rare. However, as with any strictly defined phenomenon, it is plausible to consider that the criteria used in this study is limiting the outcome of this analysis. In order to fully understand the strength of PTC surface winds, the NWS high-wind criteria

in Table 1.1 was relaxed (Table 2.6.). The relaxed criteria were based on the PTC standard deviations of both sustained (± 2.5 m s^{-1}) and gust (± 2.0 m s^{-1}) high-wind reports. Using these deviations, the original NWS high-wind criteria were set to the following wind velocities of: 10.5 m s^{-1} for sustained and 20 m s^{-1} for gusts. For this study, three standard deviations were used to account for any possible differences, while still maintaining a wind threshold above 10 m s^{-1}.

As of result, an additional 3,492 PTC high-wind records (3,093 PTC-SWEs and 399 PTC-GWEs) were observed (Table 2.7). In this study, 66% (50) of all PTCs produced SWEs while only 28% (21) produced GWEs. The highest monthly frequencies of both criterion occurred during September and October (Fig. 2.22). Specifically, 81% of all SWE and GWE observations were recorded during these two months. This agrees with earlier findings where most PTC-HWEs occur when the peak PTC development period is at its maximum during the Atlantic hurricane season. Out of 46 TSs, 32 transitioned to PTC, with high-wind observations during September and October under this revised scale. Despite lower frequency of PTC transitions during May-June, these events still produce more high-wind reports when compared to July and August.

Fig. 2.23a shows that nearly every state within the study area was affected by PTCs with SWEs. Two primary axes of SWEs were observed along the eastern U.S. coastline and the southern Great Lakes region. This high frequency of SWEs is likely due to ETC tracks at middle-to-higher latitudes. Another PTC-HWE maximum was found over the southeastern U.S. A considerable decrease in PTC-SWE reports is evident in the Great Plains and upper Great Lakes, and Gulf Coast regions. Kruk et al. (2010) stated that areas demonstrated a lesser likelihood of receiving PTC winds. Hart

and Evans (2001) explained that landfalling TSs along the Gulf of Mexico tend to dissipate before entering into a favorable baroclinic environment, in result not allowing PTC high winds to occur in these particular regions. In contrast, the distribution of PTC-GWEs is more confined to the Ohio Valley and eastern U.S. coastal regions (Fig. 2.23b). PTC-GWEs are less prominent and observed throughout the Gulf Coast and Great Plains regions. The unavailability of wind-gust data prior to the 1970's could be hindering the actual number of high-wind reports throughout the entire study area.

The contribution of NCWEs and CWEs produced by PTCs had similar results as found in the previous section. First, this study found that 99% of all simplified PTC-HWEs were classified as NCWEs under the new criteria**.** Moreover, 81% of all NCWEs were observed over the months of September and October. CWEs are uncommon and not are typically observed with landfalling PTCs**.**

Lastly, both adjusted high winds (sustained and gust), were typically located on the right flank of PTCs. Specifically, 60% of SWEs and 57% of GWEs were observed on the upstream flank of the migrating storm system. The primary wind direction for PTC-SWEs occurred from the northeast quadrant (0°-90°) with a secondary direction arising from southeast quadrant (90°-180°)(Fig. 2.24a). Furthermore, a similar wind preference is found for PTC-GWEs (Fig. 2.25a). Specifically, 46% of all GWEs observations were reported between 0°-90° and 31% observed from 180°-270°. These results concur with the findings found in the previous section that the strongest winds develop on the inflow side of TSs. These findings are supported by Powell (1982), which found that the strongest winds associated with landfalling TS are found in the front-right quadrant of the system. The analysis also revealed that the highest wind velocity frequencies for SWEs

and GWEs occur at the threshold minimums (Fig 2.24b and Fig. 2.25b). A sharp decline in frequency for both wind scales indicate that PTC usually produce wind speeds lower then required by the mandates set by the NWS. It was found that 63% of all SWEs and 58% of all GWEs were observed within 2 m s^{-1} of the revised wind scale.

2.5 Conclusions

The North Atlantic basin is a common place for intense TSs to develop. In recent years, a great deal of research has been focused understanding the dynamical changes that occur during the TSs transition to PTC, particularly at middle-to-higher latitudes. Understanding how TSs evolve as they enter into these baroclinic environments is important for forecasters. The ability to accurately forewarn and advise people of the possible hazards can help reduce the number of fatalities and damage costs for the areas affected by any PTCs. This study extends our knowledge on PTCs by focusing on cyclones that affected the U.S. and produced high winds, according to the typical NWS high-wind criteria.

HURDAT data was used to track and identify 301 TSs that transitioned to PTCs within the Atlantic and Gulf of Mexico basins during 1951-2009. Only 23% (76) of the 301 PTCs were analyzed for high winds that occurred over the eastern U.S. These systems typically start their transition to PTC classification between the latitudes of 41°-45° N and migrate in a northeasterly direction. Overall, 80% of all PTCs began their transition phase above 35° N. Hart and Evans (2001) found that the delay warming in SSTs of the Atlantic basin, ETC development, increase Coriolis parameter, and baroclinic instability are major contributors for PTC transitions to occur in higher latitudes. The

monthly frequency and distribution of PTC development suggests that the spatial location of baroclinic conditions and ETCs are critical to whether or not a TS will make the transition to a PTC. Specifically, the peak frequency of PTC transition occurs during the months of September and October with 60% of all TSs evolving to PTC status. These results are further supported by the work of Hart and Evans (2001) which found that 50% of all TSs became classified as PTC.

The results from this study also determined that it is uncommon for U.S. landfalling PTCs to produce high-wind events that meet the NWS high-wind criteria. Specifically, < 1% of all high-wind observations during 1951-2009 was contributed from PTCs during the study period. Therefore, this study shows that most of high winds within the U.S. are caused by other atmospheric phenomena and processes. Regardless of the low frequency, 98% of all PTC-HWEs were classified as sustained NCWEs. The nonconvective dominance may likely be due to the loss of deep convection and upper-level dynamical during the transition to PTC.

The maximum concentrations of PTC-HWEs were located over the Mid-Atlantic and New England regions or above 40° N. The migration and initiation of PTCs supports the findings of other high-wind observations across areas. In addition, the overall distribution of all high-wind observations showed that the highest concentrations of NCWEs occur along the northeastern seaboard, followed by the Great Plains and Midwest regions. In contrast, the lowest frequency of PTC-CWEs was found over northeastern U.S.

Next, the typical NWS high-wind scale was reduced to account for other PTC wind events that were omitted by the criteria. As a result, 3,492 of events were included,

but with similar findings. For example, the highest frequency of PTC-HWEs occurred during September and October. The distribution of high-wind events showed that nearly every state east of the Rockies was affected by a PTC. The largest number of PTC-HWEs was observed in the Mid-Atlantic, Midwest, and New England regions. In addition, the majority of high-wind observations (both sustained and gust) occurred from the upstream flank of the migrating PTC. Previous work has shown that the strongest winds associated with landfalling TS are found on the right flank (Powell, 1982). In comparison, Lacke et al. (2007) found that the tendency for NCWEs to occur from a southwest direction over the Great Lakes region is a result of mid-latitude cyclone dynamics. Durkee et al. (2011) concluded that isallobaric wind was the primary contributor of producing the November 2003 NCWE over the Great Lakes region as well. Finally, PTC wind velocities were most common near set the minimum threshold values of the adjusted wind speeds. These findings further demonstrate that the likelihood PTC to produce high winds based on the NWS definition is relatively rare and unexpected.

In conclusion, this thesis examined the high-wind climatology for landfalling PTCs over the U.S. during 1951-2009. Future work will focus on broadening the dataset to include all landfalling TSs. By doing so, forecasters may understand how TS wind fields change upon making landfall over the U.S. Other avenues of research would be to investigate PTC-HWEs for the providence of Nova Scotia. This assumption was made based on the migration and density of PTC observations that occur in this higher latitude region. In addition, current work is being conducted by Durkee et al. (forthcoming) on producing a comprehensive high-wind climatology for the eastern U.S. using this particular high-wind dataset. Further examination of high-wind observations may shed

light on the understanding of the dynamics and evolution of ETCs that occur over the U.S.

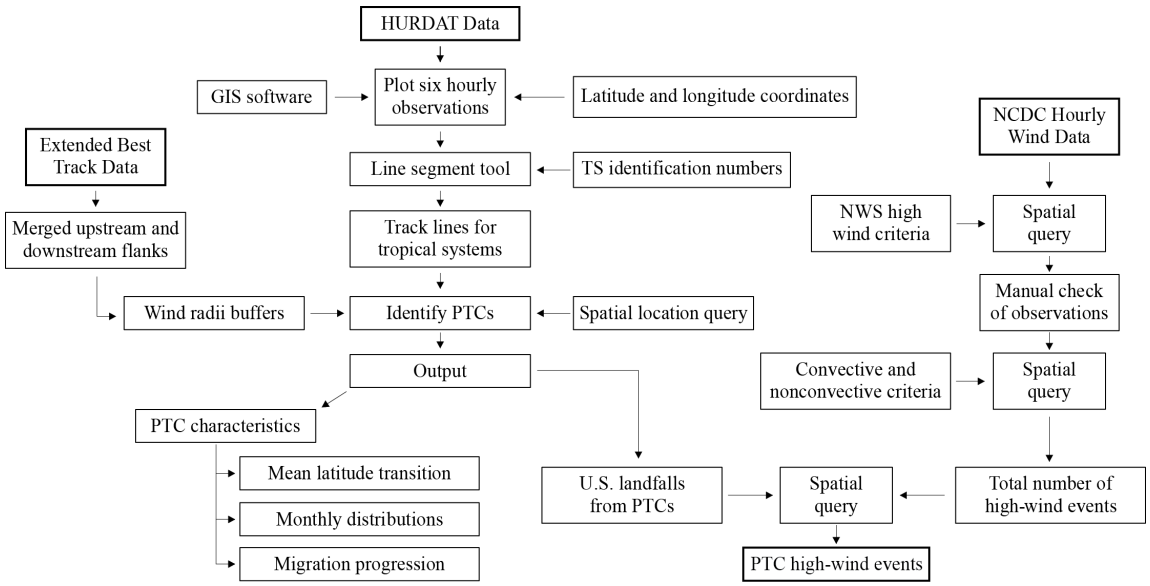

Fig. 2.1. A flow diagram demonstrating PTC and high-wind event identifying and tracking schemes.

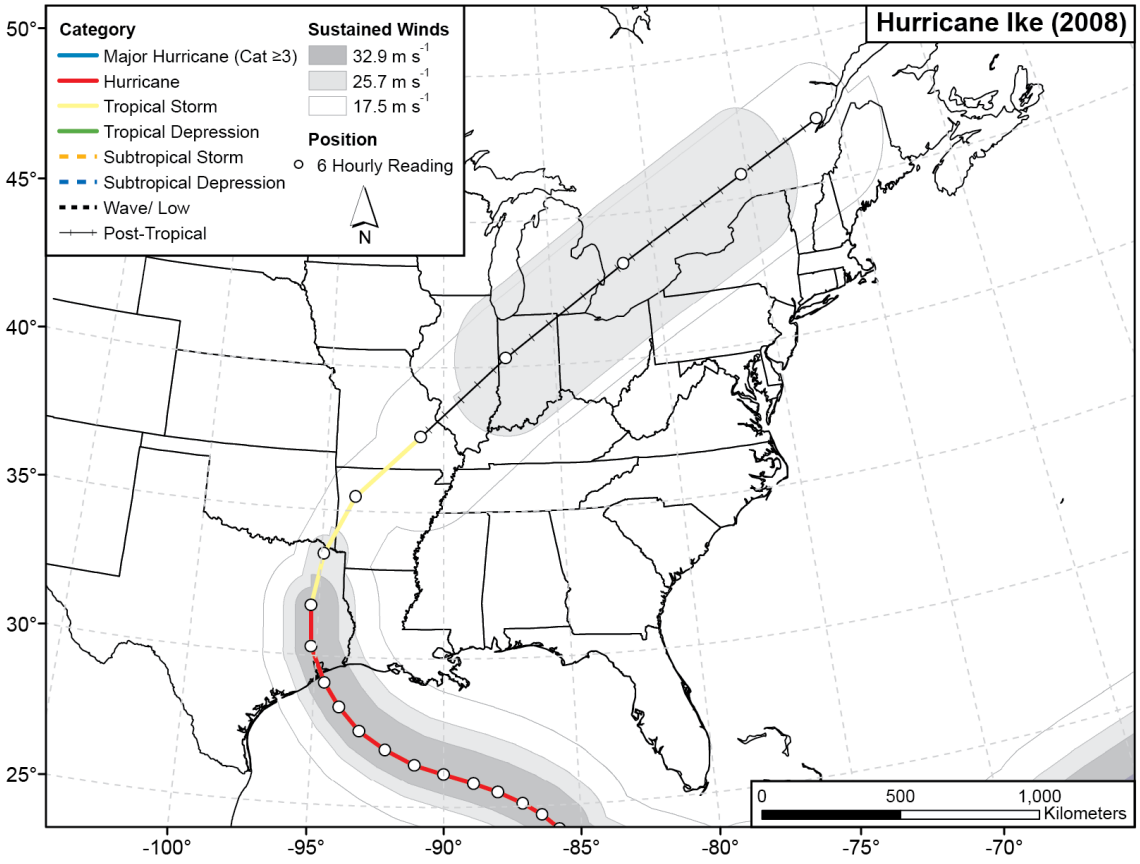

Fig. 2.2. Hurricane Ike (2008) landfall track based on six hourly observations and mean maximum extent of winds (MEW) 17.5, 25.7, and 32.9 m s^{-1} buffers.

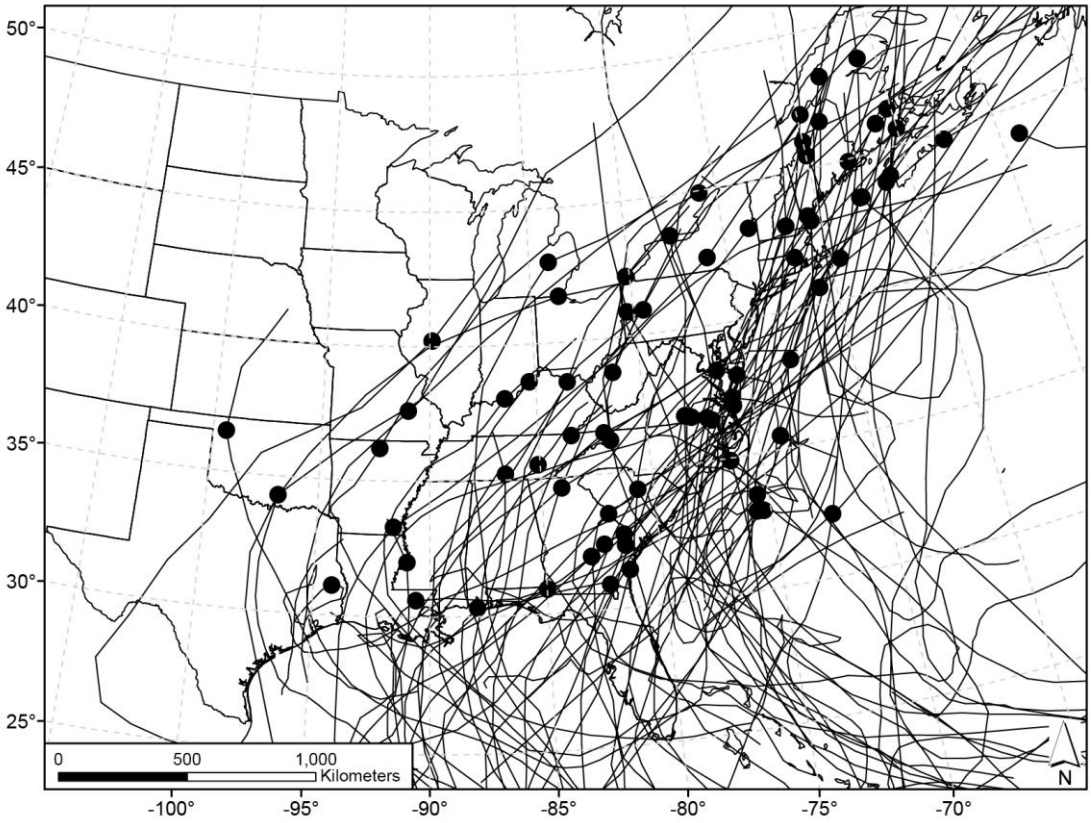

Fig. 2.3. Tracks of the 76 TSs analyzed for high-wind observations from 1951-2009. The black dot represents the point of PTC transition as defined by NHC.

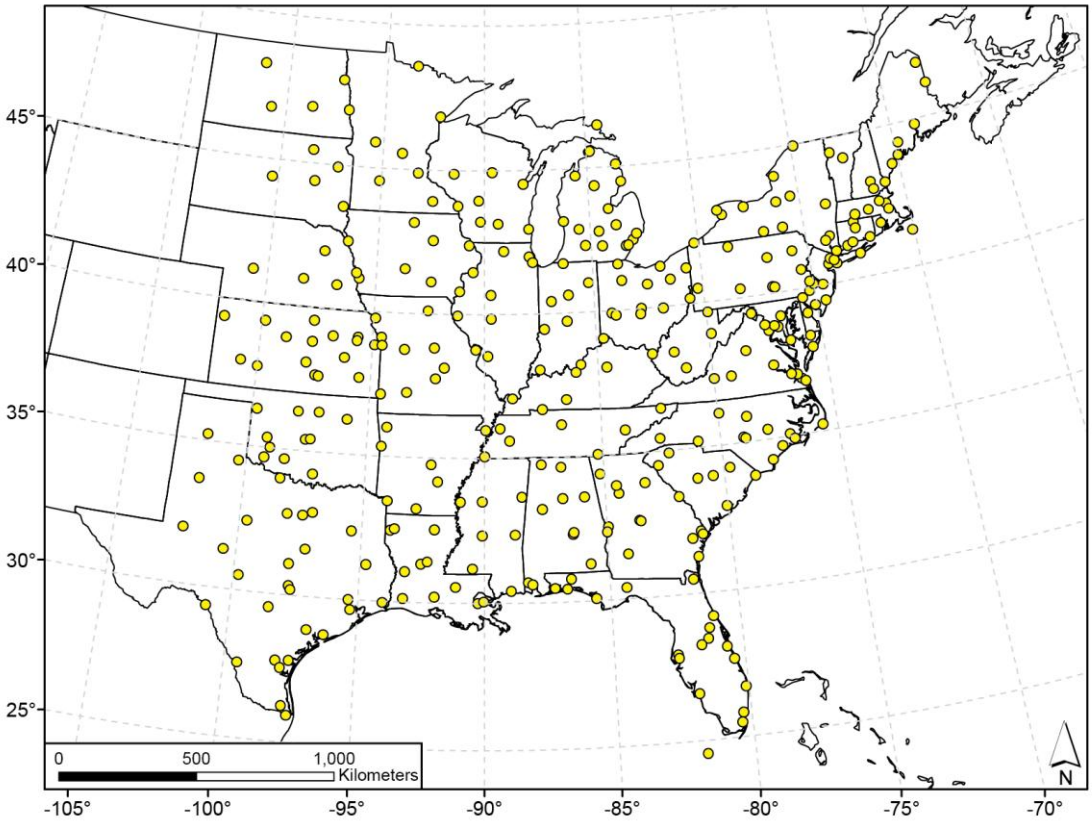

Fig. 2.4. The distribution of the 331 first-order stations used for the study region.

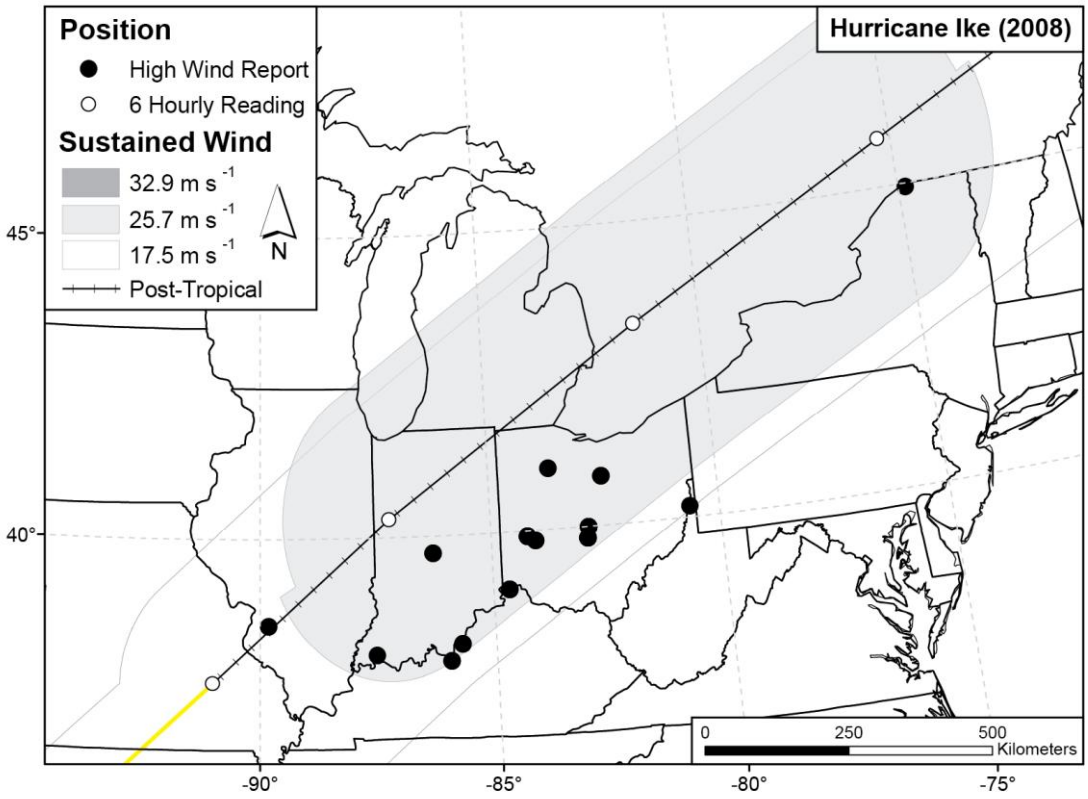

Fig. 2.5. High-wind reports observed from the first-order stations during the PTC phase of Hurricane Ike in 2008.

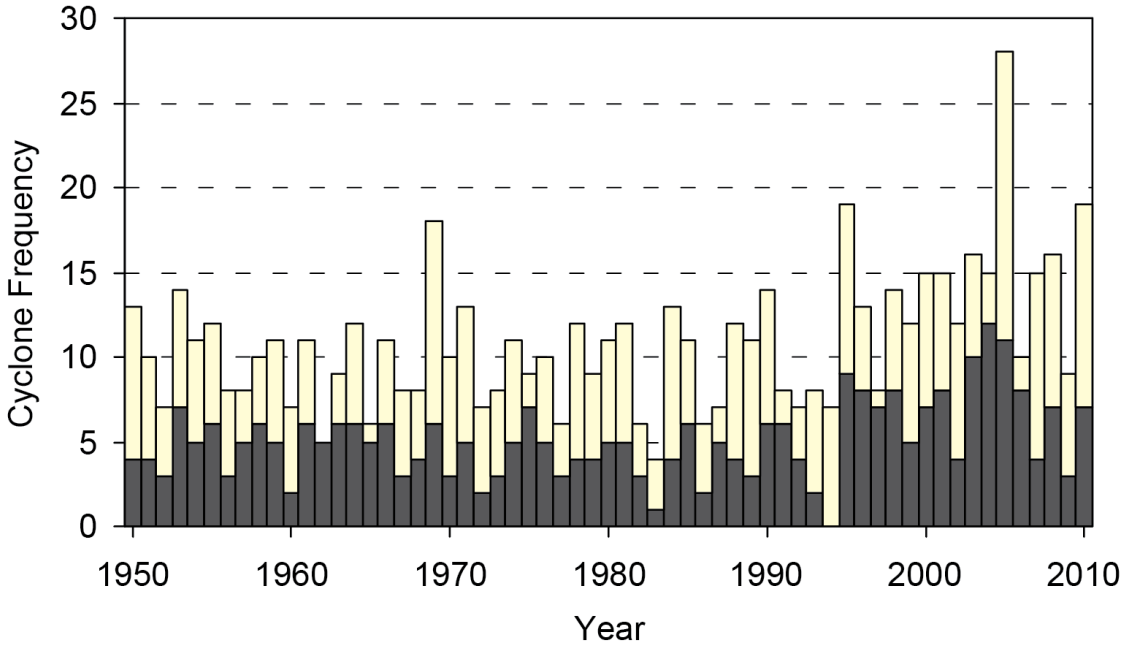

Fig. 2.6. The yearly distribution of TSs (tan) and PTCs (black) classified by the NHC from 1950-2010.

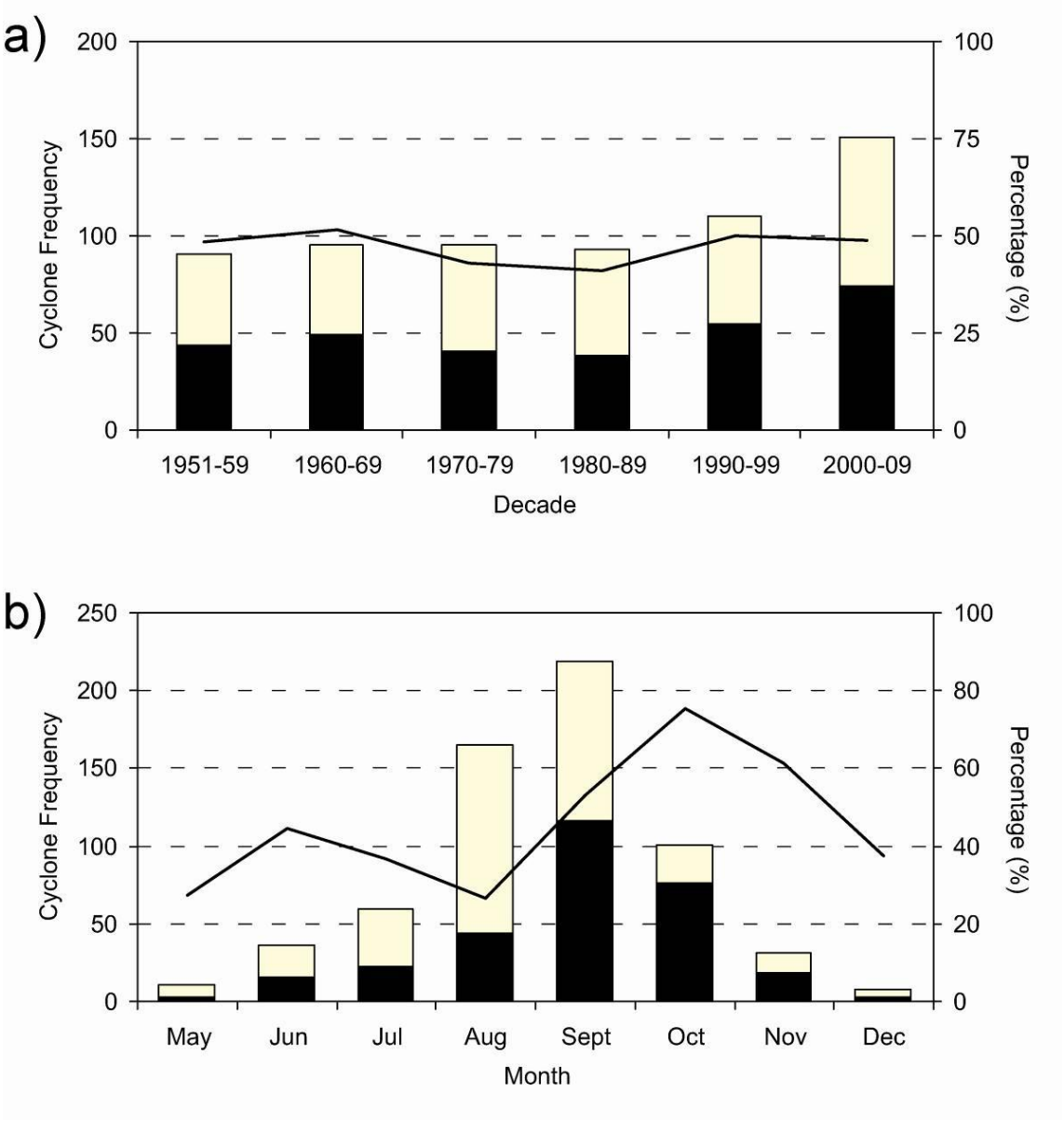

Fig. 2.7. The distribution of TSs (tan) and PTCs (black) by (a) decade and (b) monthly from 1951-2009. The black line represents the percent of TSs classified as PTC.

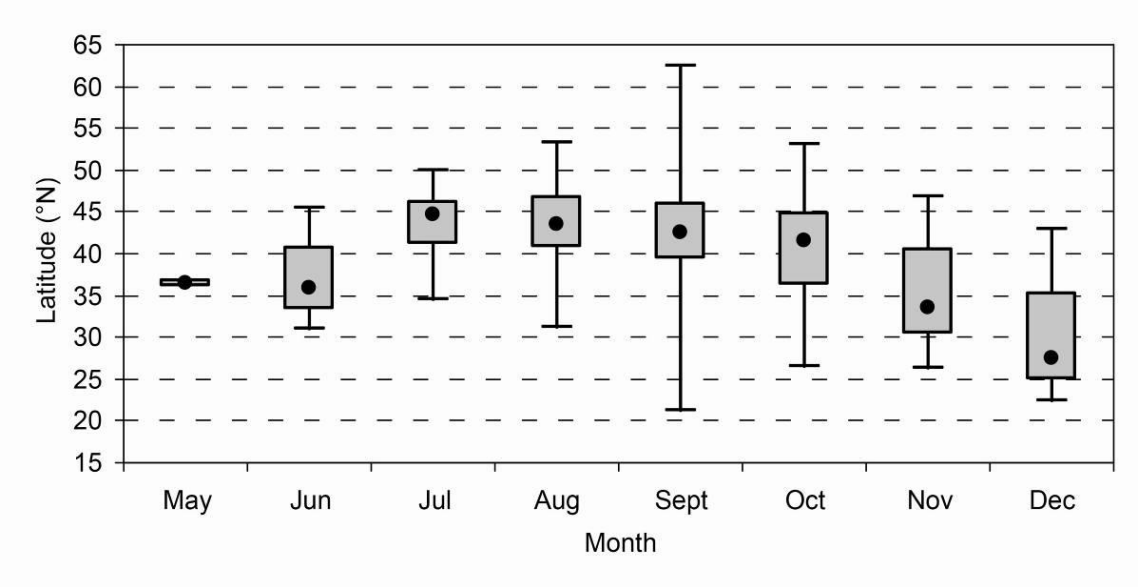

Fig. 2.8. Box plots of PTC transition locations May-December. A black circle represents the median latitude transition during each month.

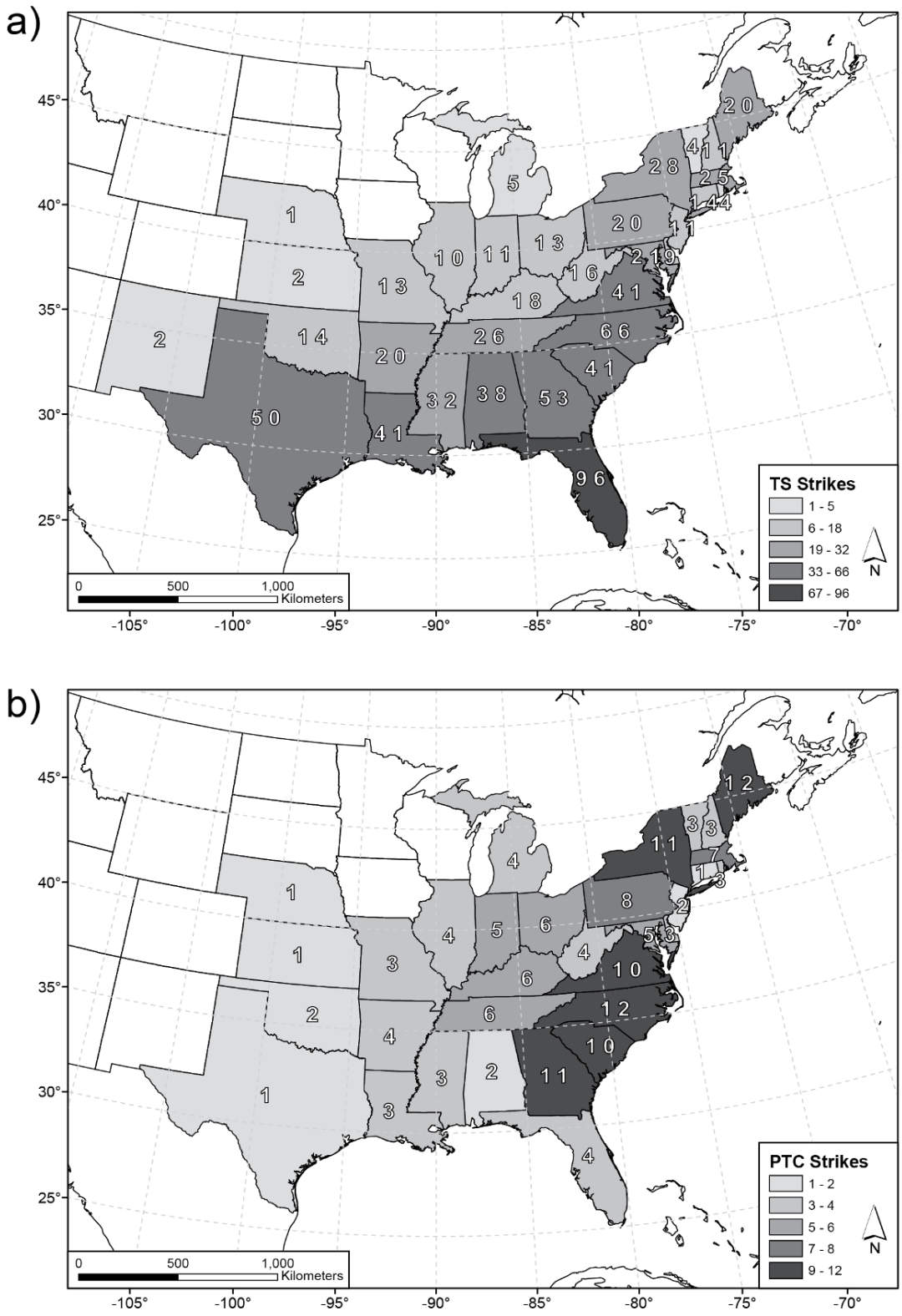

Fig. 2.9. Total number of (a) TSs and (b) PTCs observed by state.

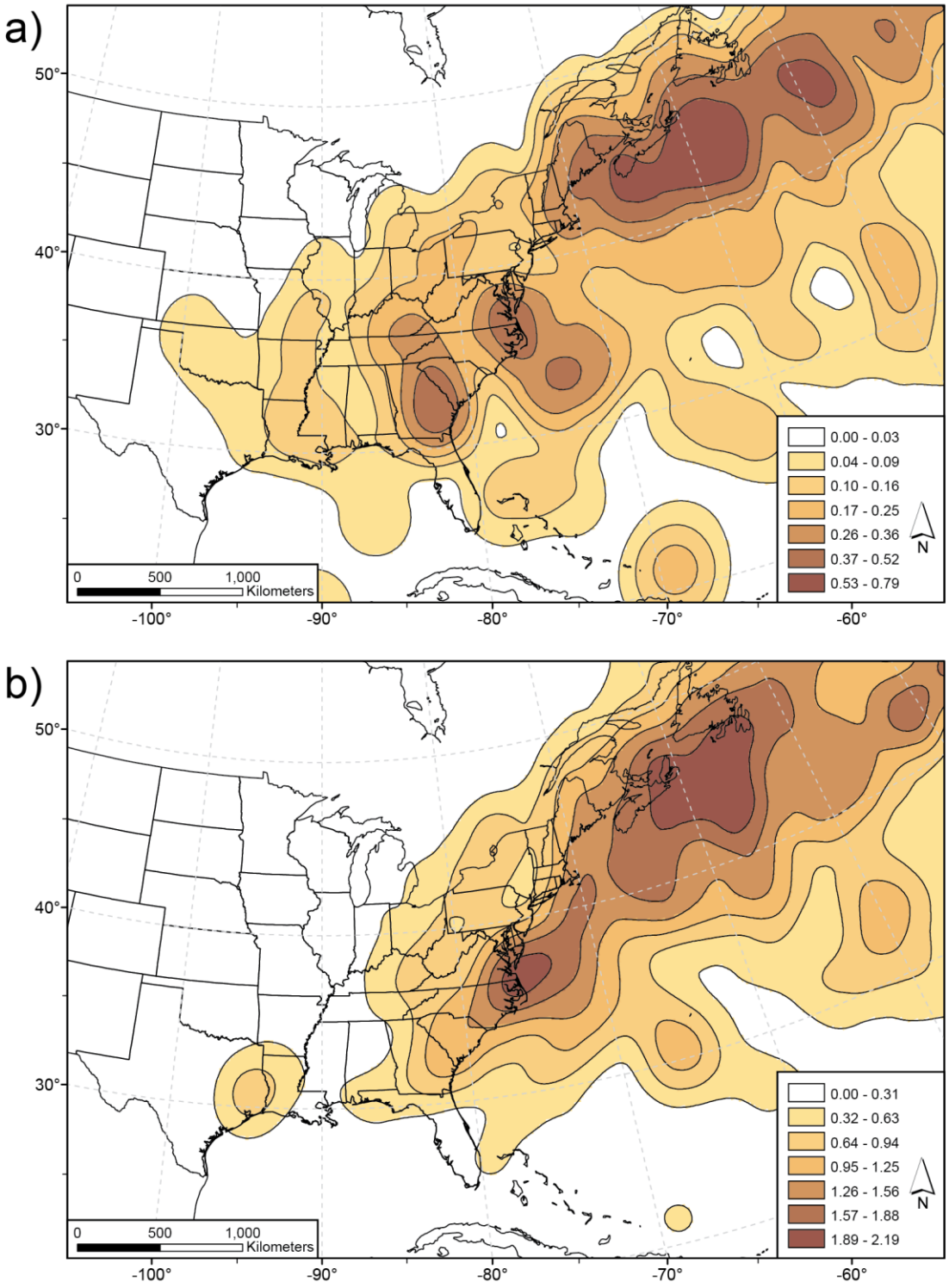

Fig. 2.10. Kernel density estimation plot of (a) PTC transitions and (b) all PTC observations.

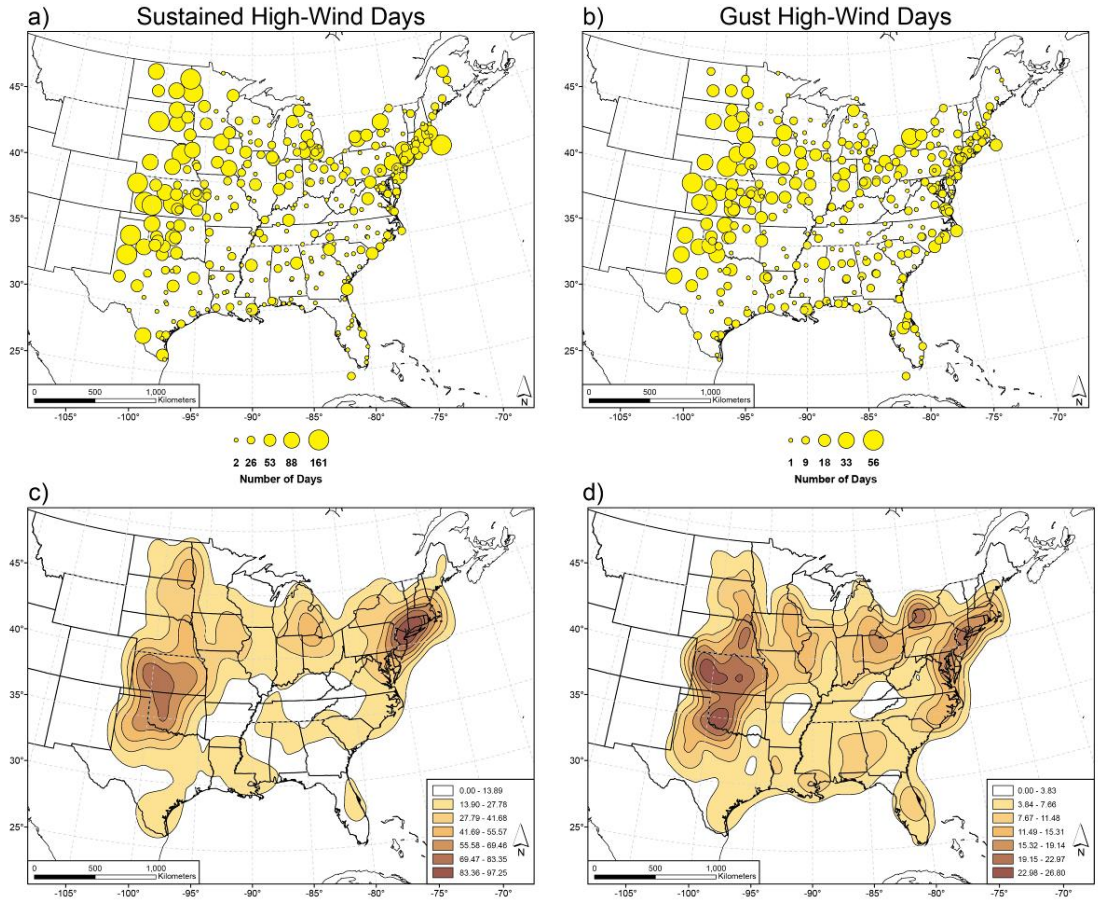

Fig. 2.11. The distribution of high-wind days and kernel density estimations for (a and c) SWEs and (b and d) GWEs.

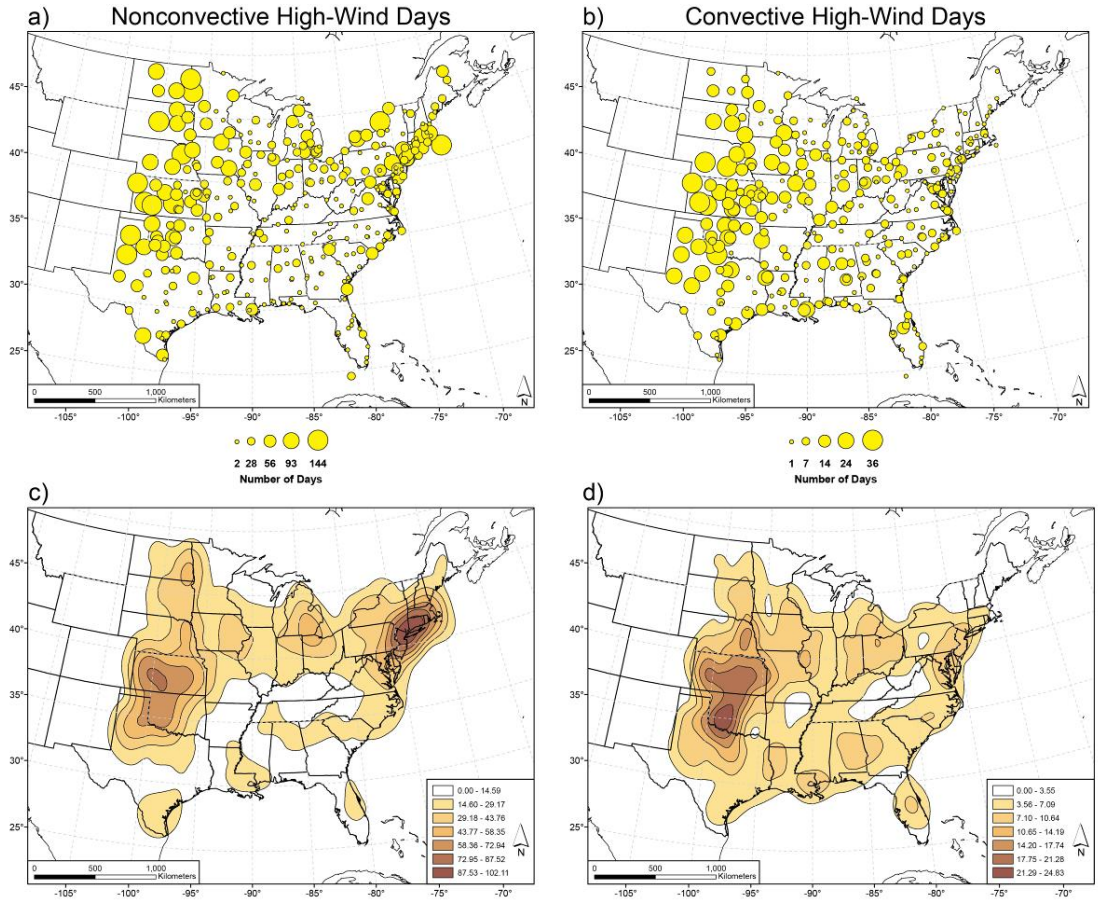

Fig. 2.12. As in Fig. 2.11 except for (a and c) NCWEs and (b and d) CWEs.

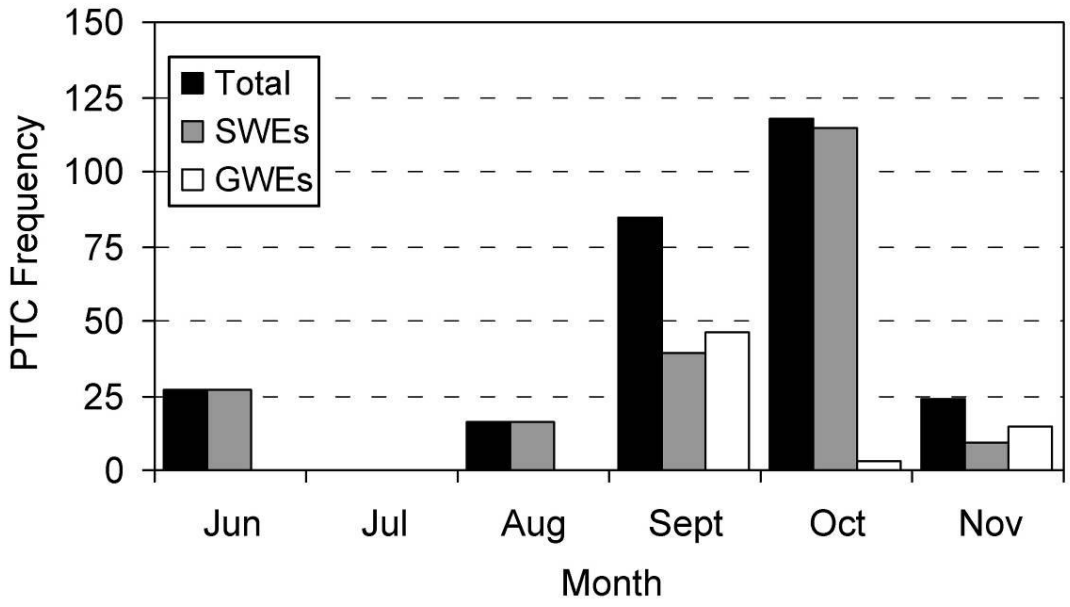

Fig. 2.13. The total monthly frequencies of PTC observations based on the typical NWS high-wind criteria for SWEs and GWEs.

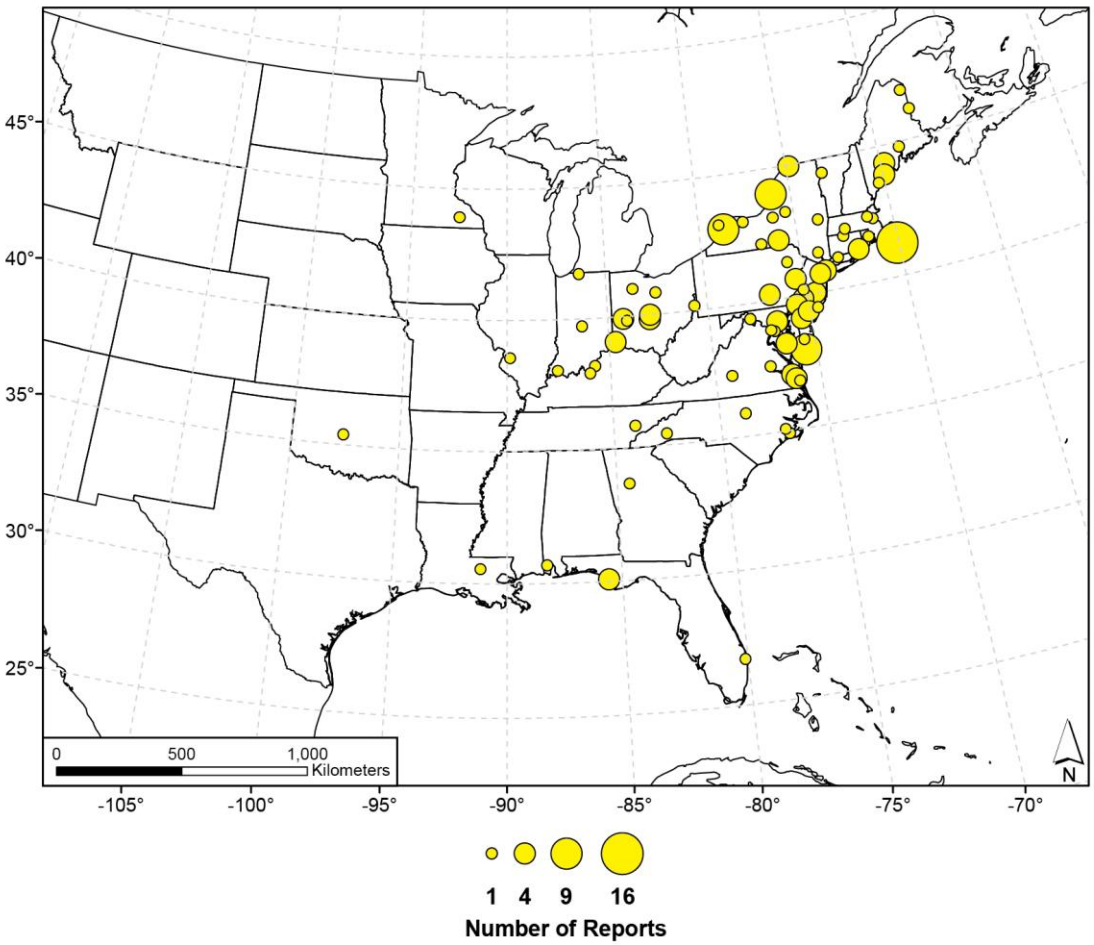

Fig. 2.14. The total distribution of high-wind observations contributed by PTCs based on the current NWS high-wind criteria.

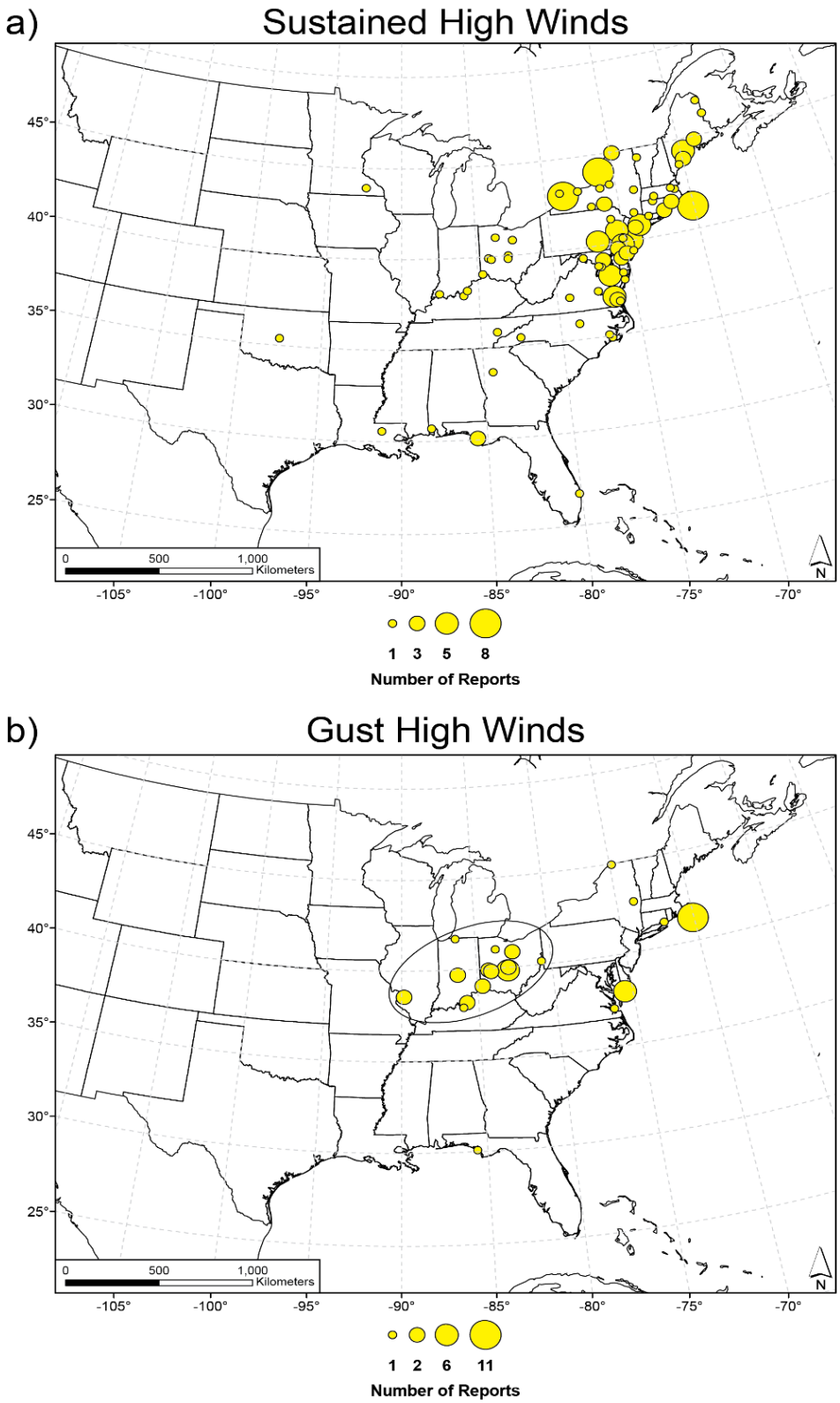

Fig. 2.15. As in Fig. 2.14 except for (a) sustained and (b) gust observations. Black oval shows high-wind reports from Hurricane Ike (2008).

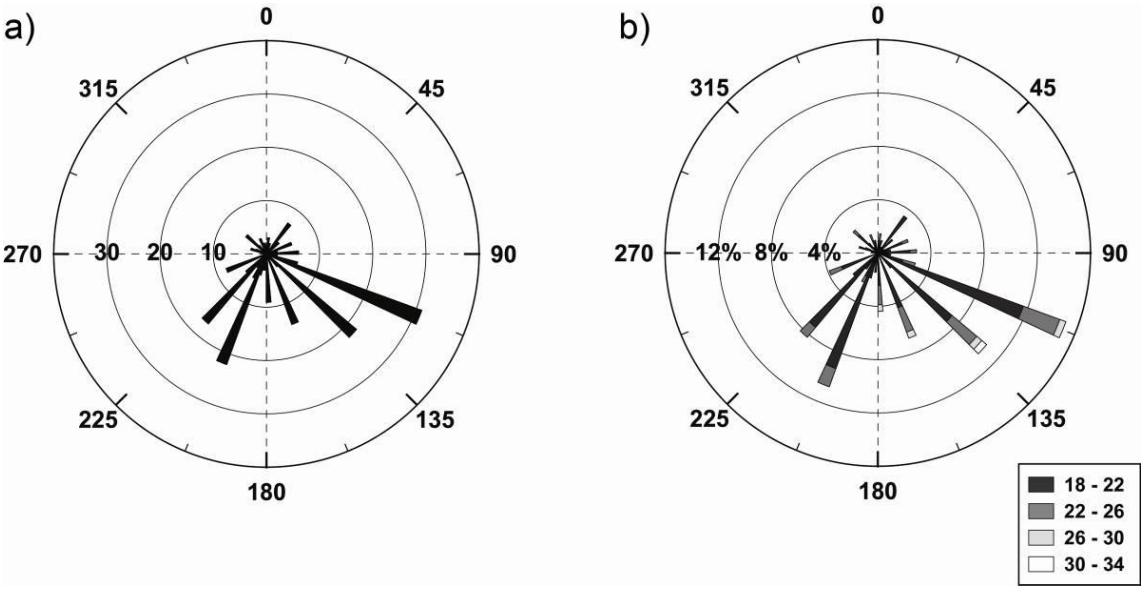

Fig. 2.16. Wind rose for sustained PTC-HWEs, which indicates the frequency of wind observations based on (a) direction and (b) speed. Units of wind speed are in m s^{-1}.

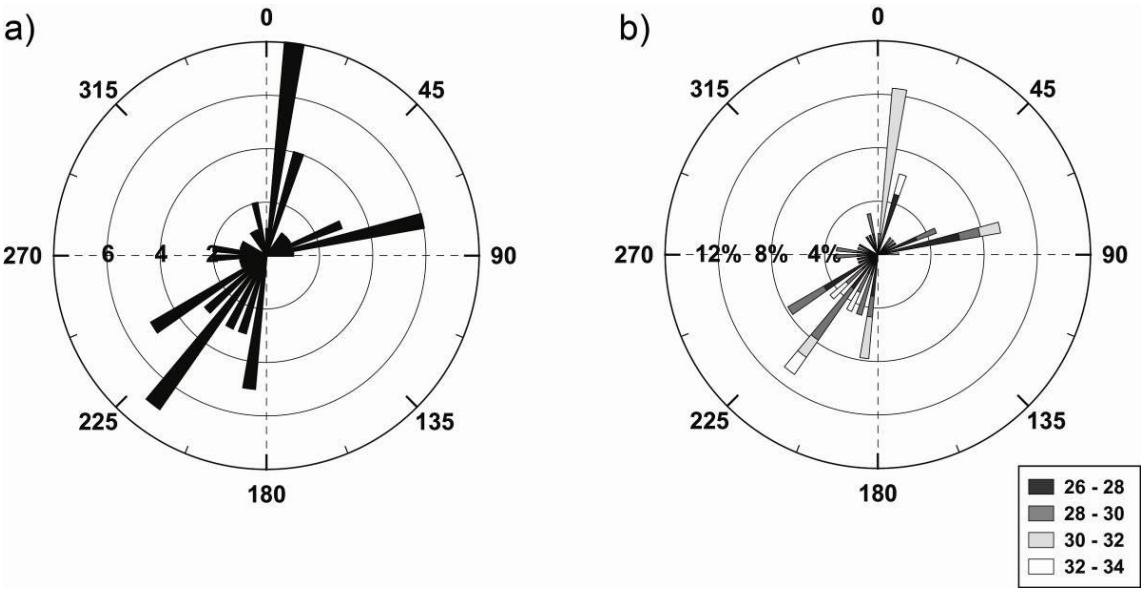

Fig. 2.17. As in Fig. 2.16 except for gust PTC-HWEs.

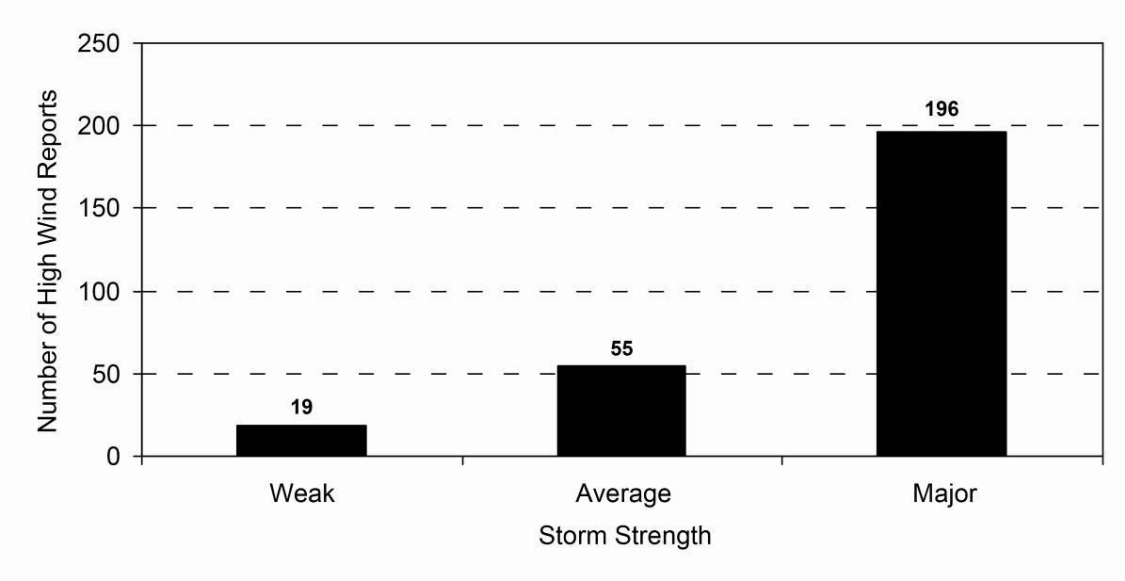

Fig. 2.18. Total number of high-wind reports based on the maximum storm strength achieved PTC during its life cycle.

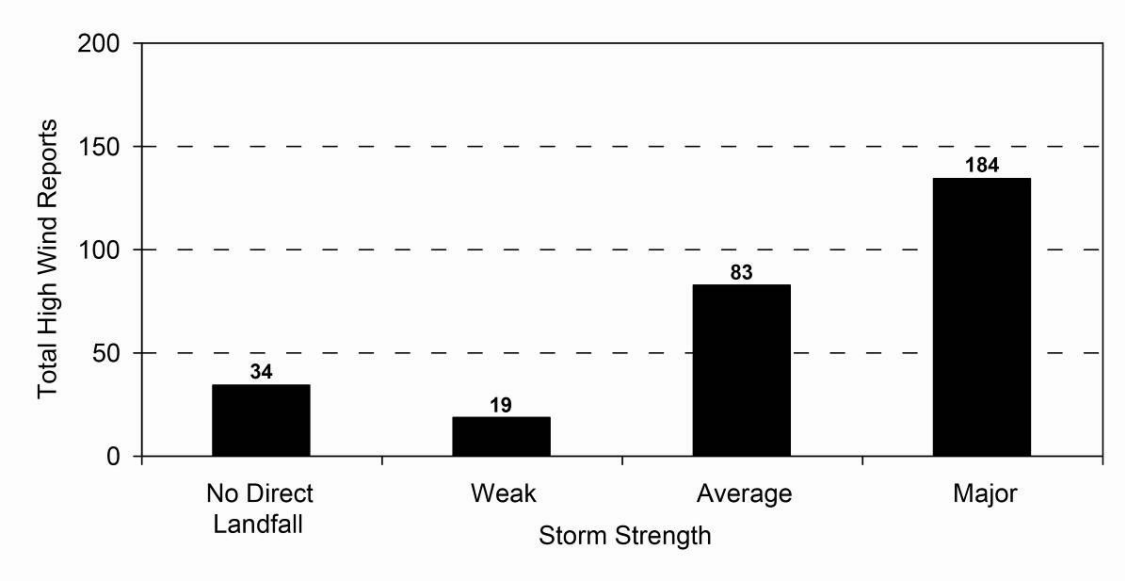

Fig. 2.19. As in Fig. 2.18 except based on the initial landfall strength.

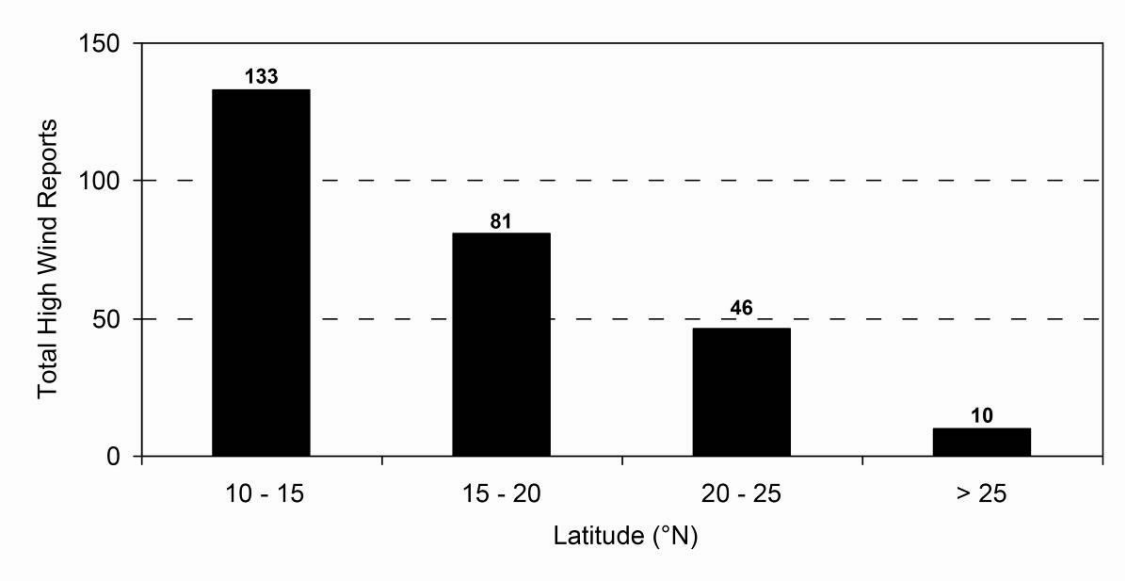

Fig. 2.20. As in Fig. 2.18 except based on the origin of the system.

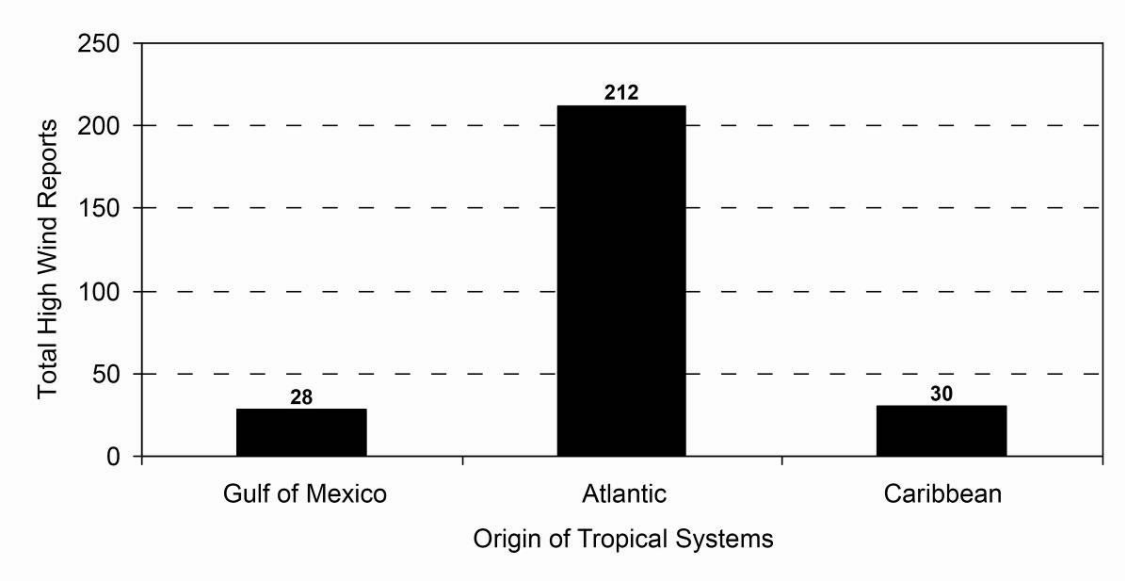

Fig. 2.21. As in Fig. 2.18 except based on the origin basin.

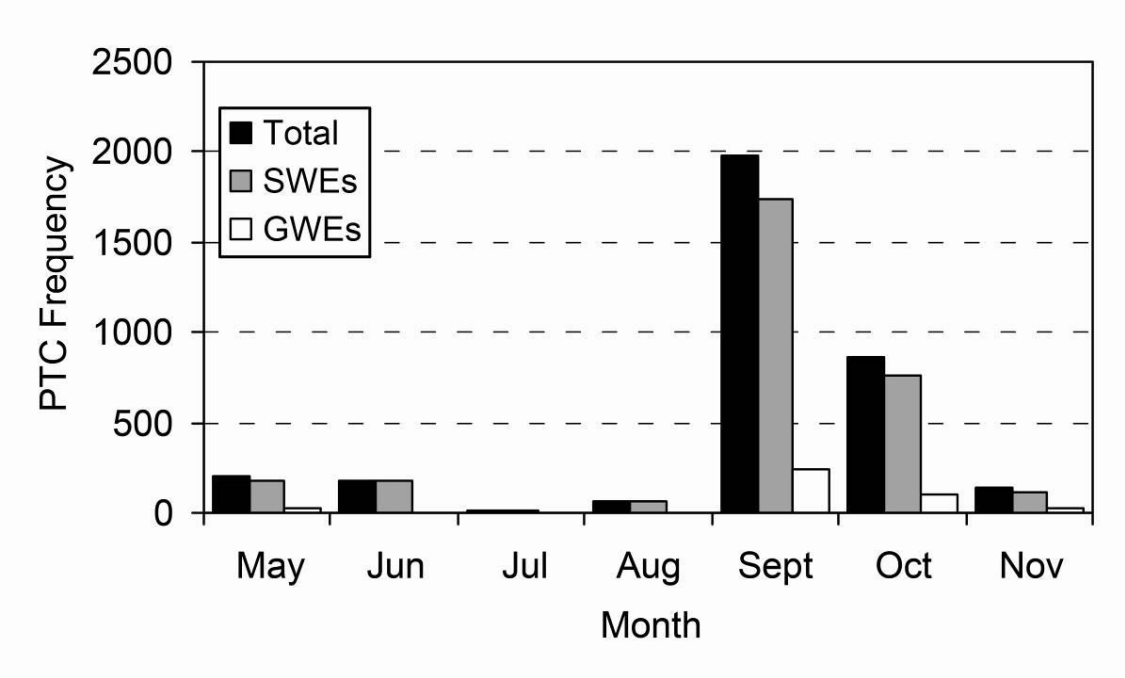

Fig. 2.22. As in Fig. 2.13 except for the adjusted high-wind scale.

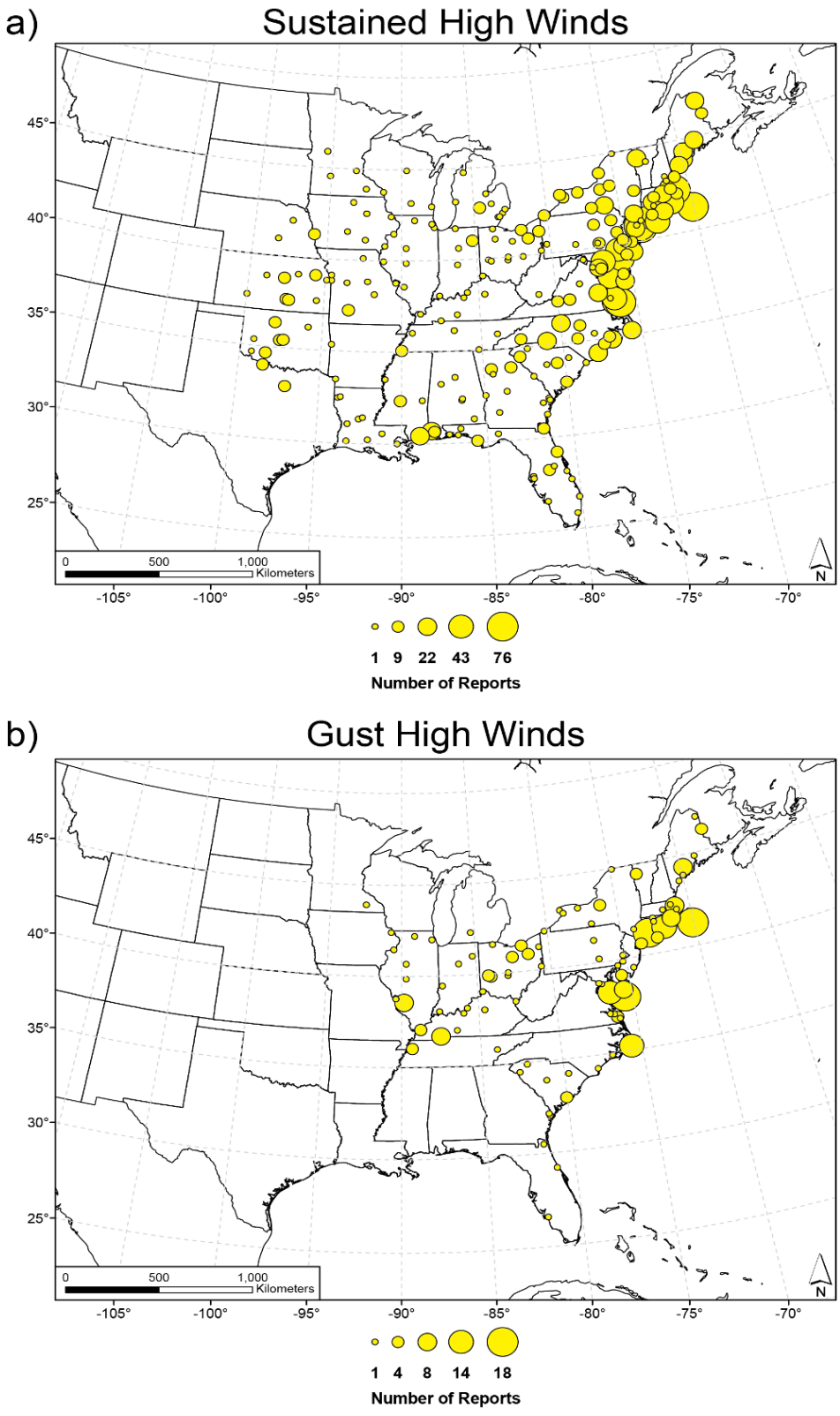

Fig. 2.23. The distribution of high-wind observations classified as (a) sustained and (b) gust based on the adjusted wind scale.

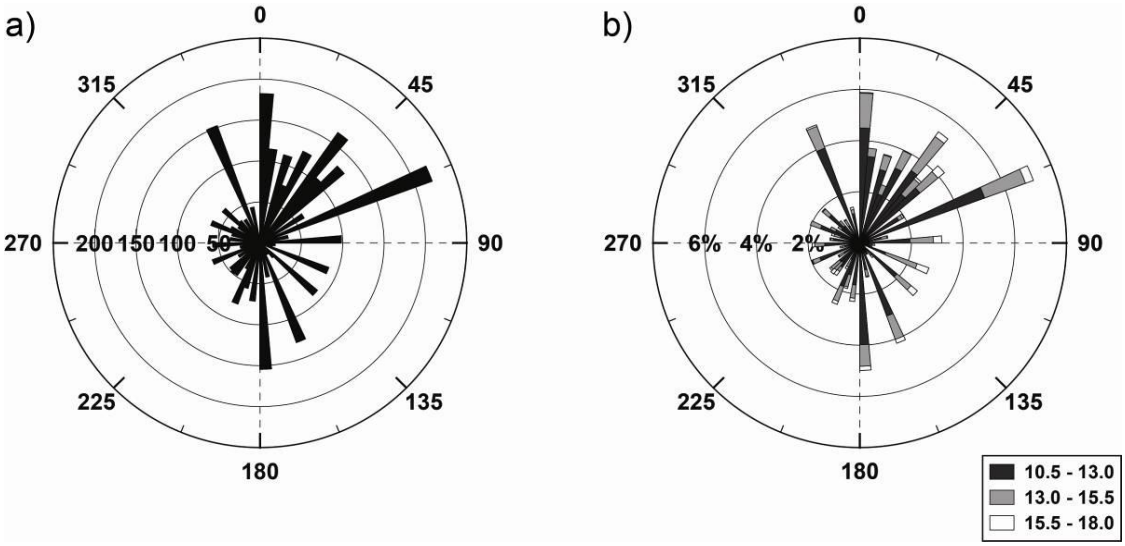

Fig. 2.24. Wind rose for sustained PTC-HWEs based on the reduced wind criteria, which indicates the frequency of wind observations based on (a) direction and (b) speed. Units of wind speed are in m s^{-1}.

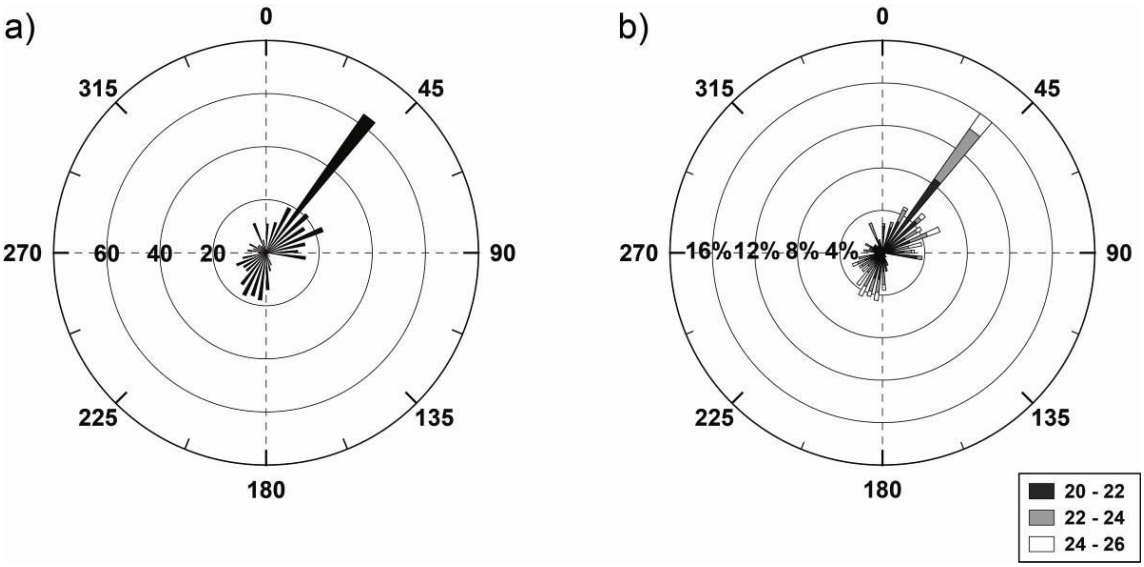

Fig. 2.25. As in Fig. 2.24 except for gust PTC-HWEs.

Table 2.1. Typical National Weather Service (NWS) high-wind criteria based on sustained and gust observations.

National Weather Service (NWS) High-Wind Criteria		
Criterion	**Speed**	**Duration**
Sustained	≥ 18 m s^{-1} (40 mph)	≥ 1 hour
Gust	≥ 26 m s^{-1} (58 mph)	For any duration

Table 2.2. Sample HURDAT observations of Hurricane Katrina (2005) as classified by the NHC by its location, strength, and time.

Year	Month	Day	Hour (UTC)	Name	Latitude	Longitude	Speed (kts)	Pressure (mb)	Category
2005	8	23	1800	KATRINA	23.100	-75.100	30	1008	TD
2005	8	24	0000	KATRINA	23.400	-75.700	30	1007	TD
2005	8	24	0600	KATRINA	23.800	-76.200	30	1007	TD
2005	8	24	1200	KATRINA	24.500	-76.500	35	1006	TS
2005	8	24	1800	KATRINA	25.400	-76.900	40	1003	TS
2005	8	25	0000	KATRINA	26.000	-77.700	45	1000	TS
2005	8	25	0600	KATRINA	26.100	-78.400	50	997	TS
2005	8	25	1200	KATRINA	26.200	-79.000	55	994	TS
2005	8	25	1800	KATRINA	26.200	-79.600	60	988	TS
2005	8	26	0000	KATRINA	25.900	-80.300	70	983	H1
2005	8	26	0600	KATRINA	25.400	-81.300	65	987	H1
2005	8	26	1200	KATRINA	25.100	-82.000	75	979	H1
2005	8	26	1800	KATRINA	24.900	-82.600	85	968	H2
2005	8	27	0000	KATRINA	24.600	-83.300	90	959	H2
2005	8	27	0600	KATRINA	24.400	-84.000	95	950	H2
2005	8	27	1200	KATRINA	24.400	-84.700	100	942	H3
2005	8	27	1800	KATRINA	24.500	-85.300	100	948	H3
2005	8	28	0000	KATRINA	24.800	-85.900	100	941	H3
2005	8	28	0600	KATRINA	25.200	-86.700	125	930	H4
2005	8	28	1200	KATRINA	25.700	-87.700	145	909	H5
2005	8	28	1800	KATRINA	26.300	-88.600	150	902	H5
2005	8	29	0000	KATRINA	27.200	-89.200	140	905	H5
2005	8	29	0600	KATRINA	28.200	-89.600	125	913	H4
2005	8	29	1200	KATRINA	29.500	-89.600	110	923	H3

2005	8	29	1800	KATRINA	31.100	-89.600	80	948	H1
2005	8	30	0000	KATRINA	32.600	-89.100	50	961	TS
2005	8	30	0600	KATRINA	34.100	-88.600	40	978	TS
2005	8	30	1200	KATRINA	35.600	-88.000	30	985	TD
2005	8	30	1800	KATRINA	37.000	-87.000	30	990	TD
2005	8	31	0000	KATRINA	38.600	-85.300	30	994	PTC
2005	8	31	0600	KATRINA	40.100	-82.900	25	996	PTC

Table 2.3. Average wind radii for the merged upstream and downstream flanks based on TS strength and wind velocity. Units are kilometers.

Category	**17.5 m s^{-1} Left**	**17.5 m s^{-1} Right**	**25.7 m s^{-1} Left**	**25.7 m s^{-1} Right**	**32.9 m s^{-1} Left**	**32.9 m s^{-1} Right**
PTC	217	356.5	257	299	83	65
Tropical Storm	121	186	67.5	100	0	0
Category-1	148	240	85	134	53	80
Category-2	211	300	123	193	70	118.5
Category-3	221	328	139	206.5	83	135
Category-4 Category-5	208	268	117	163	70	105.5
** Wind radii developed by Kruk et al. (2010)*						

Table 2.4. T-test significance based on decadal comparisons for (a) PTCs and (b) TSs. 95% confidence interval indicates significant differences between each decade of the study. The arrows and color schemes show the significant differences between each decade.

a) Post-Tropical Cyclones

Decade	1950	1960	1970	1980	1990
1960				0.013	
1970				0.028	
1980					
1990					
2000					

b) Tropical Systems

Decade	1950	1960	1970	1980	1990
1960					
1970				0.015	
1980			0.002		
1990		0.044			
2000	0.006				

Table 2.5. Total number of PTC-HWEs based on the storm type and NWS high-wind criteria.

Name	Year	Sustained Nonconvective	Sustained Convective	Gust Nonconvective	Gust Convective
Florence	1953	4	0	1	0
Carol	1954	16	0	0	0
Edna	1954	7	0	0	0
Hazel	1954	102	2	0	0
Flossy	1956	5	0	0	0
Audrey	1957	26	0	0	0
Carla	1961	1	0	0	0
Hilda	1964	2	0	0	0
David	1979	2	0	0	0
Frederic	1979	0	0	1	0
Gilbert	1988	1	0	0	1
Notnamed	1991	8	0	2	0
Josephine	1996	1	0	1	0
Arlene	2005	0	1	0	0
Ernesto	2006	6	0	10	0
Noel	2007	9	0	15	0
Ike	2008	13	0	33	0

Table 2.6. As in Table 2.1 except for the adjusted high-wind scale.

Adjusted High-Wind Scale Criteria		
Criterion	**Speed**	**Duration**
Sustained	≥ 10.5 m s^{-1} (23 mph)	≥ 1 hour
Gust	≥ 20 m s^{-1} (45 mph)	For any duration

Table 2.7. As in Table 2.5 except for the adjusted high-wind scale.

Name	Year	Sustained Nonconvective	Sustained Convective	Gust Nonconvective	Gust Convective
Notnamed	1952	47	1	0	0
Carol	1953	1	0	0	0
Florence	1953	71	0	0	0
Carol	1954	61	1	0	0
Edna	1954	52	0	0	0
Hazel	1954	304	3	0	0
Flossy	1956	378	2	0	0
Audrey	1957	127	4	0	0
Gracie	1959	44	0	0	0
Brenda	1960	2	0	0	0
Donna	1960	7	0	0	0
Carla	1961	283	0	0	0
Frances	1961	1	0	0	0
Hilda	1964	75	1	0	0
Isbell	1964	40	7	0	0
Notnamed	1965	9	0	0	0
Candy	1968	3	0	0	0
Gerda	1969	1	0	0	0
Carrie	1972	4	0	0	0
David	1979	31	0	7	0
Frederic	1979	46	1	15	1
Alicia	1983	1	0	0	0
Danny	1985	3	0	0	0
Gloria	1985	11	0	2	0
Gilbert	1988	73	2	9	3
Hugo	1989	98	0	16	0

Marco	1990	0	0	4	0
Notnamed	1991	139	0	45	0
Allison	1995	4	0	0	3
Opal	1995	40	0	3	0
Josephine	1996	135	0	45	3
Earl	1998	34	0	9	0
Floyd	1999	112	0	6	0
Gordon	2000	4	0	0	0
Isabel	2003	53	0	0	0
Charley	2004	1	0	0	0
Frances	2004	37	0	1	0
Hermine	2004	1	0	0	0
Ivan	2004	82	0	3	0
Jeanne	2004	40	0	2	0
Arlene	2005	1	0	0	0
Cindy	2005	16	0	0	0
Alberto	2006	7	1	2	0
Ernesto	2006	145	0	72	0
Andrea	2007	181	0	23	0
Barry	2007	17	0	1	0
Noel	2007	92	0	27	0
Gustav	2008	7	0	0	0
Hanna	2008	5	0	0	0
Ike	2008	120	0	97	0
Ida	2009	24	0	0	0

CHAPTER 3

SUMMARY AND CONCLUSIONS

3.1 Overview

Atlantic and Gulf of Mexico basin tropical systems (TSs) are primary driven by atmospheric conditions, sea surface temperatures (SSTs), and physiographic characteristics. This combination of tropical easterlies, warm SSTs gradients, and surface wind convergence along the intertropical convergence zone (ITCZ) help create TSs that often leave behind devastating affects across the eastern United States. Surface winds that develop within TSs usually reach their peak magnitude prior to landfall and eventually decay in magnitude as the cyclone moves farther inland away from its energy source (Kaplan and DeMaria 1995). Despite the advancements in computer modeling, improved weather instrumentation, and forecasting theory, meteorologists still remained challenged in trying to accurately predict how TS wind fields will evolve as the system enter various upper-atmospheric and surface conditions at middle-to-high latitudes (Jones et al. 2003). In many cases, a portion of these TSs make landfall and/or moved into latitudes above 35° N and eventually transition from warm to cold-core systems, otherwise known as post-tropical cyclones (PTCs). The primary goal of this thesis is to provide a climatological perspective of PTCs and resulting high winds.

The majority of the research has focused on understanding PTC transition by investigating the various large-scale baroclinic and dynamic environments (Sinclair 1993; Harr and Elsberry 2000; Klein et al. 2000; Hart 2003; Jones et al. 2003; Kitabatake

2008). In order to complete their analysis of PTC's dynamics, many of the studies had to conduct basic climatologies for their region of interest (Foley and Hanstrum 1994; Klein et al. 2000; Hart and Evans 2001; Sinclair 2002; Jones et al. 2003; Kitabatake 2008). Further, some North Atlantic PTC studies only focused on particular events that underwent reintensification or encountered various large-scale dynamics (Thorncroft and Jones 2000; Evans and Prater-Mayes 2004; McTaggart-Cowan et al. 2004; Augustí-Panareda et al. 2005; Evans and Hart 2008; Hulme and Martin 2009). A recent study performed by Kruk et al. (2010) used wind radii buffers to estimate the likelihood of PTC winds based on return intervals for the U.S. Despite these research efforts, no formal studies have explicitly analyzed the spatial distribution of landfalling PTC surface high winds over the U.S.

3.2 Summary

The purpose of this thesis was to improve our understanding of PTC high-wind events (HWEs) by using the typical National Weather Service (NWS) high-wind criteria. During 1951-2009, 76 out of 301 PTCs classified by the NHC were examined. This study showed that 0.8% (270) high-wind observations and 0.6 % (121) high-wind days were contributed from PTCs. Results from this analysis also found that nearly (98%) of all PTCs-HWEs were classified as nonconvective high-wind events (NCWEs). PTC-HWEs were primarily observed in three regions: Great Lakes, Mid-Atlantic, and New England regions. These results agree with the overall findings that convective high-wind events (CWEs) are not usually observed with any migrating system over the northeastern U.S. and it can be concluded that PTC-HWEs are rarely CWEs in nature.

Previous work by Kruk et al. (2010) showed TSs that transition to PTC are observed at middle-to-higher latitudes. Our study showed that 75% of all PTC-HWEs were observed during the peak of the North Atlantic hurricane season (September-October). Hart and Evans (2001) concluded that the highest likelihood of PTC transitions occurred during these particular months. The study by Hart and Evans (2001) also found that the delay warming in SSTs of the Atlantic basin, extratropical cyclone (ETC) development, increase Coriolis parameter, and baroclinic instability are major contributors for PTC transitions to occur in higher latitudes. Results from this study showed that 61% of all PTC transitions occurred during September and October.

An adjusted high-wind speed scale was developed to understand PTC surface high winds over the U.S. The relaxed criteria were based on the PTC standard deviations of both sustained ($\pm$ 2.5 m s^{-1}) and gust ($\pm$ 2.0 m s^{-1}) high-wind reports. As a result, an additional 3,492 PTC high-wind records [3,093 PTC sustained wind events (SWEs) and 399 PTC gust wind events (GWEs)] were observed. It was found that nearly every state east of the Rocky Mountains was affected by PTCs. The highest frequency of SWEs and GWEs were observed along the eastern seaboard with a secondary axis along the Great Lakes region. Despite the decrease in wind velocity, a minimum number of high-wind reports were observed within the southeastern U.S. and Great Plains regions. Hart and Evans (2001) found that TS landfalls along Gulf of Mexico coastlines dissipate more rapidly, preventing them to enter into a baroclinic environment that can support PTC growth. This study also showed that the strongest winds associated with PTCs are located on the upstream flank of the system, with a secondary axis in the southwest quadrant of the migrating system. Powell (1982) demonstrated that the strongest winds

of a landfalling TS are located on the upstream flank in the northern hemisphere. The greatest frequency of SWEs (63%) and GWEs (58%) occurred within 2 m s^{-1} of the relaxed high-wind scale. This result shows that the surface winds from landfalling PTCs generally do not produce high winds that meet the current NWS criteria and the adjusted high-wind scale.

3.3 Conclusions

Results from this thesis broaden our background on PTCs, in particular with respect to PTC-HWEs over the U.S. Previous studies have been primarily focused on understanding the dynamic and large-scale conditions have on PTCs through the world (Foley and Hanstrum 1994; Harr and Elsberry 2000; Klein et al. 2000; Sinclair 2002; Jones et al. 2003; Hart 2003; among others). This thesis has shown that PTC surface winds rarely produce high-wind events that meet the typical NWS high-wind criteria. Despite, the minimum fraction (<1%) of PTC-HWEs found during the study, recent PTCs [e.g., Perfect Storm (1991) and Hurricane Ike (2008)] have shown the capability of producing damaging and life-threatening winds to the U.S.

Further investigation should examine high winds of all landfalling U.S. TSs. This type of study would allow forecasters to understand how surface high winds change as they progress inland. In addition, this future project would grant forecasters the ability to better predict and forewarn citizens and emergency management of the possible hazards that could exist with the approaching storm system. Another possible point of research would be to analyze PTC-HWEs that occurred over the Canadian providence of Nova Scotia. As described in this paper, a high density of PTC transitions was observed within

this particular region. Lastly, perhaps the work presented here will raise awareness and develop a greater understanding of PTC wind characteristics, so that people are less vulnerable to the possible threats that can exist with landfalling PTCs over the U.S.

APPENDIX

Distribution of PTC-HWEs based on the typical NWS high-wind criteria.

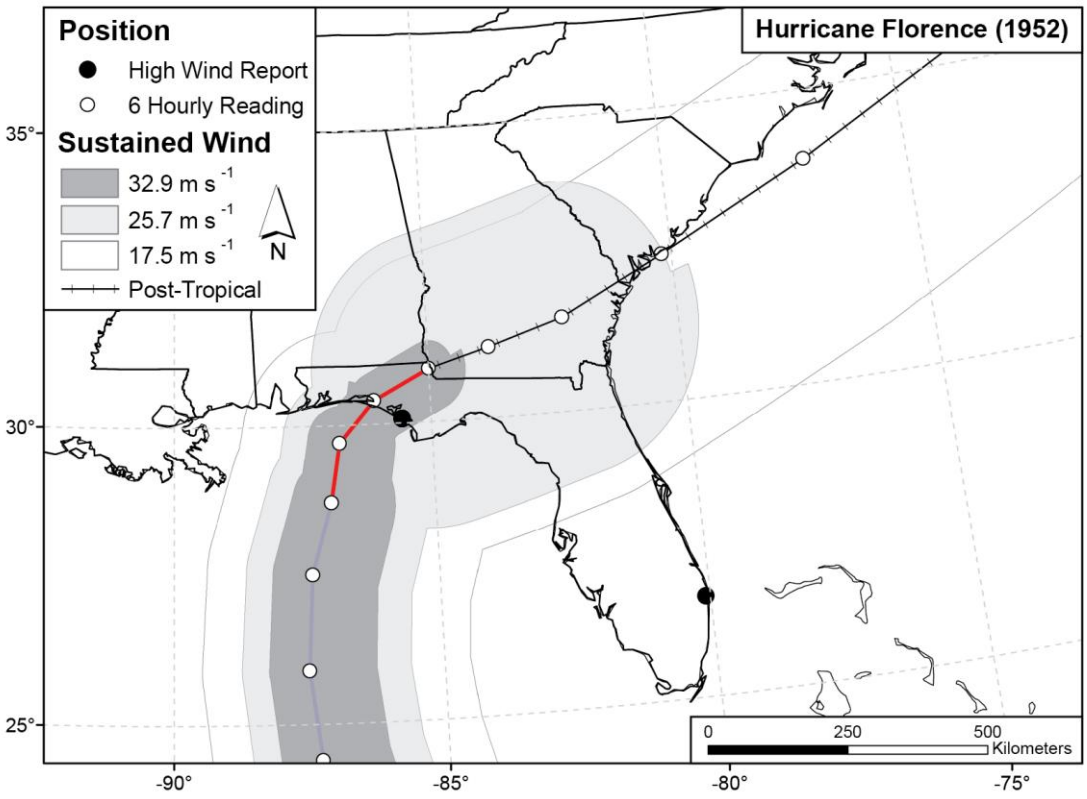

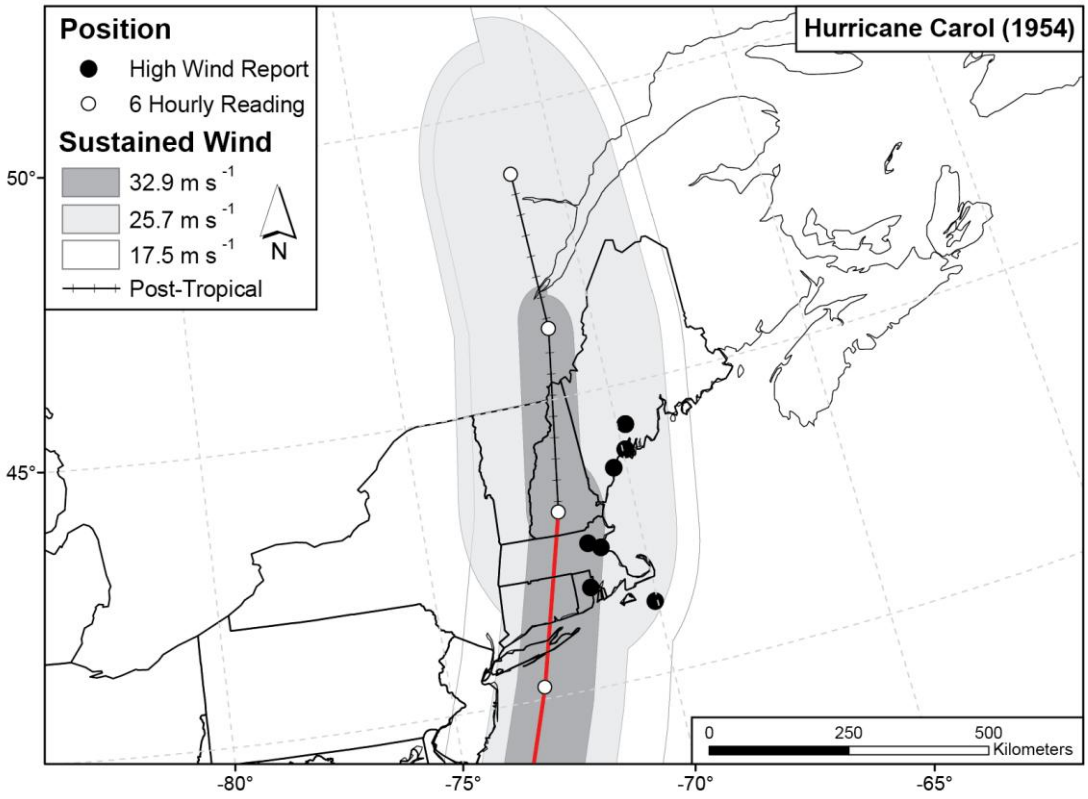
Position
High Wind Report
6 Hourly Reading
Sustained Wind
32.9 m s -1
25.7 m s -1
17.5 m s -1
Post-Tropical
N
Hurricane Carol (1954)
50°
45°
-80°
-75°
-70°
-65°
0
250
500
Kilometers

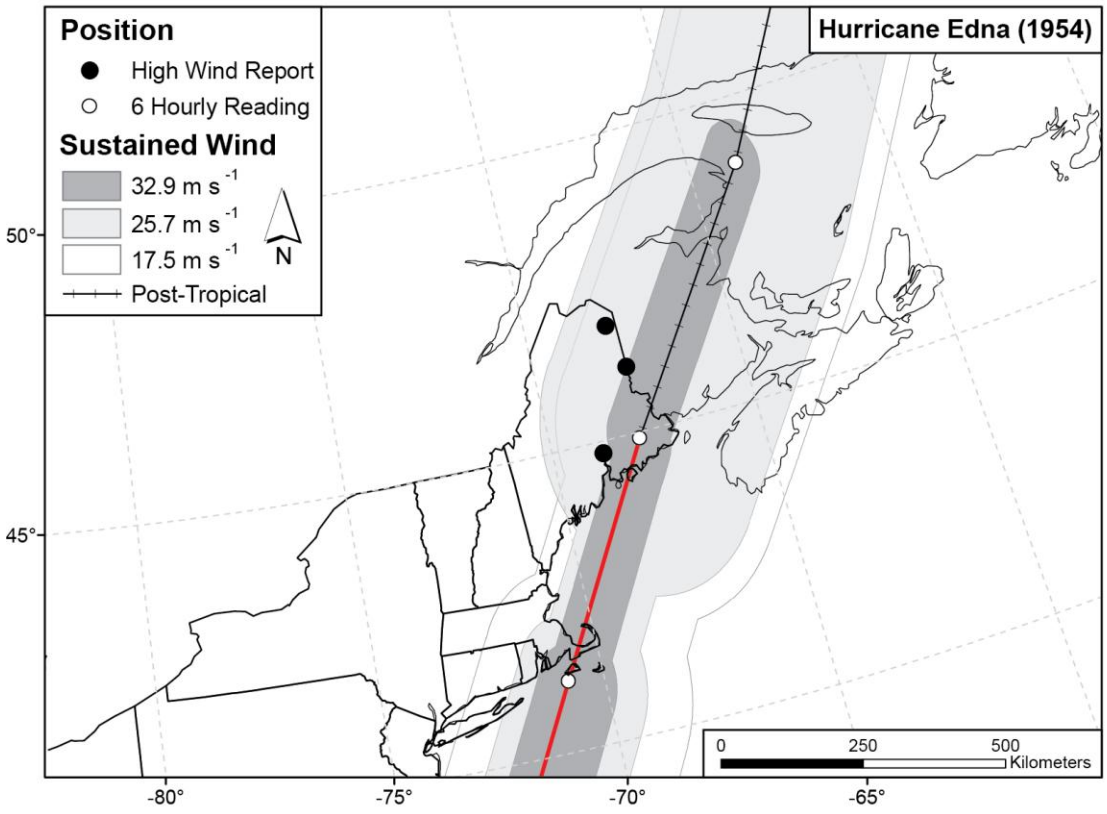
Position
High Wind Report
6 Hourly Reading
Sustained Wind
32.9 m s -1
25.7 m s -1
17.5 m s -1
Post-Tropical
N
Hurricane Edna (1954)
50°
45°
-80°
-75°
-70°
-65°
0
250
500
Kilometers

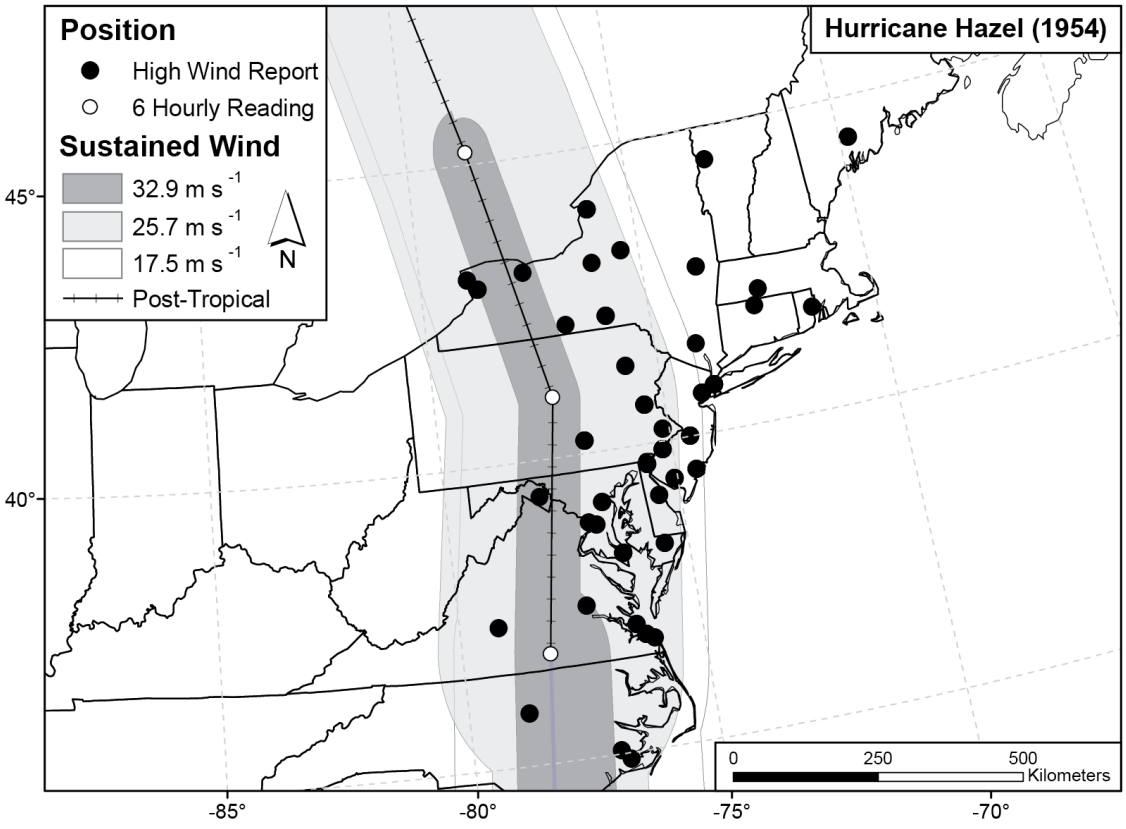
Position
High Wind Report
6 Hourly Reading
Sustained Wind
32.9 m s -1
25.7 m s -1
17.5 m s -1
Post-Tropical
N
Hurricane Hazel (1954)
45°
40°
-85°
-80°
-75°
-70°
0
250
500
Kilometers

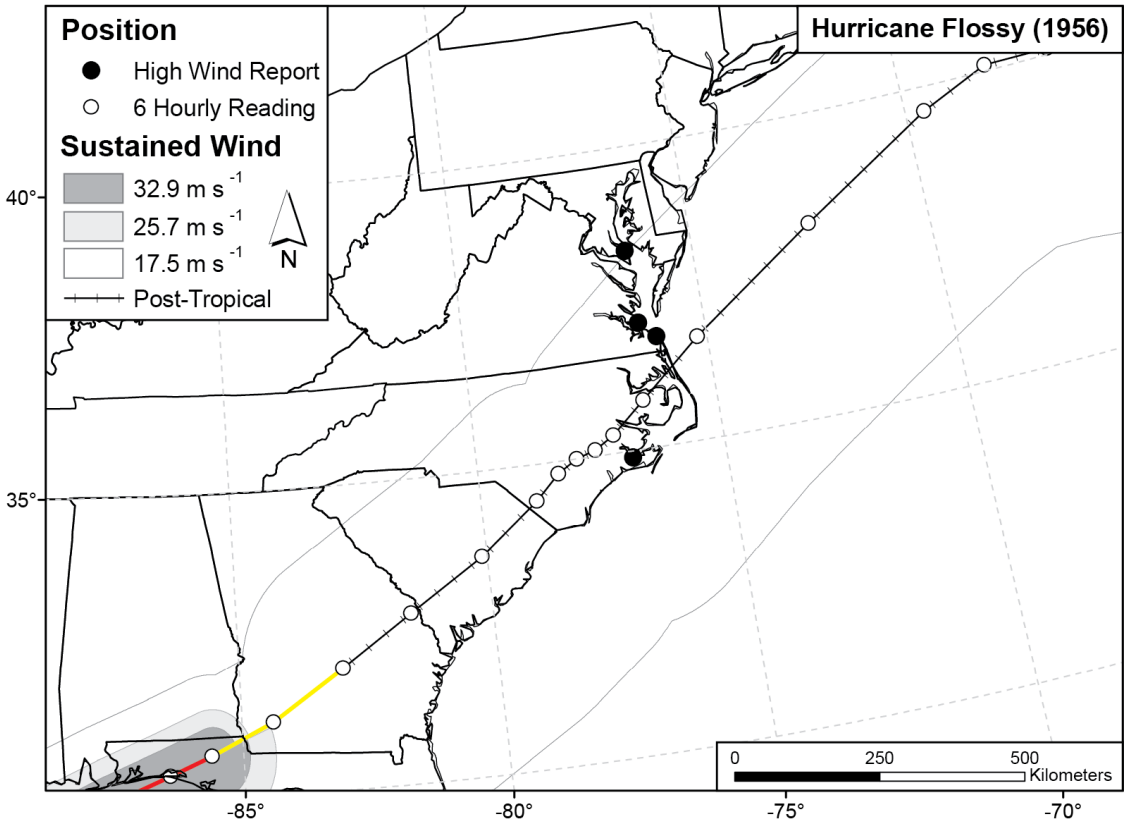
Position
High Wind Report
6 Hourly Reading
Sustained Wind
32.9 m s -1
25.7 m s -1
17.5 m s -1
Post-Tropical
N
Hurricane Flossy (1956)
40°
35°
-85°
-80°
-75°
-70°
0
250
500
Kilometers

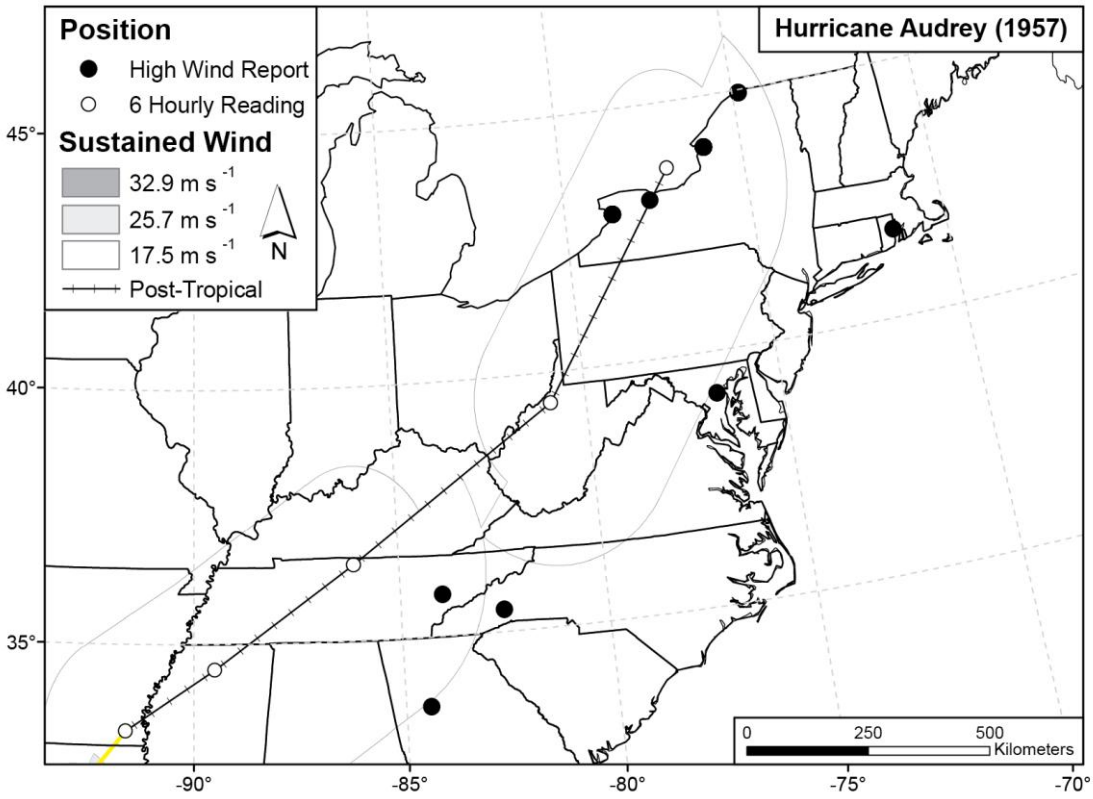
Position
High Wind Report
6 Hourly Reading
Sustained Wind
32.9 m s -1
25.7 m s -1
17.5 m s -1
Post-Tropical
N
Hurricane Audrey (1957)
45°
40°
35°
-90°
-85°
-80°
-75°
-70°
0
250
500
Kilometers

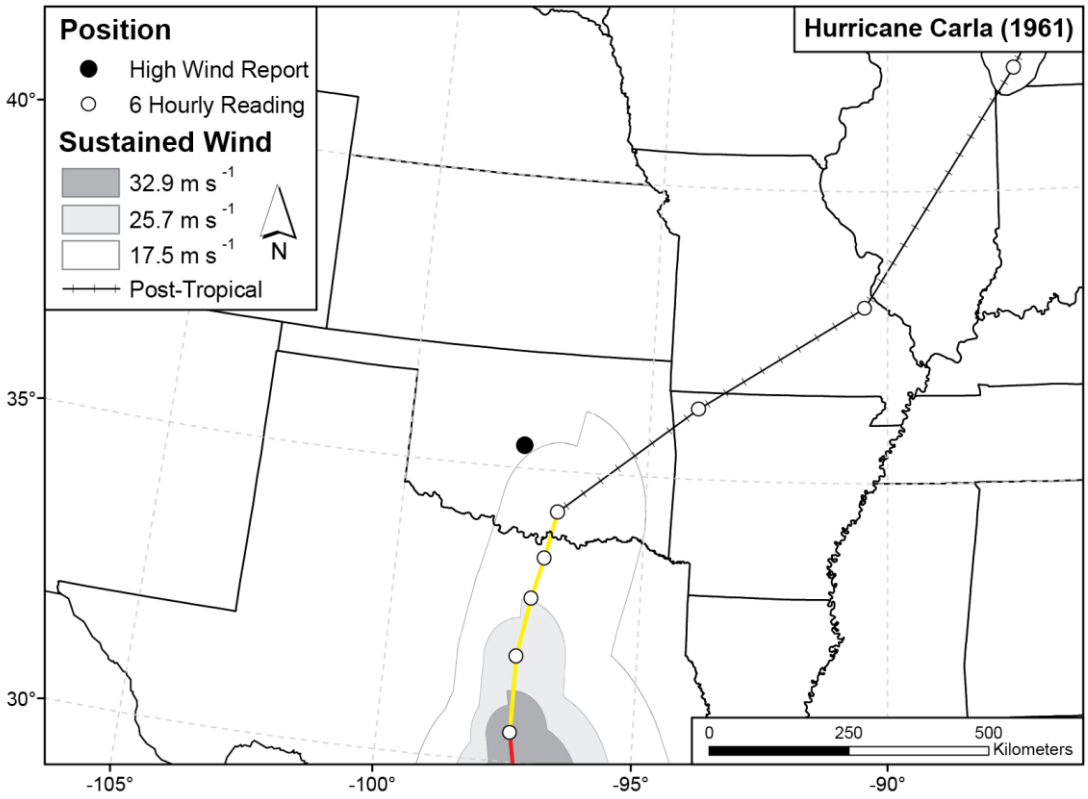
Position
High Wind Report
6 Hourly Reading
Sustained Wind
32.9 m s -1
25.7 m s -1
17.5 m s -1
Post-Tropical
N
Hurricane Carla (1961)
40°
35°
30°
-105°
-100°
-95°
-90°
0
250
500
Kilometers

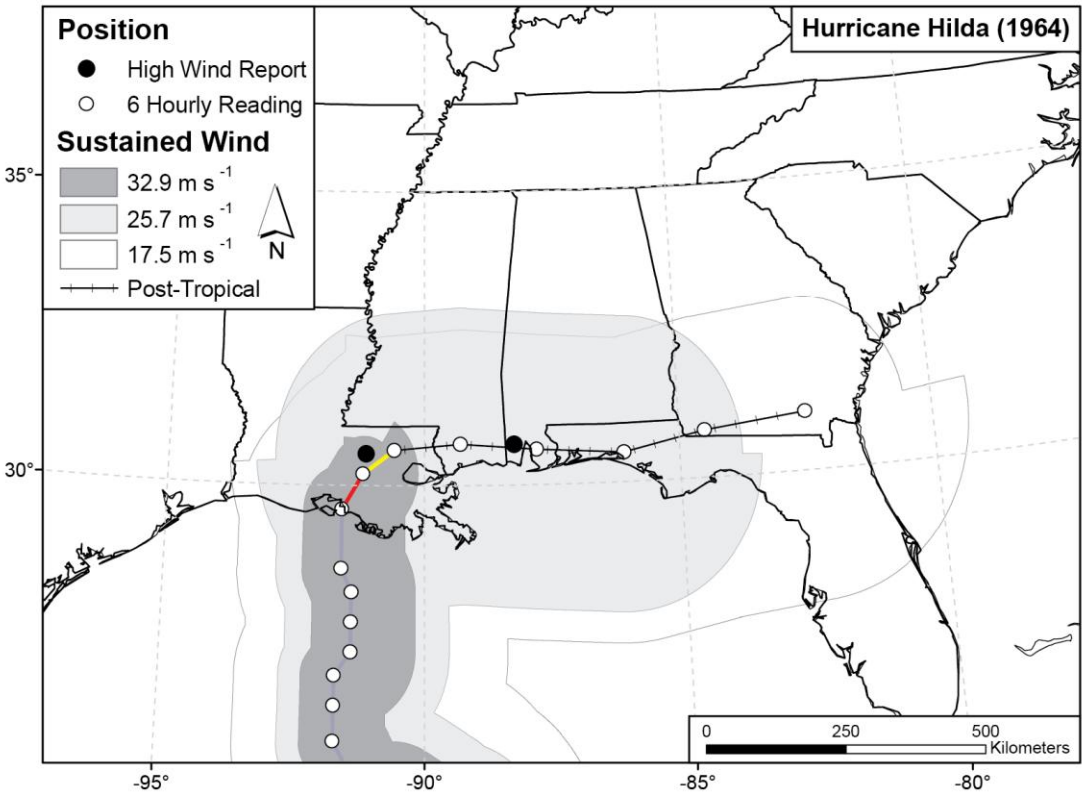
Position
High Wind Report
6 Hourly Reading
Sustained Wind
32.9 m s -1
25.7 m s -1
17.5 m s -1
Post-Tropical
N
Hurricane Hilda (1964)
35°
30°
-95°
-90°
-85°
-80°
0
250
500
Kilometers

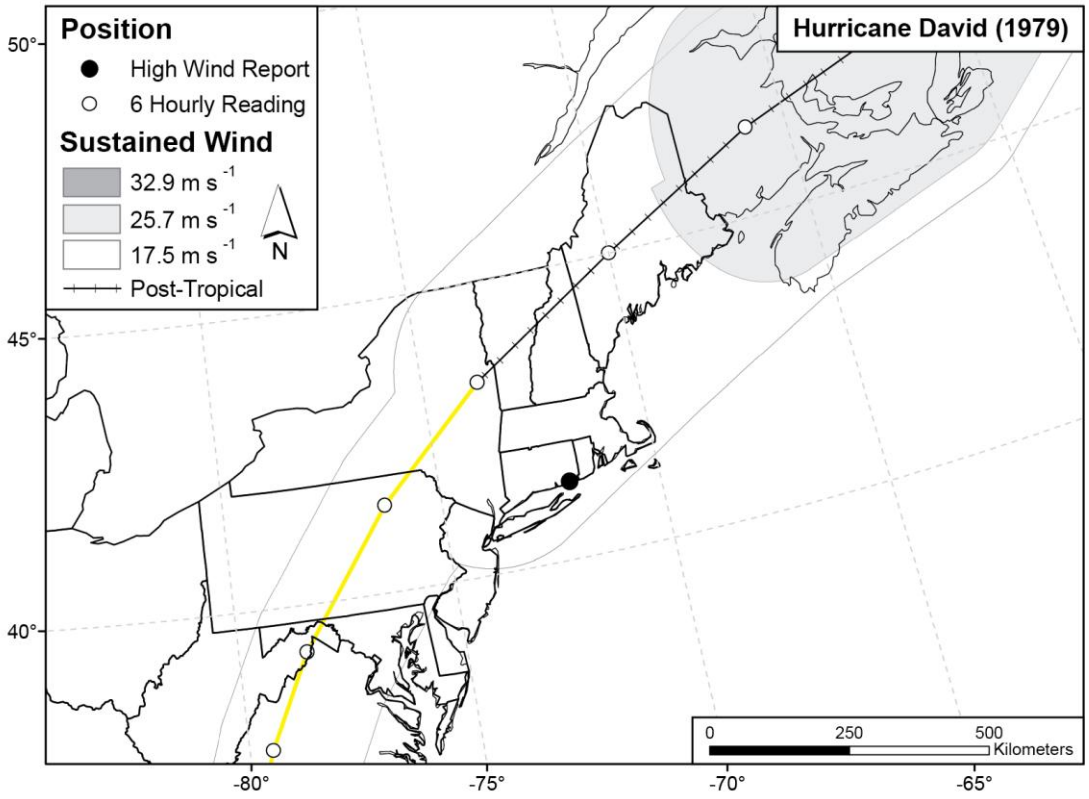
Position
High Wind Report
6 Hourly Reading
Sustained Wind
32.9 m s -1
25.7 m s -1
17.5 m s -1
Post-Tropical
N
Hurricane David (1979)
50°
45°
40°
-80°
-75°
-70°
-65°
0
250
500
Kilometers

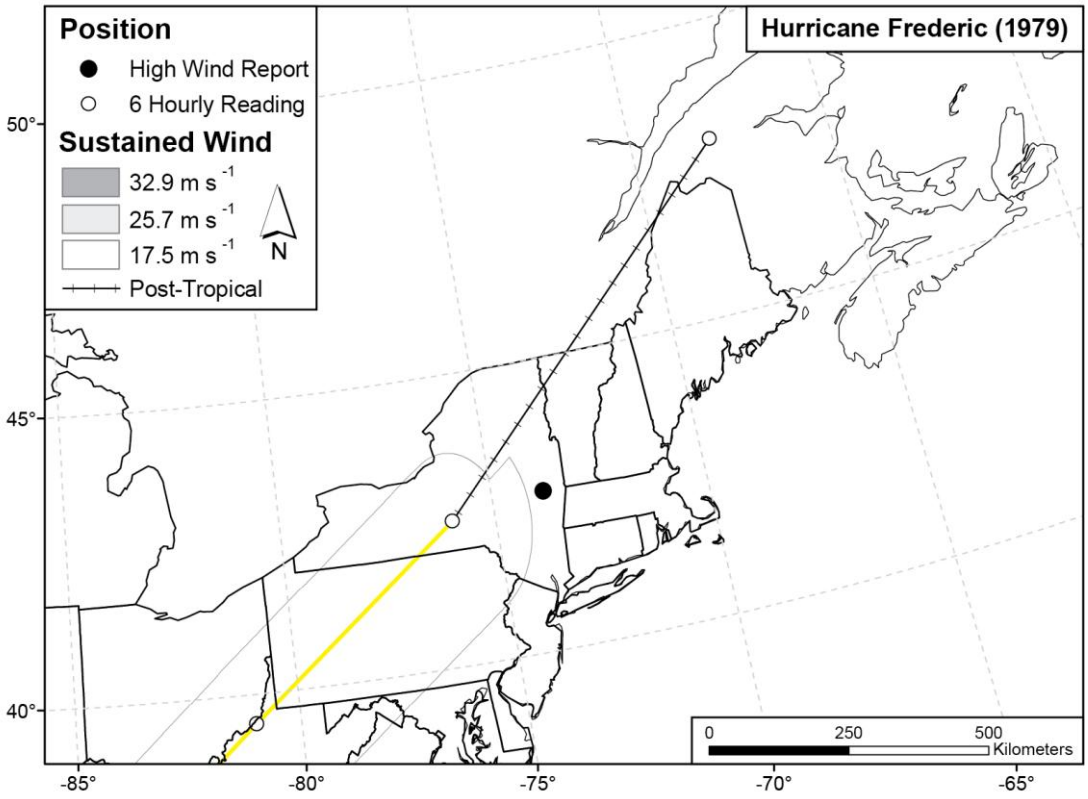
Position
High Wind Report
6 Hourly Reading
Sustained Wind
32.9 m s -1
25.7 m s -1
17.5 m s -1
Post-Tropical
N
Hurricane Frederic (1979)
50°
45°
40°
-85°
-80°
-75°
-70°
-65°
0
250
500
Kilometers

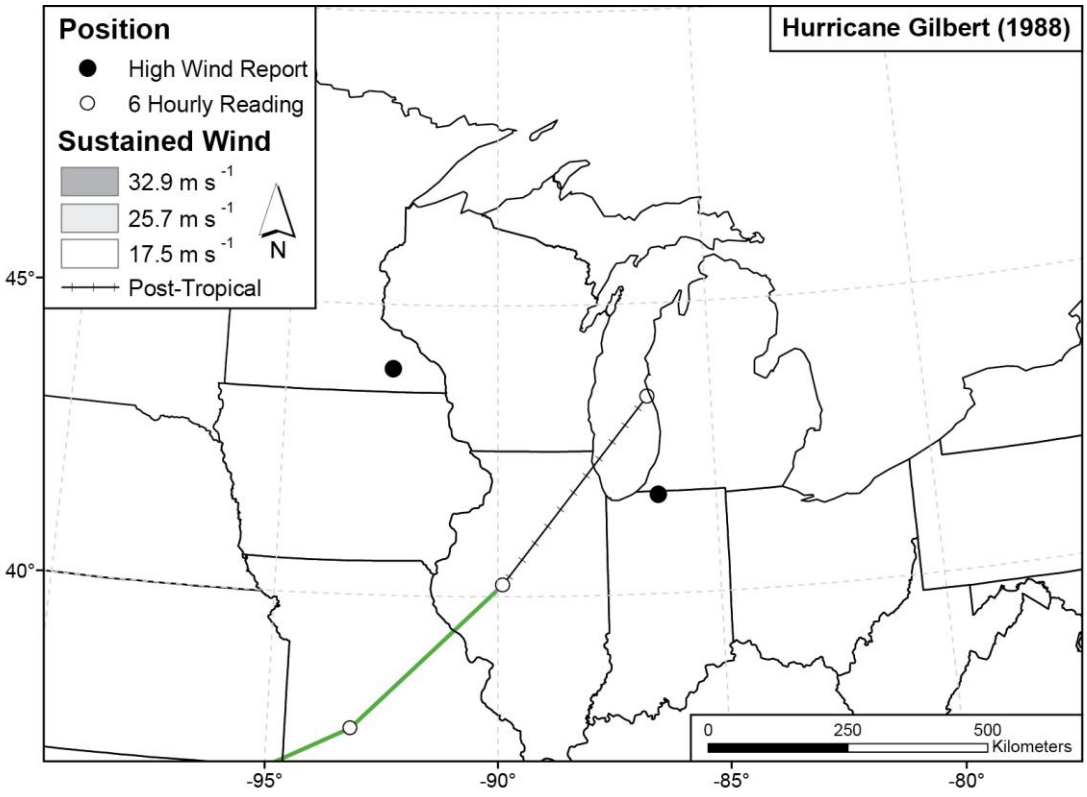
Position
High Wind Report
6 Hourly Reading
Sustained Wind
32.9 m s -1
25.7 m s -1
17.5 m s -1
Post-Tropical
N
Hurricane Gilbert (1988)
45°
40°
-95°
-90°
-85°
-80°
0
250
500
Kilometers

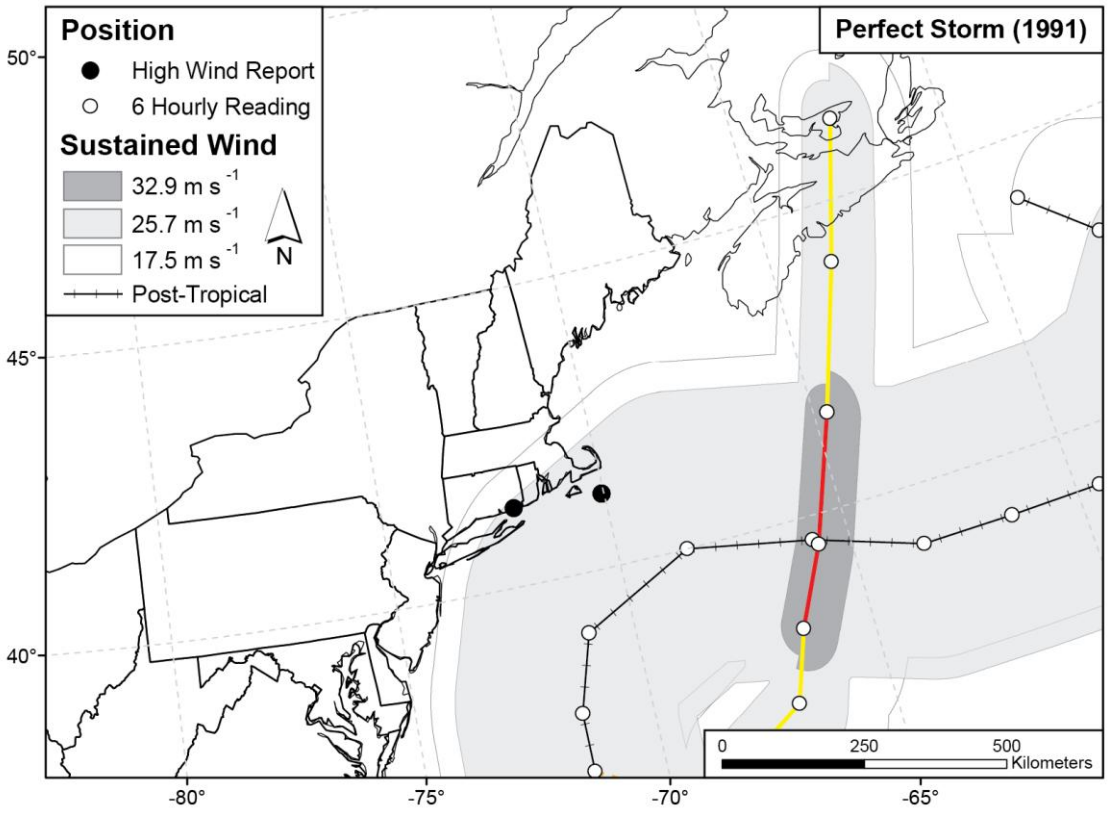
Position
High Wind Report
6 Hourly Reading
Sustained Wind
32.9 m s -1
25.7 m s -1
17.5 m s -1
Post-Tropical
N
Perfect Storm (1991)
50°
45°
40°
-80°
-75°
-70°
-65°
0
250
500
Kilometers

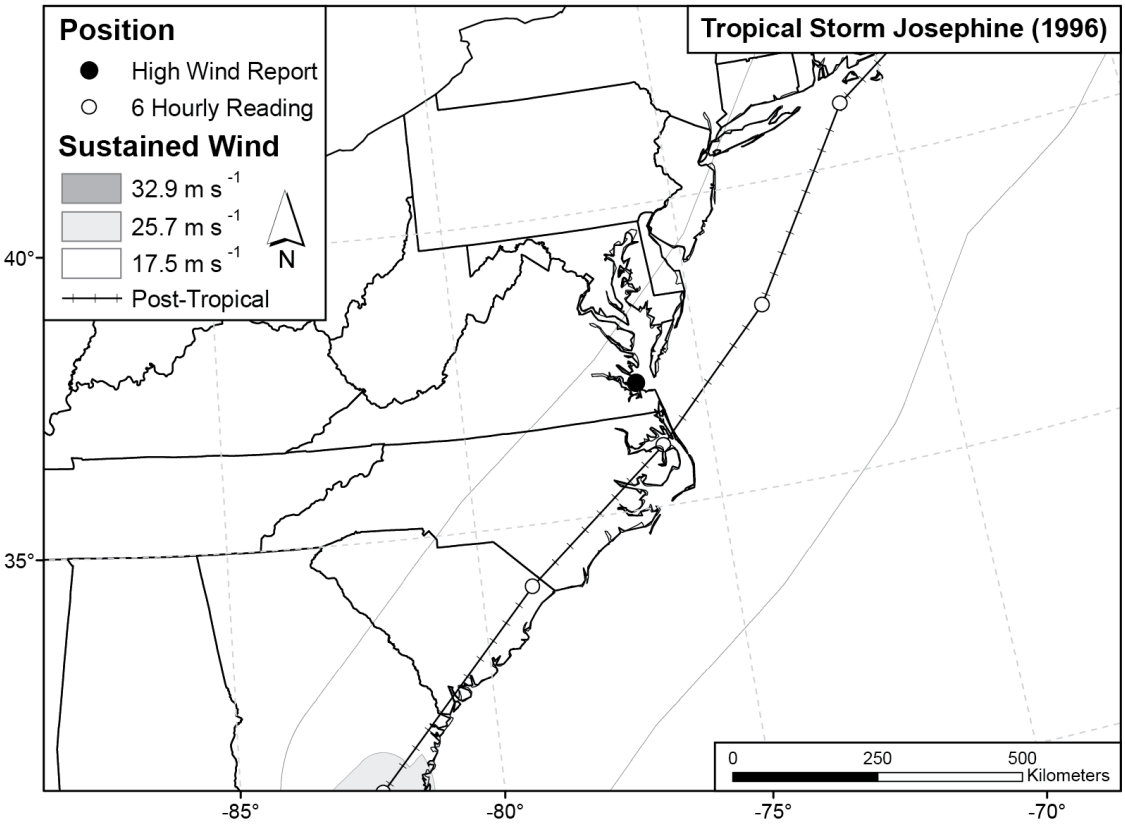
Position
High Wind Report
6 Hourly Reading
Sustained Wind
32.9 m s -1
25.7 m s -1
17.5 m s -1
Post-Tropical
N
Tropical Storm Josephine (1996)
0
250
500
Kilometers
40°
35°
-85°
-80°
-75°
-70°

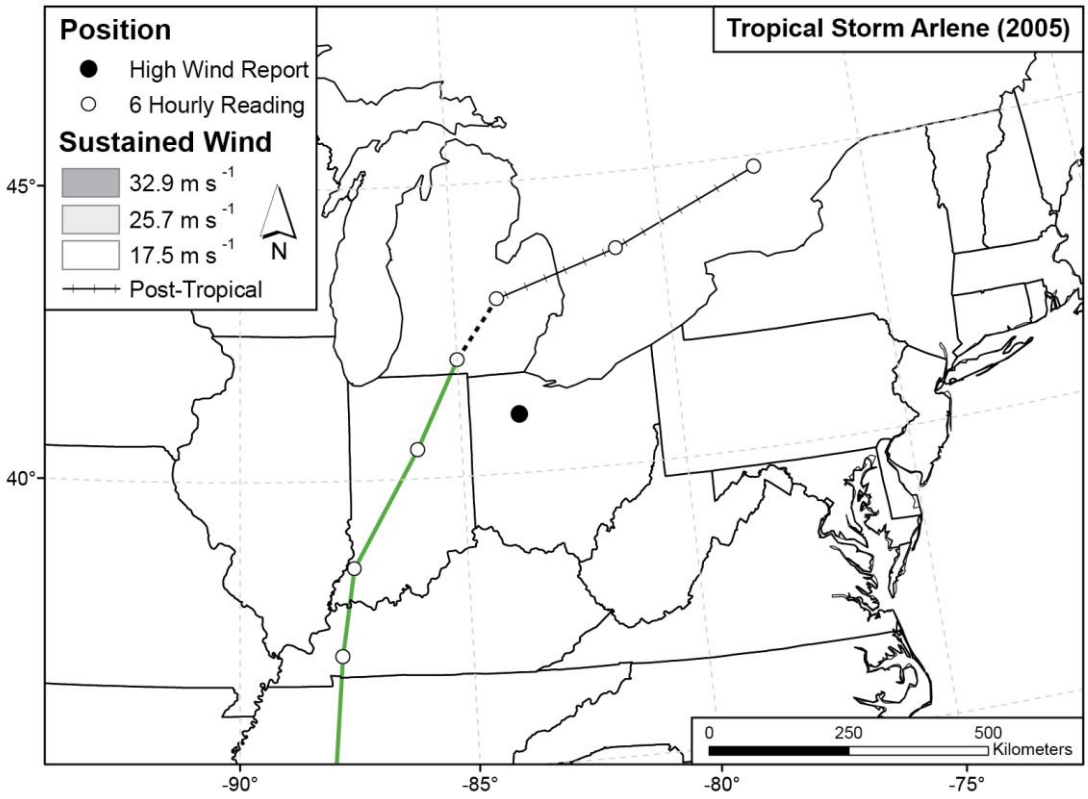
Position
High Wind Report
6 Hourly Reading
Sustained Wind
32.9 m s -1
25.7 m s -1
17.5 m s -1
Post-Tropical
N
Tropical Storm Arlene (2005)
0
250
500
Kilometers
45°
40°
-90°
-85°
-80°
-75°

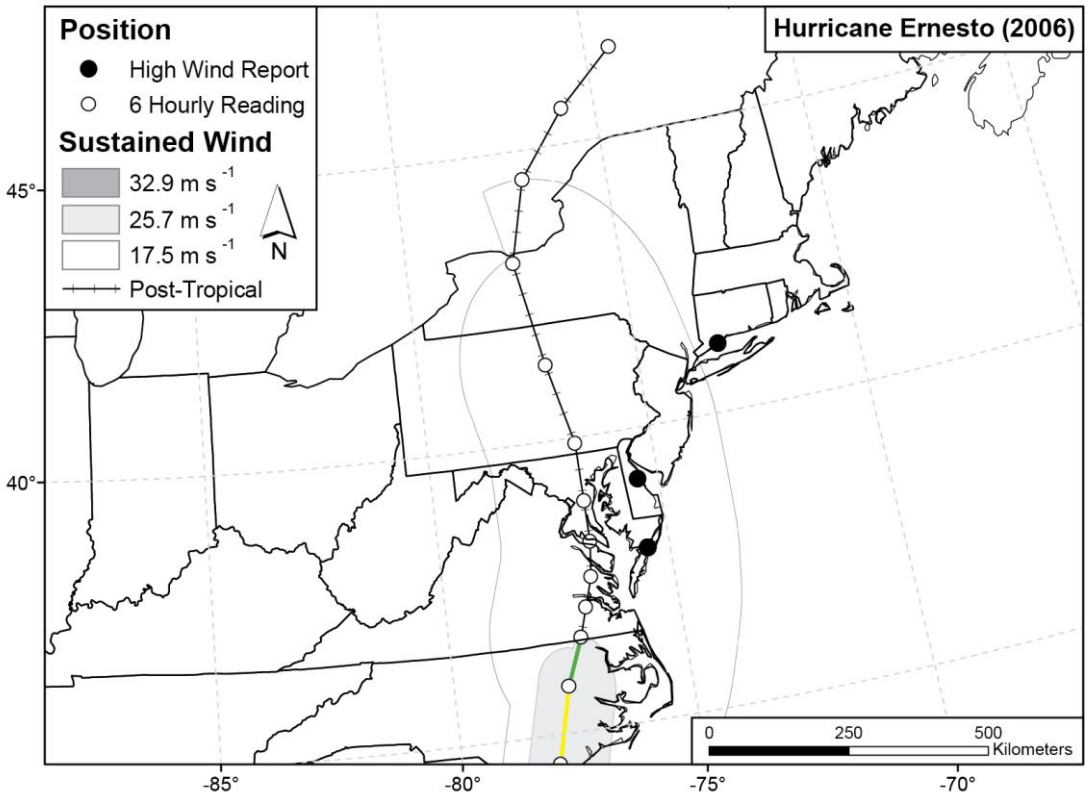
Position
High Wind Report
6 Hourly Reading
Sustained Wind
32.9 m s -1
25.7 m s -1
17.5 m s -1
Post-Tropical
N
Hurricane Ernesto (2006)
0
250
500
Kilometers
45°
40°
-85°
-80°
-75°
-70°

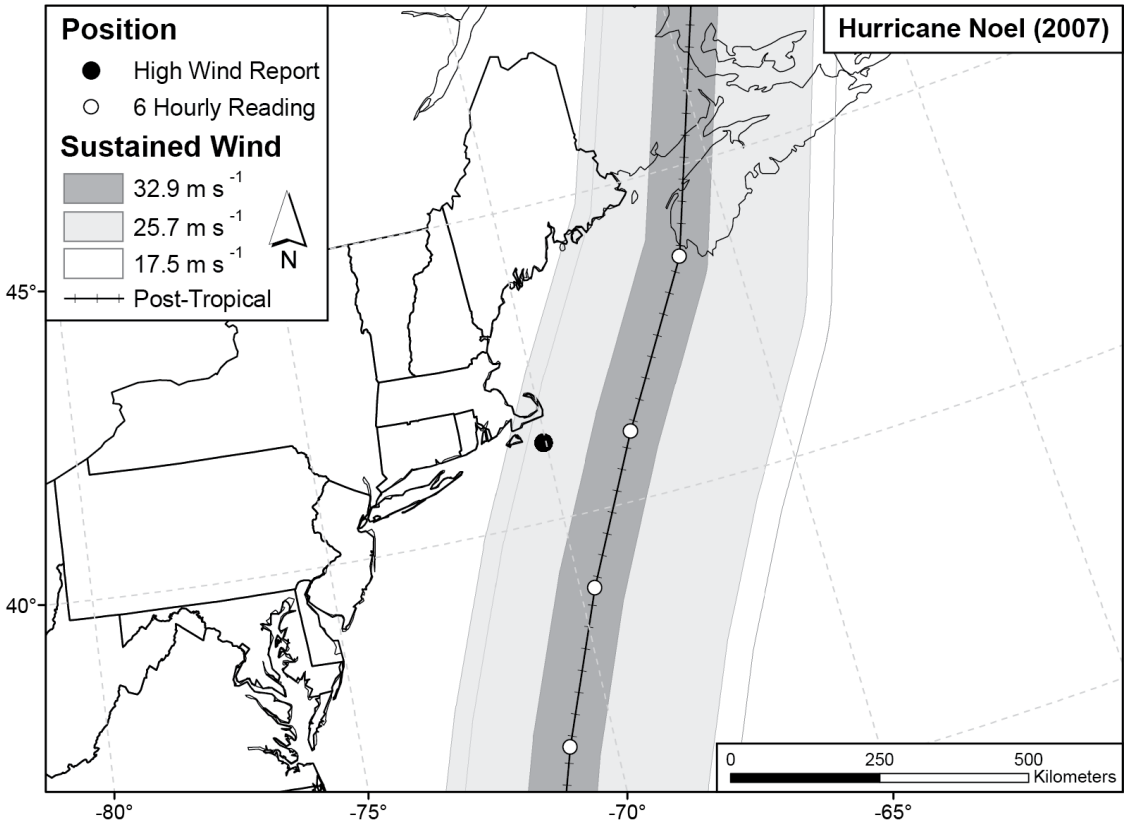
Position
High Wind Report
6 Hourly Reading
Sustained Wind
32.9 m s -1
25.7 m s -1
17.5 m s -1
Post-Tropical
N
Hurricane Noel (2007)
0
250
500
Kilometers
45°
40°
-80°
-75°
-70°
-65°

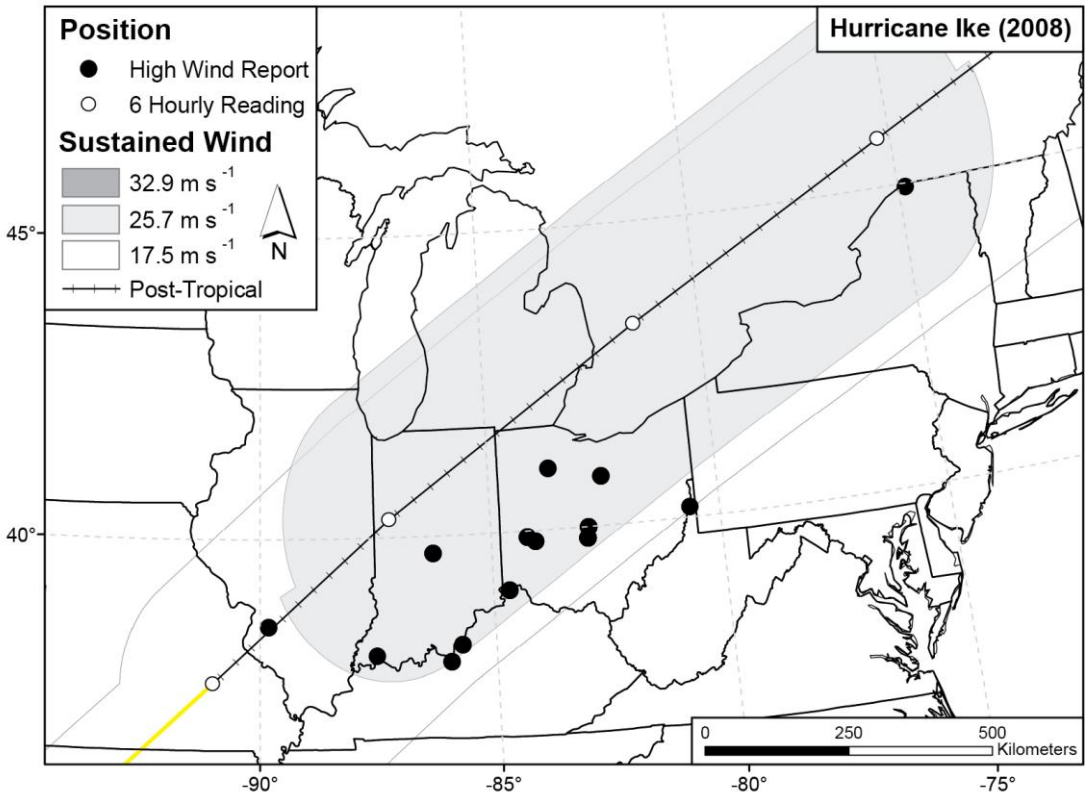
Position
High Wind Report
6 Hourly Reading
Sustained Wind
32.9 m s -1
25.7 m s -1
17.5 m s -1
Post-Tropical
N
Hurricane Ike (2008)
45°
40°
-90°
-85°
-80°
-75°
0
250
500
Kilometers

REFERENCES

Agustí-Panareda, A., S.L. Gray, G.C. Craig, and C. Thorncroft, 2005: The Extratropical Transition of Tropical Cyclone Lili (1996) and Its Crucial Contribution to a Moderate Extratropical Development. *Mon. Wea. Rev.*, **133**, 1562-1573.

Arnott, J.M., J.L. Evans, and F. Chiaromonte, 2004: Characterization of Extratropical Transition Using Cluster Analysis, *Mon. Wea. Rev*., **132**, 2916-2937.

Ashley, W.S., and A.W. Black, 2008: Fatalities Associated with Nonconvective High-Wind Events in the United States. *J. Appl. Meteor. Climatol.*, **47**, 717-725.

Asuma, J.V., 2010: Cool-Season High-Wind Events in the Northeast U.S. Unpublished Thesis, Department of Atmospheric and Environmental Sciences, University at Albany State University of New York, Albany, New York.

Black, A.W., and W.S. Ashley, 2010: Nontornadic convective wind fatalities in the United States. *Nat. Hazards*, **54**, 355-366.

Bosart, L.F., and J.A. Bartlo, 1991: Tropical Storm Formation in a Baroclinic Environment. *Mon. Wea. Rev*., **119**, 1979-2013.

Brown, D. P., 2007: Tropical Cyclone Report, Hurricane Noel, 28 October –2 November 2007: National Hurricane Center. [Available online at http://www.nhc.noaa.gov /pdf/TCR-AL162007_Noel.pdf].

Chen, T., S. Wang, and A.J. Clark, 2008: North Atlantic Hurricanes Contributed by African Easterly Waves North and South of the African Easterly Jet. *J. Climate*, **21**, 6767-6776.

Czajkowski, J., K. Simmons, and D. Sutter, 2011: An analysis of coastal and inland fatalities in landfalling US hurricanes. *Nat. Hazards*, 1-19, [online publication].

Dacre, H.F., and S.L. Gray, 2009: The Spatial Distribution and Evolution Characteristics of North Atlantic Cyclones, *Mon. Wea. Rev.*, **137**, 99-115.

DeGaetano, A.T., 1997: A Quality-Control Routine for Hourly Wind Observations. *J. Atmos. Oceanic Technol.*, **14**, 308-317.

Demuth, J.L., M. DeMaria, and J.A. Knaff, 2006: Improvement of Advanced Microwave Sounding Unit Tropical Cyclone Intensity and Size Estimation Algorithms. *J. Appl. Meteor. Climatol.*, **45**, 1573-1581.

Doswell, C.A., 2001: Severe Convective Storms—An Overview. *Meteorological Monographs*, **28**, 1-26.

———, H.E. Brooks, and M.P. Kay, 2005: Climatological Estimates of Daily Local Nontornadic Severe Thunderstorm Probability for the United States. *Wea. Forecasting*, **20**, 577-595.

Durkee, J. D., C. M. Fuhrmann, J. A. Knox, and J. D. Frye, 2011: Ageostrophic contributions to a nonconvective high-wind event in the Great Lakes region. *National Weather Digest*, [accepted, pending revisions].

Eichler, T., and W. Higgins, 2006: Climatology and ENSO-Related Variability of North American Extratropical Cyclone Activity. *J. Climate*, **19**, 2076-2093.

Evans, E., and R.E. Hart, 2008: Analysis of the Wind Field Evolution Associated with the Extratropical Transition of Bonnie (1998). *Mon. Wea. Rev.*, **136**, 2047-2065.

Evans, J.L., and R.E. Hart, 2003: Objective Indicators of the Life Cycle Evolution of Extratropical Transition for Atlantic Tropical Cyclones. *Mon. Wea. Rev.*, **131**, 909-925.

———, and B.E. Prater-Mayes, 2004: Factors Affecting the Posttransition Intensification of Hurricane Irene (1999). *Mon. Wea. Rev.*, **132**, 1355-1368.

Foley, G. R., and B. N. Hanstrum, 1994: The capture of tropical cyclones by cold fronts off the west coast of Australia. *Wea. Forecasting,* **9,** 577-592.

Harr, P.A., and R.L. Elsberry, 2000: Extratropical Transition of Tropical Cyclones over the Western North Pacific. Part I: Evolution of Structural Characteristics during the Transition Process. *Mon. Wea. Rev.*, **128**, 2613-2633.

———, ———, and T.F. Hogan, 2000: Extratropical Transition of Tropical Cyclones over the Western North Pacific. Part II: The Impact of Midlatitude Circulation Characteristics. *Mon. Wea. Rev.*, **128**, 2634-2653.

Hart, R.E., and J.L. Evans, 2001: A Climatology of the Extratropical Transition of Atlantic Tropical Cyclones. *J. Climate*, **14**, 546-564.

———, 2003: A cyclone phase space derived from thermal wind and thermal asymmetry. *Mon. Wea. Rev.*, **131,** 585-616.

———, ———, and C. Evans, 2006: Synoptic Composites of the Extratropical Transition Life Cycle of North Atlantic Tropical Cyclones: Factors Determining Posttransition Evolution. *Mon. Wea. Rev.*, **134**, 553-578.

Ho, F. P., J. C. Su, K. L. Hanevich, R. J. Smith, and F. P. Richards, 1987: Hurricane climatology for the Atlantic and Gulf Coasts of the United States. NOAA Tech. Rep. NWS 38, U.S. Department of Commerce, Washington, DC, 195 pp.

Horgan, K.L., D.M. Schultz, J.E. Hales, S.F. Corfidi, and R.H. Johns, 2007: A Five-Year Climatology of Elevated Severe Convective Storms in the United States East of the Rocky Mountains. *Wea. Forecasting*, **22**, 1031-1044.

Hulme, A.L., and J.E. Martin, 2009: Synoptic- and Frontal-Scale Influences on Tropical Transition Events in the Atlantic Basin. Part I: A Six-Case Survey. *Mon. Wea. Rev*., **137**, 3605-3625.

Jones, S.C., P.A. Harr, J. Abraham, L.F. Bosart, P.J. Bowyer, J.L. Evans, D.E. Hanley, B.N. Hanstrum, R.E. Hart, F. Lalaurette, M.R. Sinclair, R.K. Smith, and C. Thorncroft, 2003: The Extratropical Transition of Tropical Cyclones: Forecast Challenges, Current Understanding, and Future Directions. *Wea. Forecasting*, **18**, 1052-1092.

Kamburova, P.L., and F.H. Ludlam, 1966: Rainfall evaporation in thunderstorm downdrafts. *Quart. J. Roy. Meteor*. Soc., **92**, 510-518.

Kaplan, J., and M. DeMaria. 1995. A Simple Empirical Model for Predicting the Decay of Tropical Cyclone Winds after Landfall. *J. Appl. Meteor.*, **34**, 2499-2512.

———, and ———, 2001: On the Decay of Tropical Cyclone Winds after Landfall in the New England Area. *J. Appl. Meteor.*, **40**, 280-286.

Kelly, D.L., J.T. Schaefer, and C.A. Doswell, 1985: Climatology of Nontornadic Severe Thunderstorm Events in the United States. *Mon. Wea. Rev*., **113**, 1997–2014.

Kitabatake, N., 2002: Extratropical transformation of Typhoon Vicki (9807): Structural change and the role of upper tropospheric disturbances. *J. Meteor. Soc. Japan*, **80,** 229-247.

———, 2008: Extratropical Transition of Tropical Cyclones in the Western North Pacific: Their Frontal Evolution. *Mon. Wea. Rev*., **136**, 2066-2090.

Klein, P.M., P.A. Harr, and R.L. Elsberry, 2000: Extratropical Transition of Western North Pacific Tropical Cyclones: An Overview and Conceptual Model of the Transformation Stage, *Wea. Forecasting*, **15**, 373-395.

Klemp, J.B., 1987: Dynamics of Tornadic Thunderstorms, *Ann. Rev. Fluid Mech*., **19**, 369-402.

Klimowski, B.A., M.J. Bunkers, M.R. Hjelmfelt, and J.N. Covert, 2003: Severe Convective Windstorms over the Northern High Plains of the United States. *Wea. Forecasting*, **18**, 502-519.

Knox, J.A., 2004: Non-convective windstorms in the Midwest United States: Surface and satellite climatologies. Preprints, *22nd Conf. on Severe Local Storms*, Hyannis, MA, Amer. Meteor. Soc.

———, J. D. Frye, J. D. Durkee, and C. M. Fuhrmann, 2011: Non-convective high-winds associated with extratropical cyclones. *Geography Compass*, **5**, 63-89.

Kruk, M. C., E.J. Gibney, D.H. Levinson, and M. Squires, 2010: A Climatology of Inland Winds from Tropical Cyclones for the Eastern United States. *J. Appl. Meteor. Climatol.*, **49**, 1538-1547.

Kurtz, J., and J. Martinelli, 2010: Climatology of cold-season non-convective wind events for the north central Plains. *35th Annual Meeting*, Tucson, AZ, National Weather Association.

Lacke, M. C., J. A. Knox, J. D. Frye, A. E. Stewart, J. D. Durkee, C. M. Fuhrmann, and S. M. Dillingham, 2007: A climatology of cold-season non-convective wind events in the Great Lakes region. *J. Climate*, **20**, 6012-6222.

Landsea, C.W., 1993: A Climatology of Intense (or Major) Atlantic Hurricanes. *Mon. Wea. Rev.*, **121**, 1703-1713.

Lemon, L.R., and C.A. Doswell, 1979: Severe Thunderstorm Evolution and Mesocyclone Structure as Related to Tornadogenesis. *Mon. Wea. Rev.*, **107**, 1184–1197.

Martin, J., and C.E. Konrad, 2006: Directional characteristics of potentially damaging wind gusts in the Southeast United States. *Physical Geography*, **27**, 155-169.

Matano, H., and M. Sekioka, 1971: On the synoptic structure of Typhoon Cora, 1969, as the compound system of tropical and extratropical cyclones. *J. Meteor. Soc. Japan*, **49,** 282-295.

McTaggart-Cowan, R., J. R. Gyakum, and M. K. Yau, 2004: The Impact of Tropical Remnants on Extratropical Cyclogenesis: Case Study of Hurricanes Danielle and Earl (1998). *Mon. Wea. Rev.*, **132**, 1933-1951.

Merrill, R. T., 1993: Tropical cyclone structure. Global Guide to Tropical Cyclone Forecasting, WMO/TD-No. 560, Rep. TCP-31, World Meteorological Organization, Geneva, Switzerland, 2.1-2.60.

Mesquita, M.D.S., N.G. Kvamsto, A. Sorteberg, and D.E. Atkinson, 2008: Climatological properties of summertime extra-tropical storm tracks in the Northern Hemisphere, *Tellus*, **60**, 557-569.

Niziol, T.A. and T.J. Paone, 2000: A climatology of non-convective high-wind events in western New York State. NOAA Tech. Memor., NWS ER-91, 36 pp.

Palmén, E., 1958: Vertical circulation and release of kinetic energy during the development of Hurricane Hazel into an extratropical storm. *Tellus*, **10,** 1-23.

Powell, M. D., 1982: The transition of the Hurricane Frederic boundary-layer wind fields from the open Gulf of Mexico to landfall. *Mon. Wea. Rev.*, **110,** 1912-1932.

Raible, C. C., P. M. Della-Marta, C. Schwierz, H. Wernli, and R. Blender, 2008: Northern Hemisphere Extratropical Cyclones: A Comparison of Detection and Tracking Methods and Different Reanalyses. *Mon. Wea. Rev.*, **136**, 880-897.

Rappaport, E.N., 2000: Loss of Life in the United States Associated with Recent Atlantic Tropical Cyclones. *Bull. Amer. Meteor. Soc.*, **81**, 2065-2073.

Reitan, C.H., 1974: Frequencies of Cyclones and Cyclogenesis for North America, 1951–1970. *Mon. Wea. Rev.*, **102**, 861-868.

Ritchie, E.A., and R.L. Elsberry, 2003: Simulations of the Extratropical Transition of Tropical Cyclones: Contributions by the Midlatitude Upper-Level Trough to Reintensification. *Mon. Wea. Rev.*, **131**, 2112–2128.

Schmidlin, T.W., 2009: Human fatalities from wind-related tree failures in the United States, 1995-2007. *Nat. Hazards*, **50**, 13-25.

Schoen, J., and W. S. Ashley, 2011: A climatology of fatal convective wind events by storm type. *Wea. Forecasting*. **26**, 109-121.

Sinclair, M. R., 1993: A diagnostic study of the extratropical precipitation resulting from Cyclone Bola. *Mon. Wea. Rev.*, **121,** 2690-2707.

———, 2002: Extratropical transition of southwest Pacific tropical cyclones. Part I: Climatology and mean structure changes. *Mon. Wea. Rev.*, **130,** 590-609.

———, 2004: Extratropical Transition of Southwest Pacific Tropical Cyclones. Part II: Midlatiutde Circulation Characteristics. *Mon. Wea. Rev.*, **132**, 2145-2168.

Smith, B.T., A.C. Winters, C.M. Mead, A.R. Dean, and T.E. Castellanos, 2010: Measured severe wind gust climatology of thunderstorms for the contiguous United States, 2003-2009. Preprints, *25th Conf. on Severe Local Storms*, Denver, CO, Amer. Meteor. Soc.

Srivastava, R. C., 1985: A Simple Model of Evaporatively Driven Dowadraft: Application to Microburst Downdraft. *J. Atmos. Sci*., **42**, 1004-1023

Stoppkotte, E.M., A.D. Lee, S. Pavlow, and R. Baker, 2009: 14 September 2008 Ohio Valley High-wind Event Associated with the remnants of Hurricane Ike. Preprints, *23rd Conf. on Weather Analysis and Forecasting*, Omaha, NE Amer. Meteor. Soc., 13B.3.

Thorncroft,C., and S.C. Jones, 2000: The Extratropical Transitions of Hurricanes Felix and Iris in 1995. *Mon. Wea. Rev*., **128**, 947-972.

Ulbirch, U., G.C. Leckebush, and J.G. Pinto, 2009: Extra-tropical cyclones in the present and future climate: a review. *Theor. Appl. Climatol*., **96**, 117-131.

Wakimoto, R.M., 2001: Convectively Driven High Wind Events. *Meteorological Monographs*, **28**, 255-298.

Wang, X.L., V.R. Swail, and F. W. Zwiers, 2006: Climatology and Changes of Extratropical Cyclone Activity: Comparison of ERA-40 with NCEP-NCAR Reanalysis for 1958-2001. *J. Climate*, **19**, 3145-3166.

Wernli, H., and C. Schwierz, 2006: Surface Cyclones in the ERA-40 Dataset (1958-2001). Part I: Novel Identification Method and Global Climatology. *J. Atmos. Science*, **63**, 2486-2507.

Whittaker, L.M., and L.H. Horn, 1984: Northern Hemisphere Extratropical Cyclone Activity for Four Mid-Season Months, *Int. J. Climatology*, **4**, 297-310.